ATTACHMENT TO WCR

PETROGRAPHIC ANALYSIS REPORT

ANEMONE 1 & 1A

(W997)

DEC 1989

2349

89/426

FINAL REPORT

Core Services of Australia Pty Limited

Petroleum Reservoir Engineering Data

891426

CLIENT: PETROFINA EXPLORATION AUSTRALIA S.A.

WELL: ANEMONE #1 & 1A

Core Services of Australia Pty Limited

Petroleum Reservoir Engineering Data

PETROGRAPHIC ANALYSIS REPORT

ANEMONE #1, #1A

N.M. LEMON, S.E. PHILLIPS & N.S. MEAKIN

National Centre for Petroleum Geology and Geophysics
G.P.O. Box 498
ADELAIDE,
S.A. 5001.

December 1989.

INDEX

DISCLAIMER

1. SUMMARY

A series of samples from Anemone #1 and #1A in the Gippsland Basin were forwarded to the National Centre for Petroleum Geology and Geophysics via Core Services of Australia Pty. Ltd. by the well operator, Petrofina Exploration Australia S.A.. The samples were received on 3rd. August, 11th. and 25th. September and 2nd. October, 1989. The details of the samples are as follows:-

Anemone #1	Cuttings samples, washed		4530-35 metres 4560-65 metres 4600-05 metres
Anemone #1A	Cuttings samples, washed		4530-35 metres 4535-40 metres 4540-45 metres
		unwashed	4530-35 metres 4535-40 metres 4540-45 metres 4545-50 metres
Anemone #1A	Junk sub samples	4575 metres, one sample 4676 metres, six samples	

No core was available from the hole due to difficult drilling conditions.

This report is a compilation of individual reports on each group of samples. The summary covers all samples. Each previous report is included as an appendix.

The work requested varied with each batch of samples. Thin section preparation, brief petrologic descriptions and photomicroscopy were required for all samples. Particular attention was to be paid to lithology, cement composition, diagenetic sequence and the presence and nature of any hydrocarbon staining. Grain size analysis by microscopy was done on the cuttings from Anemone #1A. XRD scans on selected bulk samples from Anemone #1A were run to assist with clay mineralogy. Compositions of the junk sub samples were determined by point counting. Requests for some work were modified in consultation with the client to provide the most efficient approach to the answer required. Combined SEM - EDS analysis was done on three of the junk sub samples.

All of the samples analysed were similar in that they were all feldsarenites to sub-felsarenites with a similar source area. Most of the samples were immature, both texturally and mineralogically. Moderate to poor sorting was accompanied by angular to subangular grains. Grains in the samples ranged in size from very fine sand to granules. Grain size analysis on the cuttings samples from Anemone #1A semi quantified these characteristics, despite the grinding associated with cuttings samples. The high feldspar content of most samples indicates their mineralogical immaturity.

The source area for the sandstones was almost exclusively granite. The indications of this are the low strain, vacuole filled quartz grains, the abundance of feldspars including othoclase, microcline, perthite and some plagioclase, occassional distinctive grains with a granophyric texture, minor muscovite and biotite, and, especially in the larger grains, rock fragments easily identifiable as granite.

The cuttings samples showed contamination from overlying formations. Between 5% and 10% of the chips were silty micrite, organic rich siltstones and mudstones and/or glauconitic siltstones.

The determination of matrix content in all of the samples was difficult to impossible. Cuttings samples invariably break through the matrix, cement and pore spaces, the weaker parts of the rock, exposing that material to erosion during drilling and sample return to the surface. Very little cement or matrix was seen adhering to the chips. It is highly likely that junk sub samples would be heavily impregnated by drilling mud, having been broken from the edge of the hole. It was difficult to distinguish bewteen mud and matrix until XRD scans on the washed and unwashed cuttings from Anemone #1A allowed discrimination of the drilling mud on barite content. Matrix contents of between 8% and 2% were then estimated for samples 4676a to 4676f.

As with matrix determination, porosity determination in the majority of these samples was difficult. No primary porosity was preserved in the cuttings samples but there were some interesting occurrences of secondary porosity. Micro porosity is associated with the alteration of plagioclase to sericite and kaolin but experience elsewhere suggests that this may only be effective with respect to the very lightest hydrocarbons. Many of the feldspar grains show dissolution porosity. Plagioclase has been removed from feldspar grains to give a "Swiss cheese" texture to those grains. Those initial sites have focussed further dissolution so that some grains are now a mere skeleton showing the original twinning. Most of the feldspar dissolution porosity is large enough to be effective provided it is interconnected through primary intergranular porosity.

Primary porosity was not observed in any of the cuttings samples due to the nature of those samples. It was observed in the junk sub samples but there it was a minor proportion of each sample. This could be related to the nature of the samples. Junk sub collection may concentrate on the more competant hard bands in the sequence; those with more matrix and/or cement. The junk sub samples show low primary porosity due to high matrix content and strong compactional influences. Carbonate and clay cement occlude much of the remaining porosity with minor quartz and traces of pyrite and anatase cements. Of the clays, pore-lining illite, pore filling dickite (a kaolin form) and late stage fibrous and bridging illite were observed. All reduce primary porosity but have associated micro porosity. The late stage illite is likely to be particularly harmful in reducing permeability.

The diagenetic sequence determined from the junk sub samples is the most complete because these samples are likely to be the most cemented (see above) and are intact. The observations from the cuttings samples, while disjointed, are in agreement with those from the junk sub samples. The diagenetic sequence is as follows:-

Earliest Micrite cement
Siderite spar
Compaction and quartz corrosion
Feldspar alteration
Pore-lining illite
Pore-filling dickite and quartz overgrowth
Dolomite and ankerite cement, dissolution
Illite fibre growth, bridging framework grains and on kaolin
Latest Anatase

The position of hydrocarbon generation and migration is difficult to determine as so little of it was seen in the tight junk sub samples or the disaggregated cuttings. It does, however, post date the feldspar alteration and possibly the pore-filling dickite.

2. APPENDIX I

ANEMONE #1, Cuttings decriptions

INDEX

2.1 INTRODUCTION

This report contains a brief petrographic description of three cuttings samples from reservoir sands in Anemone #1 well in the Gippsland Basin. The client, Petrofina Exploration Australia, specifically requested an assessment of the grain and cement mineralogy, identification of any clay matrix and the description of any oil staining. Photomicroscopy was done after a telephone conversation with the client.

Cuttings samples from the following depths were analysed:-

4530-4535 metres
4560-4565 metres
4600-4605 metres

2.2 METHODS

All samples were briefly described in "hand" specimen. They were then impregnated and glued into a single mount with araldite. Blue dye was used in the araldite to facilitate the description of porosity. The slides cut from the mounted grains were systematically scanned to determine their lithology and cement and porosity relationships. All percentages are based on visual estimates, not point counts.

2.3 CUTTINGS PETROGRAPHY

2.3.1 Anemone #1, cuttings sample, 4530-4535 metres

Macro description
White, fine to very coarse grained feldsarenite with angular to subangular grains and a few dark grey shale chips.

Micro description
The slide shows a poorly sorted, very fine to very coarse feldsarenite. However, this does not reflect the true grain size and distribution as most of the grains have been fractured by the drilling rather than liberated. The grains are now shard-like with very sharp edges or cleavage fragments of feldspars. Some grains have traces of matrix and cement still attached which show the original grains to be angular to subangular and possibly medium to coarse sand sized.

The majority of the grains have been derived from a granitic source. There are a few polycrystalline grains of quartz and K feldspar and quartz plus muscovite which clearly suggest a granitic origin. Individual quartz grains are unstrained to weakly strained with lines of vacuoles, all igneous features. K feldspars, orthoclase and and microcline are common and there are numerous grains of perthite, the distinctive intergrowth of plagioclase in K feldspar, also suggestive of a granitic source.

There are a few grains of highly strained metamorphic quartzite and a few sedimentary grains of very fine sandstone with an illitic matrix that show other than a granite source.

Many of the feldspar grains show alteration to sericite. This is particularly so with plagioclase, where the alteration is almost complete and has associated kaolin and microporosity development. The K feldspars only show incipient sericite alteration that gives those grains a dirty brown appearance under plane polarized light. Biotite grains show alteration to chlorite with the consequent release of iron as finely divided magnetite.

Secondary porosity is apparent where the plagioclase component of the perthite grains has been removed to produce a "Swiss cheese" texture.

Some grains show cementation by a sparry carbonate, probably dolomite. This has corroded the adjacent framework grains, both quartz and feldspar. Many of the individual grains have deeply embayed edges and these could be the result of more extensive carbonate cement, now removed. There are a few large single crystals of carbonate up to 0.5mm long.

There are a few chips of organic rich siltstone in the sample. These contain glauconite grains, small spherical foraminifera fossils and finely disseminated pyrite. Siltstone also rims some of the finer sand grains, suggesting that there may be some silty interbeds in the sequence.

Rare chips contain booklets of kaolin. It is unclear whether these are originally a pore filling form or a replacement of feldspar. Apart from the carbonate, there is minimal cement. There are no quartz overgrowths and only traces of authigenic feldspar.

There are the faintest traces of pale brown hydrocarbon staining in the microporosity of the completely sericitized grains.

Composition

Quartz	49%
Orthoclase	20%
Microcline	5%
Plagioclase	3%
Biotite	1%
Muscovite	2%
Sedimentary grains	1%
Mudstone chips	1%
Carbonate	4%
Sericite	8%
Kaolin	1%
Secondary porosity	4%

2.3.2 Anemone #1, cuttings sample, 4560-4565 metres

Macro description
A pale grey, poorly sorted, very fine to very coarse feldsarenite with silty matrix and some chips of grey shale.

Micro description
The slide shows very fine to fine sand sizes with a few medium grains. These sizes are not representative of the original rock as nearly all fragments have been generated during drilling. Some original outlines shown by rims of illitic clay (matrix?) suggest subrounded grains.

The grains are dominantly from a granitic source area. The quartz grains are weakly strained with lines of vacuoles. There is a high proportion of K feldspar with numerous grains of perthite. Biotite is a common accessory mineral and commonly shows alteration to chlorite. Plagioclase is present in minor amounts but is almost invaribly highly altered to sericite and kaolin. The K feldspars show incipient sericite alteration which gives the grains a dusty appearance.

Although the majority of the grains in the sample are separated, the main cement appears to be carbonate microspar (probably dolomite). This occurs between the framework grains, etching both the quartz and feldspar, and as recrystallized micrite. Etching of microcline is pronounced and is associated with both microspar and some micrite.

Cementation of the whole sample appears to be minor with only traces of clay and minor authigenic feldspar overgrowth apart from the carbonate. It is difficult to tell whether the rare small groups of kaolin booklets were original pore filling or feldspar replacement.

Secondary porosity is particularly evident in some of the feldspar grains. Plagioclase has been completely removed from perthite and there has been some dissolution of orthoclase and microcline.

There are a few chips of muddy siltstone and silty mudstone in the sample. No traces of hydrocarbons were seen.

Composition

Quartz	45%
Orthoclase	22%
Microcline	6%
Plagioclase	2%
Biotite	3%
Mudstone chips	2%
Carbonate	3%
Sericite	10%
Kaolin	1%
Authigenic feldspar	1%
Secondary porosity	5%

2.3.3 Anemone #1, cuttings sample, 4600-4605 metres

Macro description
A pale grey, very fine to coarse grained feldsarenite with subangular grains and a silty matrix.

Micro description
The slide shows mainly very fine to medium sand sizes but many of the finer chips are fragments generated by drilling. The sample appears to have been a reasonably well sorted, fine to medium feldsarenite. Most grains are angular to subangular although some are subrounded.

As with the other two cuttings samples, the grains have been derived from a granitic source area. There is a high proportion of K feldspars, including distinctive perthite grains. The quartz grains are unstrained or weakly strained and shows lines of vacuoles. Muscovite and biotite are also present. There are, however, a few polycrystalline grains of highly strained quartz suggesting minor input from a metamorphic source.

There has been substantial sericite alteration of the feldspar grains, particularly the plagioclase grains. These have completely altered to a mass of sericite with some associated fine grained kaolin. This reaction generates microporosity between the remaining clay minerals. Booklets of kaolin were also seen replacing a feldspar in a polycrystalline grain.

Only minor amounts of cement were seen in the sample. The main cement component is carbonate, both as individual, liberated grains and some still attached to framework grains where etching of those grain surfaces is evident. Minor pore-lining illite occurs and this is followed by pore-filling kaolin.

The development of secondary porosity is quite extensive in this sample. Plagioclase has been removed from perthite grains to give a "Swiss cheese" appearance to those grains. Some microcline grains have been skeletonized to leave just a grid outline of the familiar "cross-hatched" twinning.

Some silty matrix holds a few of the very fine sand grains together and there are a few chips of organic-rich, silty mudstone, some with a micritic matrix.

Hydrocarbon staining is present as dark, bituminous rims on intergrown carbonate grains ansd as light brown stains preserved in deeply etched embayments on the framework grains.

Composition

Quartz	38%
Orthoclase	15%
Microcline	10%
Plagioclase	2%
Biotite	2%
Muscovite	2%
Silty matrix	2%
Mudstone chips	3%
Carbonate	4%
Sericite	10%
Illite	1%
Kaolin	3%
Secondary porosity	8%

2.4. CONCLUSIONS

The three cuttings samples described above are all related in that they have been derived from a dominantly granitic source area. The majority of quartz grains suggest an igneous origin with low strain and lines of vacuoles. There is a high proportion of feldspar, particularly the potassium rich feldspars, orthoclase and microcline. There are also grains with the distinctive granite-associated perthitic feldspar intergrowths and granophyric quartz-feldspar intergrowths. Biotite and muscovite are common accessory minerals. There is, however, a minor metamorphic component shown by polycrystalline aggregates of highly strained quartz.

Many of the grains show alteration features which may have been initiated in the source area but have continued after deposition. Plagioclase, in particular, is often highly altered to a mass of sericite with some associated kaolin. The K feldspars are also sericitized but to a far lesser extent so that they now appear as very dirty, dusty grains under plane polarized light. Biotite alters to chlorite with the consequent release of iron as finely divided magnetite.

Most of the grains in all three samples have been crushed and broken by drilling so that the current grain size distibution does not reflect that in the formation. The few original grain edges recognized suggest that most of the grains were angular to subangular and that etching or corrosion has taken place during diagenesis.

Rare sand-sized grain aggregates show some silty matrix. There are also associated clasts of organic-rich, silty mudstone which contain some foraminifera fossils, glauconite grains and finely disseminated pyrite. Micrite is present in about half of these mudstones and is the most likely source of carbonate seen as cement in the sands.

Cements are a minimal component of the sands. The main cement by volume is sparry carbonate, possibly dolomite. This was seen adhering to some of the framework grains and as single, liberated crystals. The emplacement of carbonate has caused some etching and may be the reason for the corroded edges on many of the grains. Some groups of kaolin booklets were seen but these could be either replacement of feldspar or have a pore filling habit. Both modes of occurrence are likely. One pore was seen with an illite lining followed by pore filling kaolin.

No estimate of primary porosity could be made these crushed sands. There are, however, excellent examples of secondary porosity. Some microporosity is associated with the alteration of plagioclase to sericite and minor kaolin. This type of porosity is likely to be largely ineffective with regards to the hydrocarbon reservoir. Of greater interest, both volumetrically and economically, is the secondary dissolution porosity observed in the K feldspars. The plagioclase component of the perthite grains has been largely removed in many cases to create grains that resemble a "Swiss cheese". Many of the microcline grains show ragged edges where dissolution has taken place. Some of these grains have been skeletonized to leave just a grid outline of the distinctive cross-hatched twinning. This porosity is large enough to be effective for hyrocarbons and it is highly likely that it would be connected with the primary, intergranular porosity.

In comparison with Angler #1, the samples from Anemone #1 show the same mineralogy reflecting the same source area. However, the Anemone #1 samples have a more even distribution of carbonate cement and less authigenic feldspar. No quartz cement was observed in either hole. The feldspar dissolution seen in at these depths in Anemone #1 could have supplied the potassium which influenced the diagenesis of the Angler #1 samples.

6. FIGURES AND CAPTIONS

The following shorthand symbols have been used to annotate the photomicrographs below:-

Q	quartz
Pe	perthite
Mi	microcline
Ca	carbonate
Ad	adularia, authigenic feldspar
Se	sericite

Figure 1. Anemone #1, cuttings 4530-35 metres. (Plane polarized light) Very angular, shard-like grains fractured during drilling. Only the larger grains of quartz and perthite represent original grains as would be seen from a cored sample. The carbonate grain shown contains some hydrocarbon staining between its crystals. The composite grain arrowed, now sericite and muscovite, was originally plagioclase and muscovite. The dirty brown appearance of the perthite grain is due to incipient sericitization.

Figure 2. Anemone #1, cuttings 4530-35 metres. The same field of view as Fig.1 under crossed polars shows the intergrown feldspars in the perthite grain. Micro porous sericite can be seen in the arrowed grain from Fig.1. Carbonate grains show as bright orange-yellow.

Figure 3. Anemone #1, cuttings 4530-35 metres. (Plane polarized light) Intense dissolution of a microcline perthite grain creates considerable secondary porosity which would be connected to the primary porosity surrounding each grain.

Figure 4. Anemone #1, cuttings 4530-35 metres. The same field of view as Fig.3 under crossed polars shows crossed hatched microcline twinning still showing in the skeletonized grain.

Figure 5. Anemone #1, cuttings 4560-65 metres. (Plane polarized light) Most of the very angular grains have been fractured during drilling although the larger grains are closer to the original size and shape. The high feldspar content of this sample consists of perthite, microcline and plagioclase. The perthite grains have had their plagioclase component removed to give a "Swiss cheese" texture to the grains. There is some carbonate in the sample but its relationship to the other grains is unclear.

Figure 6. Anemone #1, cuttings 4560-65 metres. The same field of view as Fig.5 under crossed polars shows the intergrowth of feldspars in the perthite grains. The dark brown grains in Fig.5 are seen to be sericite, probably from the complete alteration of plagioclase.

Figure 7. Anemone #1, cuttings 4600-05 metres. (Plane polarized light) The larger grains in this field of view probably represent the true grain size from this interval. Some dark, hydrocarbon stained carbonate can be seen as individual grains as well as attached to, and corroding, framework grains. One dusty, incipiently sericitized feldspar grain has clear rims of adularia, or authigenic feldspar. Other feldspars show considerable dissolution.

Figure 8. Anemone #1, cuttings 4600-05 metres. The same field of view as Fig.7 under crossed polars shows that the dirty, mid-brown grains in that scene are now brightly coloured sericite, probably after plagioclase. Illitic clays rim some of the grains.

Figure 9. Anemone #1, cuttings 4600-05 metres. (Plane polarized light) A deeply corroded microcline grain. The remaining skeleton picks out the cross hatched twinning of that mineral. Such dissolution creates substantial and effective secondary porosity.

PE906850

This is an enclosure indicator page.
The enclosure PE906850 is enclosed within the container PE906849 at this location in this document.

The enclosure PE906850 has the following characteristics:

ITEM_BARCODE =	PE906850
CONTAINER_BARCODE =	PE906849
NAME =	Core Photomicrograph
BASIN =	GIPPSLAND
PERMIT =	VIC/P20
TYPE =	WELL
SUBTYPE =	PHOTOMICROGRAPH
DESCRIPTION =	Core Photomicrograph, very angular shard-like grains fractured during drilling, (figure 1 from attachment to WCR--Petrographic Analysis Report) for Anemone-1 & 1A
REMARKS =	
DATE_CREATED =	31/12/89
DATE_RECEIVED =	17/01/90
W_NO =	W997
WELL_NAME =	ANEMONE-1 & 1A
CONTRACTOR =	CORE SERVICES OF AUSTRALIA
CLIENT_OP_CO =	PETROFINA EXPLORATION AUSTRALIA S.A.

PE906851

This is an enclosure indicator page.
The enclosure PE906851 is enclosed within the container PE906849 at this location in this document.

The enclosure PE906851 has the following characteristics:

ITEM_BARCODE =	PE906851
CONTAINER_BARCODE =	PE906849
NAME =	Core Photomicrograph
BASIN =	GIPPSLAND
PERMIT =	VIC/P20
TYPE =	WELL
SUBTYPE =	PHOTOMICROGRAPH
DESCRIPTION =	Core Photomicrograph, intergrown feldspars in the perthite grain, (figure 2 from attachment to WCR--Petrographic Analysis Report) for Anemone-1 & 1A
REMARKS =	
DATE_CREATED =	31/12/89
DATE_RECEIVED =	17/01/90
W_NO =	W997
WELL_NAME =	ANEMONE-1 & 1A
CONTRACTOR =	CORE SERVICES OF AUSTRALIA
CLIENT_OP_CO =	PETROFINA EXPLORATION AUSTRALIA S.A.

PE906852

This is an enclosure indicator page.
The enclosure PE906852 is enclosed within the container PE906849 at this location in this document.

The enclosure PE906852 has the following characteristics:

ITEM_BARCODE =	PE906852
CONTAINER_BARCODE =	PE906849
NAME =	Core Photomicrograph
BASIN =	GIPPSLAND
PERMIT =	VIC/P20
TYPE =	WELL
SUBTYPE =	PHOTOMICROGRAPH
DESCRIPTION =	Core Photomicrograph, dissolution of microline perthite grain, (figure 3 from attachment to WCR--Petrographic Analysis Report) for Anemone-1 & 1A
REMARKS =	
DATE_CREATED =	31/12/89
DATE_RECEIVED =	17/01/90
W_NO =	W997
WELL_NAME =	ANEMONE-1 & 1A
CONTRACTOR =	CORE SERVICES OF AUSTRALIA
CLIENT_OP_CO =	PETROFINA EXPLORATION AUSTRALIA S.A.

(Inserted by DNRE - Vic Govt Mines Dept)

PE906853

This is an enclosure indicator page.
The enclosure PE906853 is enclosed within the container PE906849 at this location in this document.

The enclosure PE906853 has the following characteristics:

ITEM_BARCODE =	PE906853
CONTAINER_BARCODE =	PE906849
NAME =	Core Photomicrograph
BASIN =	GIPPSLAND
PERMIT =	VIC/P20
TYPE =	WELL
SUBTYPE =	PHOTOMICROGRAPH
DESCRIPTION =	Core Photomicrograph, hatched microline twinning, (figure 4 from attachment to WCR--Petrographic Analysis Report) for Anemone-1 & 1A
REMARKS =	
DATE_CREATED =	31/12/89
DATE_RECEIVED =	17/01/90
W_NO =	W997
WELL_NAME =	ANEMONE-1 & 1A
CONTRACTOR =	CORE SERVICES OF AUSTRALIA
CLIENT_OP_CO =	PETROFINA EXPLORATION AUSTRALIA S.A.

(Inserted by DNRE - Vic Govt Mines Dept)

PE906854

This is an enclosure indicator page.
The enclosure PE906854 is enclosed within the container PE906849 at this location in this document.

The enclosure PE906854 has the following characteristics:

ITEM_BARCODE =	PE906854
CONTAINER_BARCODE =	PE906849
NAME =	Core Photomicrograph
BASIN =	GIPPSLAND
PERMIT =	VIC/P20
TYPE =	WELL
SUBTYPE =	PHOTOMICROGRAPH
DESCRIPTION =	Core Photomicrograph, angular grains of perthite, microline and plagioclase, (figure 5 from attachment to WCR--Petrographic Analysis Report) for Anemone-1 & 1A
REMARKS =	
DATE_CREATED =	31/12/89
DATE_RECEIVED =	17/01/90
W_NO =	W997
WELL_NAME =	ANEMONE-1 & 1A
CONTRACTOR =	CORE SERVICES OF AUSTRALIA
CLIENT_OP_CO =	PETROFINA EXPLORATION AUSTRALIA S.A.

PE906855

This is an enclosure indicator page.
The enclosure PE906855 is enclosed within the container PE906849 at this location in this document.

The enclosure PE906855 has the following characteristics:

ITEM_BARCODE =	PE906855
CONTAINER_BARCODE =	PE906849
NAME =	Core Photomicrograph
BASIN =	GIPPSLAND
PERMIT =	VIC/P20
TYPE =	WELL
SUBTYPE =	PHOTOMICROGRAPH
DESCRIPTION =	Core Photomicrograph, intergrowth of feldspars in the perthite grains, (figure 6 from attachment to WCR--Petrographic Analysis Report) for Anemone-1 & 1A
REMARKS =	
DATE_CREATED =	31/12/89
DATE_RECEIVED =	17/01/90
W_NO =	W997
WELL_NAME =	ANEMONE-1 & 1A
CONTRACTOR =	CORE SERVICES OF AUSTRALIA
CLIENT_OP_CO =	PETROFINA EXPLORATION AUSTRALIA S.A.

PE906856

This is an enclosure indicator page.
The enclosure PE906856 is enclosed within the container PE906849 at this location in this document.

The enclosure PE906856 has the following characteristics:

ITEM_BARCODE = PE906856
CONTAINER_BARCODE = PE906849
NAME = Core Photomicrograph
BASIN = GIPPSLAND
PERMIT = VIC/P20
TYPE = WELL
SUBTYPE = PHOTOMICROGRAPH
DESCRIPTION = Core Photomicrograph, brightly coloured sericite and lithic clays, (figure 8 from attachment to WCR--Petrographic Analysis Report) for Anemone-1 & 1A
REMARKS =
DATE_CREATED = 31/12/89
DATE_RECEIVED = 17/01/90
W_NO = W997
WELL_NAME = ANEMONE-1 & 1A
CONTRACTOR = CORE SERVICES OF AUSTRALIA
CLIENT_OP_CO = PETROFINA EXPLORATION AUSTRALIA S.A.

(Inserted by DNRE - Vic Govt Mines Dept)

PE906857

This is an enclosure indicator page.
The enclosure PE906857 is enclosed within the container PE906849 at this location in this document.

The enclosure PE906857 has the following characteristics:

ITEM_BARCODE =	PE906857
CONTAINER_BARCODE =	PE906849
NAME =	Core Photomicrograph
BASIN =	GIPPSLAND
PERMIT =	VIC/P20
TYPE =	WELL
SUBTYPE =	PHOTOMICROGRAPH
DESCRIPTION =	Core Photomicrograph, dark hydrocarbon stained carbonate and sericitized feldspar, (figure 7 from attachment to WCR--Petrographic Analysis Report) for Anemone-1 & 1A
REMARKS =	
DATE_CREATED =	31/12/89
DATE_RECEIVED =	17/01/90
W_NO =	W997
WELL_NAME =	ANEMONE-1 & 1A
CONTRACTOR =	CORE SERVICES OF AUSTRALIA
CLIENT_OP_CO =	PETROFINA EXPLORATION AUSTRALIA S.A.

3. APPENDIX II

ANEMONE #1A, Cuttings descriptions

INDEX

3.1. INTRODUCTION

This report contains petrographic descriptions of four cuttings samples from Anemone #1A well in the Gippsland Basin. The samples were forwarded to the National Centre by Petrofina Exploration Australia S.A. via Core Services Australia Pty. Ltd. on 25th September and 2nd October, 1989. The work requested included thin section preparation, brief thin section description, rock composition by point count, thin section grain size analysis and photomicroscopy. Of particular interest to the client were the grain and cement mineralogy, nature of the diagenesis, identification of any clay matrix and the description of any oil staining. In consultation with the client, it was decided that rock composition by point count could not be satisfactorily carried out on cuttings samples and that adequate identification of clays requires an XRD scan.

The samples received were:-

Washed samples
4530-4535m
4535-4540m
4540-4545m

Unwashed samples
4530-4535m
4535-4540m
4540-4545m
4545-4550m

3.2. METHODS

All samples, washed and unwashed, were described in hand specimen. Part of each sample was then prepared as a block mount in blue-dyed araldite prior to thin section preparation. Thin sections were then scanned to determine lithology, composition by visual estimation and textural relationships where possible and then photographed.

Mounted grains were measured under the polarizing microscope to determine the average size and distribution. Care was taken to select whole grains wherever possible although numerous measurements where taken on elongate slivers as these are all that remains of many of the larger grains. The measurements were taken on the unwashed samples so that more of the finer grain sizes could be included, but even so, much of the matrix may have been ground into the drilling mud and so removed. The average size of the sixty grains measured for each sample is likely to be close to the true value but slightly underestimated due to crushing of the larger grains. The standard deviation quoted for the samples is below that expected because both the finest and coarsest fractions are missing from each sample analysed.

Part of each sample was prepared for bulk mineralogy by X-ray diffraction. This included hand grinding in acetone prior to distribution of the sample on a smear plate. Smears were run from 3^o to 75^o 2Θ, at 1^o/minute, using Co $K\alpha$ radiation, 50kV and 35mA, on a Phillips PW1050 diffractometer. Both washed and unwashed samples were run as this allowed identification of the drilling mud which assisted with the the estimatimation of porosity and matrix percentages in the junk sub samples from 4575m and 4676m in Anemone #1A, also submitted to the National Centre for petrographic analysis.

3.3. PETROGRAPHIC DESCRIPTIONS

3.3.1 Anemone #1a, cuttings, 4530-4535 metres

Macro description
A pale grey, poorly sorted, very fine to medium, angular to subrounded micaceous sub-feldsarenite with 10% chips of light grey, very fine to fine sandstone and 10% chips of grey mudstone. Many of the feldspar grains are opaque off white to pale brown grey in colour, possibly due to alteration. There is no reaction to 10% HCl. The unwashed sample was a poorly sorted, silty, very fine to coarse feldsarenite and granule conglomerate with an obvious strong hydrocarbon odour.

Micro description
The thin sections depict a moderately sorted, very fine to very coarse grained sub-feldsarenite (Figs 1,2). The framework grains are largely igneous derived quartz, unstrained with vacuole trails, and feldspars. Orthoclase and microcline show both incipient sericitization and alteration to kaolin. Microcline in particular shows dissolution along cleavage traces to produce secondary porosity (Fig.3). Grains assumed to have been plagioclase, show complete alteration to a mixture of sericite and kaolin. This is also evident in the perthite grains, where some of the plagioclase blebs have altered to sericite and some have been removed by dissolution. Muscovite grains show partial alteration to kaolin and biotite shows alteration to chlorite.

The larger grains are mainly granitic fragments although there are a few composites of sediment grains which show cement in place. This consists of an illitic rim on some of the framework grains with later pore-filling kaolin. The other cement in this sample is siderite. Small euhedral crystals were seen growing in patches of matrix and rimming some framework grains.

Some light brown to brown oil staining was seen rimming grains and in fractures.

Composition

60%	Quartz
10%	Orthoclase (and perthite)
5%	Microcline
2%	Plagioclase, completely altered to sericite/kaolin
2%	Muscovite
2%	Biotite, largely altered to chlorite
2%	Chert
3%	Cement, kaolin, illite and siderite spar
Other grains	
1%	Carbonate spar
1%	Micrite cemented very fine to fine sand
6%	Micritic mudstone with glauconite, pyrite, carbonaceous material and foraminifera.
6%	Muddy, very fine to fine sandstone with siderite cement.

The unwashed sample shows far fewer mudstone chips (2%). The fines portion of the sample is dominated by drilling mud, a dark reddish brown material glued as small blebs to the edges of the cuttings. The larger grains show a higher proportion of completely altered grains, sericite and kaolin and heavily dissolved feldspar grains. There is more cement and matrix present in the unwashed sample including illite rims on grains, small loose carbonate rhombs and isolated small pyrite crystals. There is also more light brown hydrocarbon present, in the microporosity of altered grains and in the matrix.

XRD Analysis
The XRD scan on the washed sample, (Fig.4), shows a dominance of quartz with subsidiary microcline. Orthoclase peaks are close to those of quartz and are not easliy seen. Illite forms small but broad peaks suggesting a range of compositions. Part of the reason for this is the superposition of muscovite (sericite) peaks. The kaolin form, dickite, shows as sharp minor peaks. Traces of siderite also show.

Figure 5 shows the XRD trace of the unwashed sample. A series of barite peaks clearly shows the contamination from drilling mud. Traces of halite and pyrite are also evident but there is no observable contribution to the clay fraction. Many of the peaks seen in the washed sample are somewhat subdued by the amount of barite in the unwashed sample.

3.3.2 Anemone #1A, cuttings, 4535-4540 metres.

Macro description
The washed sample was a white, poorly sorted, fine to very coarse, angular to subangular feldsarenite and granule conglomerate with 5% chips of grey to dark grey mudstone. There are a few grains of muscovite and minor biotite. Many of the feldspar grains are cleavage fragments and display alteration, seen as opaque, off white to pale brown discolouration. This is particularly apparent along grain boundaries in some of the larger, polycrystalline grains. There was no reaction to 10% HCl. The unwashed sample is mid-brown, silty and poorly sorted. Much of the colouration may be due to hydrocarbons, of which there is a strong smell.

Micro description
The slide prepared from the washed sample shows a poorly sorted, very fine to very coarse feldsarenite. The framework grains are dominated by quartz and feldspar (Figs.6,7). The quartz grains are all of igneous origin with low strain evident and trails of vacuoles. K felspar, as orthoclase, perthite and microcline, shows some alteration to sericite to give a dusty appearance. The K feldspars also show alteration to kaolin and dissolution to produce secondary porosity. It is suspected that plagioclase was present but is now completely altered to sericite and kaolin, thus producing some microporosity.

Most of the composite chips in this sample are fragments of granite, although there are a few of intact sediment. These show illitic and kaolinitic matrix bewteen some of the framework grains as well as kaolin cement entirely filling the remaining porosity. Many individual chips show clays adhering to a margin. In 50% of cases, there is a thin rind of illite between the grain and the kaolin. Quartz overgrowths form a minor part of the cement and is seen as some straight line contacts between grains and a few euhedral terminations into porosity.

Composition

54%	Quartz
10%	Orthoclase (and perthite)
8%	Microcline
2%	Plagioclase, completely altered to sericite/kaolin
3%	Muscovite, altering to kaolin
1%	Biotite, largely altered to chlorite
3%	Matrix, illitic and kaolinitic
Cements	
1%	Quartz overgrowth
6%	Kaolin
3%	Illite
Other grains	
1%	Micrite cemented siltstone, now recrystallized
4%	Glauconitic, silty, very fine to fine sandstone with abundant pyrite
4%	Organic rich siltstone
1%	dark, organic-rich mudstone

Unwashed sample
The finer material remaining in this sample is dominantly drilling mud contamination which consists of dark reddish brown, very fine illitic material. It also carries with it a lot of opaques, possibly pyrite liberated from the matrix and finer grained sediments. There are chips of carbonate and individual carbonate scalenohedra, also probably released from the matrix. A fraction more matrix than in the washed samples is seen adhering to the grains.

XRD Analysis
Quartz dominates the scan of the washed sample (Fig.8) and there are minor amounts of microcline. Traces of illite are shown by a broad peak. The character of the peak is due in part to the superposition of the muscovite (sericite) peak. Traces of the kaolin, dickite, are present and the sharpness of this peak indicates strong crystallinity of this mineral, suggesting that it is authigenic.

The scan of the unwashed sample (Fig.9) shows barite, with traces of halite and pyrite, to be the main contaminants from the drilling mud. The sub-dominant microcline peak, in comparison with Figure 8, illustrates the difficulty in getting a representative sample from small amounts of very coarse sediments.

3.3.3 Anemone #1A, cuttings, 4540-4545 metres.

Macro description
The washed sample depicted a white, moderately sorted, very fine to very coarse, angular to subrounded sub-feldsarenite with a few chips of grey mudstone. There are some muscovite flakes, both liberated and included in the larger, polycrystalline grains. Many of the feldspar grains are opaque with alteration products. There was no reaction with 10% HCl. The unwashed sample was a mid-brown colour, silty and poorly sorted with a moderately strong hydrocarbon odour.

Micro description
The sample is dominated by quartz and feldspar. The quartz all shows characteristics of an igneous origin, with low strain evident and numerous vacuole trails. The potassium feldspars are dusty with minor sericite alteration and sometimes show replacement by kaolin (Figs.10,11). Microcline and perthite show dissolution to create secondary porosity (Figs.12,13). What was plagioclase is now largely masses of sericite and kaolin.

The sample is more finely comminuted than others with nearly all grains fractured and near total liberation of grains and sub-grains. The remaining composite groups are mainly granitic fragments, siltstone and mudstone, except for two chips of carbonate cemented very fine to fine sandstone.

Composition

56%	Quartz
8%	Orthoclase (and perthite)
6%	Microcline
4%	Plagioclase, completely altered to sericite/kaolin
3%	Muscovite, kaolin alteration
1%	Biotite, largely altered to chlorite
Cement	
4%	Carbonate spar and microspar, some encasing relict quartz grains, left after corrosion.
7%	Kaolin, pore filling and replacement
7%	Illite, pore lining
Other grains	
3%	Organic rich, pyritic mudstone
1%	Organic rich, pyritic siltstone

Unwashed sample
The finer grained component in this sample is largely drilling mud; dark red-brown, very fine grained material with abundant organics and pyrite. These may have been released from the matrix or may represent incorporation into the mud of finer grained units in the sequence. There are also masses of kaolin, small cleavage fragments of feldspar and chlorite after biotite.

XRD Analysis
Figure 14, the XRD scan of the washed sample, shows quartz as the dominant mineral with minor microcline. Orthoclase is disguised by the coincidence of peaks with quartz. The dickite in the sample is strongly crystalline and therefore probably authigenic. The broad illite peak may represent a range of compositions of that mineral or more probably is a result of a combination of near-coincident illite, muscovite and sericite peaks.

The scan of the unwashed sample (Fig.15) shows barite as the main contaminant from the drilling mud with traces of halite and pyrite. No addition of clay is evident.

3.3.4 Anemone #1A, cuttings, 4545-4550 metres.

Macro description
Only an unwashed sample was provided for this interval. It depicted a mid-brown, poorly sorted, slightly silty, very fine to very coarse grained sub-feldsarenite and granule conglomerate composed of angular to sub-angular grains. The sample gave off a moderately strong hydrocarbon odour.

Micro description
Quartz and K feldspar dominate this sample. The quartz grains all display igneous characteristics; vacuole trails and low strain. Orthoclase shows incipient sericite alteration. Microcline and perthite show dissolution to create secondary porosity (Figs.16,17,18). Large masses of sericite and kaolin were probably plagioclase grains. The same alteration is seen in the plagioclase blebs of the perthite grains.

There are a few large chips in the sample. These are mainly single quartz crystals but there are some granite fragments and a few sediment composites. The cements are mainly pore filling kaolin and micritic siderite which recrystallizes to spar. This is seen attached to the framework grains where it causes some corrosion. There are good examples of pore-lining illite followed by pore-filling kaolin.

The finer parts of the sample are largely red-brown drilling mud, rimming chips and gluing small quartz grains and feldspar cleavage fragments to the larger grains.

Composition

50%	Quartz
8%	Orthoclase (and perthite)
5%	Microcline
4%	Plagioclase, completely altered to sericite/kaolin
3%	Muscovite, some kaolin alteration
2%	Biotite, largely altered to chlorite
Cement	
8%	Kaolin, pore filling and replacement
2%	Illite, pore lining
1%	Quartz, minor euhedral terminations
6%	Carbonate, micrite and spar
Other grains	
1%	Organic, pyritic siltstone
10%	Fine fraction
	7% drilling mud
	1% small masses of sericite and kaolin
	1% ground framework grains
	1% pyrite

XRD Analysis
The XRD scan of the unwashed sample (Fig.19) shows quartz to be the dominant mineral with minor microcline. (The height of the peak in this sort of scan is not indicative of the relative proportions of the minerals in the sample) The cements indicated are traces of the clays, dickite and illite, together with calcite and dolomite. Barite is the main contaminant from the drilling mud with some indication of halite.

TABLE 1

GRAIN SIZE ANALYSIS

Sample interval	Average size mm	Average size Ø	Standard deviation	Sand class	Sorting
4530-35m	0.58	0.79	0.85	coarse	moderate
4535-40m	0.53	0.92	1.03	coarse	poor
4540-45m	0.41	1.29	0.78	medium	moderate
4545-50m	0.52	0.94	1.02	coarse	poor

See METHODS for the technique used in measurement

The standard deviation measured is lower than would be expected from a core sample so that all these samples would be expected to be poorly sorted in their natural state.

3.4. CONCLUSIONS

The cuttings samples from all four intervals are very similar. They are all sub-feldsarenites and feldsarenites derived from a granitic source. The quartz grains all show low strain and abundant vacuole trails indicative of a plutonic origin. The feldspar assemblage, dominated by microcline and orthoclase, indicates a granitic source. Perthite grains, K feldspars with exsolved blebs of plagioclase, another plutonic indicator, are common Many of the larger grains are fragments of granite.

There was some contamination of the cuttings samples from overlying sequences. Up to 10% of the chips consisted of silty micrite, organic-rich siltstone and mudstone and glauconitic siltstone.

The sediment in each sample is immature, both texturally and mineralogically. The high feldspar content is the measure of mineralogical immaturity. Grain size analysis showed the average size to be coarse sand but the range from fine sand to granules shows moderate to poor sorting, as indicated by the standard deviation of the size analysis (see Table 1). The standard deviation is likely to be greater and therefore the sorting poorer in reality because the cuttings sample grains do not contain the finest sizes, which are washed away, or the coarsest sizes, which are crushed during drilling. The other indicator of textural maturity, grain roundness, varies from angular to sub-angular, also suggesting low maturity.

Many of the grains show alteration. Average grain size and shape masses of sericite and minor kaolin are probably alteration products of plagioclase. Occasional partially altered plagioclase grains were observed, usually where the plagioclase was part of a composite granitic fragment. The K feldspars, orthoclase and microcline, show incipient alteration to sericite. This gives a dusty brown appearance to the grains in plane polarized light. Some of the microcline grains, in particular, show replacement by kaolin. Some muscovite grains show alteration to kaolin and nearly all of the biotite grains show alteration to chlorite.

The term "sericite" has been used in this report to distinguish between altered feldspar grains and authigenic illite. Sericite was originally defined as fine grained muscovite derived from feldspar alteration. However, muscovite and illite are virtually indistinguishable in XRD scans or in thin section, especially when the mineral is very fine grained.

It is impossible to give any estimate of primary porosity from cuttings samples. If it were present, all the grains would be liberated through that porosity. The few composite sediment grains in each sample show matrix and cement between the framework grains but this is to be expected as something must hold those grains together during drilling and sampling to allow the composite to remain. The fact that many of the grains were splinters and chips rather than whole original grains could be a function of either the coarse original grain size or substantial cementation. The lack of material adhering to the present boundaries of the chips suggests the former and that there may be a reasonable amount of primary porosity in the undisturbed state.

Considerable secondary porosity is evident in the sample chips. This takes the form of feldspar dissolution. Microcline in particular, has been corroded along the cleavage traces to create intraparticle porosity and to enhance primary porosity. Where perthite grains have been corroded, the plagioclase blebs have provided a focus for attack. These grains resemble a "Swiss cheese".

A moderate amount of microporosity is likely to be present in undisturbed samples. This is associated with clay masses such as the alteration and replacement areas of feldspars, and with pore-filling, and to a lesser extent, pore-lining, authigenic clays.

The XRD scans on the washed samples all show quartz as the dominant mineral. Microcline varies from sub-dominant to minor but it must be remembered that relative peak height between minerals is not indicative of relative percentages. Orthoclase is disguised in the scans because most of its peaks are coincident with those of other minerals, especially quartz. The clays present in all samples are illite and dickite. The illite peaks are broad indicating either a range of compositions or as is more likely in this case, interference with muscovite (and sericite) peaks which are virtually coincident and indistinguishable. Dickite, a form of kaolin, shows as sharp peaks. This indicates a high degree of crystallinity, an indicator of authigenic origin. Siderite, dolomite (possibly ferroan) and traces of calcite were noted in the XRD scans. The calcite is probably contamination by silty micrite from overlying sequences but siderite and dolomite were observed as cements. Dolomite spar was seen adhering to framework grains and micritic siderite recrystallized to spar in areas of matrix.

Repeat XRD scans on unwashed samples from the same intervals show the nature of the contamination from drilling mud. Barite is the main contaminant with traces of halite and pyrite. The finely divided pyrite appears to have been released into the mud system from either the matrix of the sandstones or from adjacent silty intervals. There does not appear to be any additional clay in the samples from the mud system. This has implications when considering the amount of matrix in other suites of samples from the same hole, eg., those collected in the junk sub.

A partial sequence of diagenetic events built up from observations in this suite of samples is as follows:-

1. Minor amounts of authigenic quartz overgrowth
2. Some feldspar alteration (plagioclase?)
3. Pore-lining illite
4. Pore-filling dickite
5. Carbonate cement, dolomite and siderite
6. K feldspar dissolution

Stages 2 and 3 may be coincident with some alteration coating the framework feldspar grains prior to dickite precipitation. Stages 5 and 6 may also be coincident with strongly alkaline waters associated with carbonate precipitation being the agent corroding the feldspars.

A moderate to strong smell of hydrocarbons was associated with the unwashed samples. It appears that these are largely contained in the drilling mud, adding to the reddish-brown colour of that material. Some light brown to brown hydrocarbon staining was observed in thin section, usually remaining in the clay associated microporosity and in the finer secondary pore spaces.

6. FIGURES AND CAPTIONS

Figure 1. Anemone #1A, cuttings 4530-35m. (plane polarized light). Crushed grains from the washed sample show quartz as clear grains, orthoclase with dusty sericite alteration (Or), a composite grain of very fine sandstone (Co) and an organic rich siltstone (Z). Two grains of microcline show dissolution to form secondary porosity (2O).

Figure 2. Anemone #1A, cuttings 4530-35m. The same field of view as Fig.1 under crossed polars shows the grain in the centre of the scene to be a mass of sericite after plagioclase.

Figure 3. Anemone #1A, cuttings 4530-35m. (plane polarized light). The unwashed sample shows a dark globular rim of drilling mud adhering to the chips. Secondary dissolution porosity is evident in an altered perthite grain (1) and a heavily corroded microcline (2).

Figure 4. Anemone #1A, cuttings 4530-35m. XRD scan of the washed sample. Quartz (Q) is dominant with minor dickite (D) and microcline (M) and traces of illite (I) and siderite (S).

Figure 5. Anemone #1A, cuttings 4530-35m. XRD scan of the unwashed sample. Quartz (Q), dickite (D), microcline (M), and illite (I) are present as in the washed sample but barite (B) is the main contaminant from the drilling mud together with traces of halite (H) and pyrite (P).

Figure 6. Anemone #1A, cuttings 4535-40m. (Plane polarized light). A composite of sediment grains is cemented by pore-filling kaolin (K). The grains of the composite are quartz (Q) and a granite fragment (G) with a perthite grain in the centre. Some fine sand and clay matrix is attached to the chip in the lower left.

Figure 7. Anemone #1A, cuttings 4535-40m. The same field of view as Fig 6. under crossed polars confirms the kaolinitic nature of the pore filling in the composite grain and suggests that the matrix is illitic.

Figure 8. Anemone #1A, cuttings 4535-40m. XRD scan of the washed sample. Quartz (Q) is the dominant mineral with minor amounts of microcline (M). These are cemented by the clays, dickite (D) and illite (I) and traces of calcite (C).

Figure 9. Anemone #1A, cuttings 4535-40m. XRD scan of the unwashed sample. Contamination by barite (B) with traces of halite (H) and pyrite (P) is superimposed on the minerals in the washed sample, quartz (Q), dickite (D) and illite (I). The dramatic increase in the microcline (M) peak is probably a function of sampling such a coarse sediment. One or two granules of microcline in the small XRD sample appear to have biased the results.

Figure 10. Anemone #1A, cuttings 4540-45m. (Plane polarized light). The splintered chips from this sample show microcline (Mi) dissolving to create secondary porosity, biotite (Bi) altering to chlorite (Ch) and plagioclase in a composite grain altered to a mass of sericite and minor kaolin (Pl-Se). (The circular features are bubbles in the mount).

Figure 11. Anemone #1A, cuttings 4540-45m. The same field of view as Fig.10 under crossed polars confirms the observations made above and shows the rim on the central grain to be micritic carbonate.

Figure 12. Anemone #1A, cuttings 4540-45m. (Plane polarized light). Detail of a chip from this sample shows a composite microcline-orthoclase grain which has been extensively dissolved to create secondary porosity. The edge of the grain is shown in part by the dashed line. Outside that line is a primary pore now lined with illite then filled with kaolin.

Figure 13. Anemone #1A, cuttings 4540-45m. The same field of view as Fig.12 under crossed polars shows the bright yellow to white, pore-lining illite and the mid to dark grey pore-filling kaolin. Some sandy, clayey matrix is attached to one side of the chip.

Figure 14. Anemone #1A, cuttings 4540-45m. XRD scan of the washed sample. Quartz (Q) is the dominant mineral with minor microcline (M). There are traces of the clays, illite (I) and dickite (D).

Figure 15. Anemone #1A, cuttings 4540-45m. XRD scan of the unwashed sample. Contaminants from the drilling mud, barite (B) with traces of halite (H) and pyrite (P), are superimposed on the minerals observed in the clean sample, quartz (Q), microcline (M), illite (I) and dickite (D).

Figure 16. Anemone #1A, cuttings 4545-50m. (Plane polarized light). Chips from this sample show the plagioclase in perthite dissolving to create secondary porosity (2O), orthoclase (Or) with a dusty, incipient sericite alteration and micritic siderite (Si) recrystallizing to sparry scalenohedra. Dark blebs of drilling mud glue small grains of quartz and feldspar and pyrite cubes to the larger chips.

Figure 17. Anemone #1A, cuttings 4545-50m. (Plane polarized light). Detail of a composite grain from this sample shows quartz (Q) filled with vacuole trails. The are minor quartz overgrowths on some grains (arrowed). A biotite grain is partly altered to chlorite (Bi-Ch). A ragged edged microcline grain (Mi) is dusty from minor sericite alteration and shows dissolution around the margins. Any primary porosity is now filled with clays. The dark edge to the whole chip is drilling mud.

Figure 18. Anemone #1A, cuttings 4545-50m. The same field of view as Fig.17 under crossed polars shows the primary porosity to be partially lined by a thin film of illite then filled with kaolin.

Figure 19. Anemone #1A, cuttings 4545-50m. XRD scan of the unwashed sample. Quartz (Q) dominates this sample with minor amounts of microcline (M). Traces amounts of dickite (D), illite (I), calcite (C) and dolomite (D) are seen. Barite is the main contaminant from the drilling mud, with traces of halite (H).

PE906858

This is an enclosure indicator page.
The enclosure PE906858 is enclosed within the container PE906849 at this location in this document.

The enclosure PE906858 has the following characteristics:

ITEM_BARCODE =	PE906858
CONTAINER_BARCODE =	PE906849
NAME =	Core Photomicrograph
BASIN =	GIPPSLAND
PERMIT =	VIC/P20
TYPE =	WELL
SUBTYPE =	PHOTOMICROGRAPH
DESCRIPTION =	Core Photomicrograph, quartz, orthoclase with dusty sericite alteration, (figure 1 from attachment to WCR--Petrographic Analysis Report) for Anemone-1 & 1A
REMARKS =	
DATE_CREATED =	31/12/89
DATE_RECEIVED =	17/01/90
W_NO =	W997
WELL_NAME =	ANEMONE-1 & 1A
CONTRACTOR =	CORE SERVICES OF AUSTRALIA
CLIENT_OP_CO =	PETROFINA EXPLORATION AUSTRALIA S.A.

PE906859

This is an enclosure indicator page.
The enclosure PE906859 is enclosed within the container PE906849 at this location in this document.

The enclosure PE906859 has the following characteristics:

ITEM_BARCODE =	PE906859
CONTAINER_BARCODE =	PE906849
NAME =	Core Photomicrograph
BASIN =	GIPPSLAND
PERMIT =	VIC/P20
TYPE =	WELL
SUBTYPE =	PHOTOMICROGRAPH
DESCRIPTION =	Core Photomicrograph, mass of sericite after plagiclase, (figure 2 from attachment to WCR--Petrographic Analysis Report) for Anemone-1 & 1A
REMARKS =	
DATE_CREATED =	31/12/89
DATE_RECEIVED =	17/01/90
W_NO =	W997
WELL_NAME =	ANEMONE-1 & 1A
CONTRACTOR =	CORE SERVICES OF AUSTRALIA
CLIENT_OP_CO =	PETROFINA EXPLORATION AUSTRALIA S.A.

(Inserted by DNRE - Vic Govt Mines Dept)

PE906860

This is an enclosure indicator page.
The enclosure PE906860 is enclosed within the container PE906849 at this location in this document.

The enclosure PE906860 has the following characteristics:

ITEM_BARCODE =	PE906860
CONTAINER_BARCODE =	PE906849
NAME =	Core Photomicrograph
BASIN =	GIPPSLAND
PERMIT =	VIC/P20
TYPE =	WELL
SUBTYPE =	PHOTOMICROGRAPH
DESCRIPTION =	Core Photomicrograph,globular rim of drilling mud with secondary disslution porosity evident, (figure 3 from attachment to WCR--Petrographic Analysis Report) for Anemone-1 & 1A
REMARKS =	
DATE_CREATED =	31/12/89
DATE_RECEIVED =	17/01/90
W_NO =	W997
WELL_NAME =	ANEMONE-1 & 1A
CONTRACTOR =	CORE SERVICES OF AUSTRALIA
CLIENT_OP_CO =	PETROFINA EXPLORATION AUSTRALIA S.A.

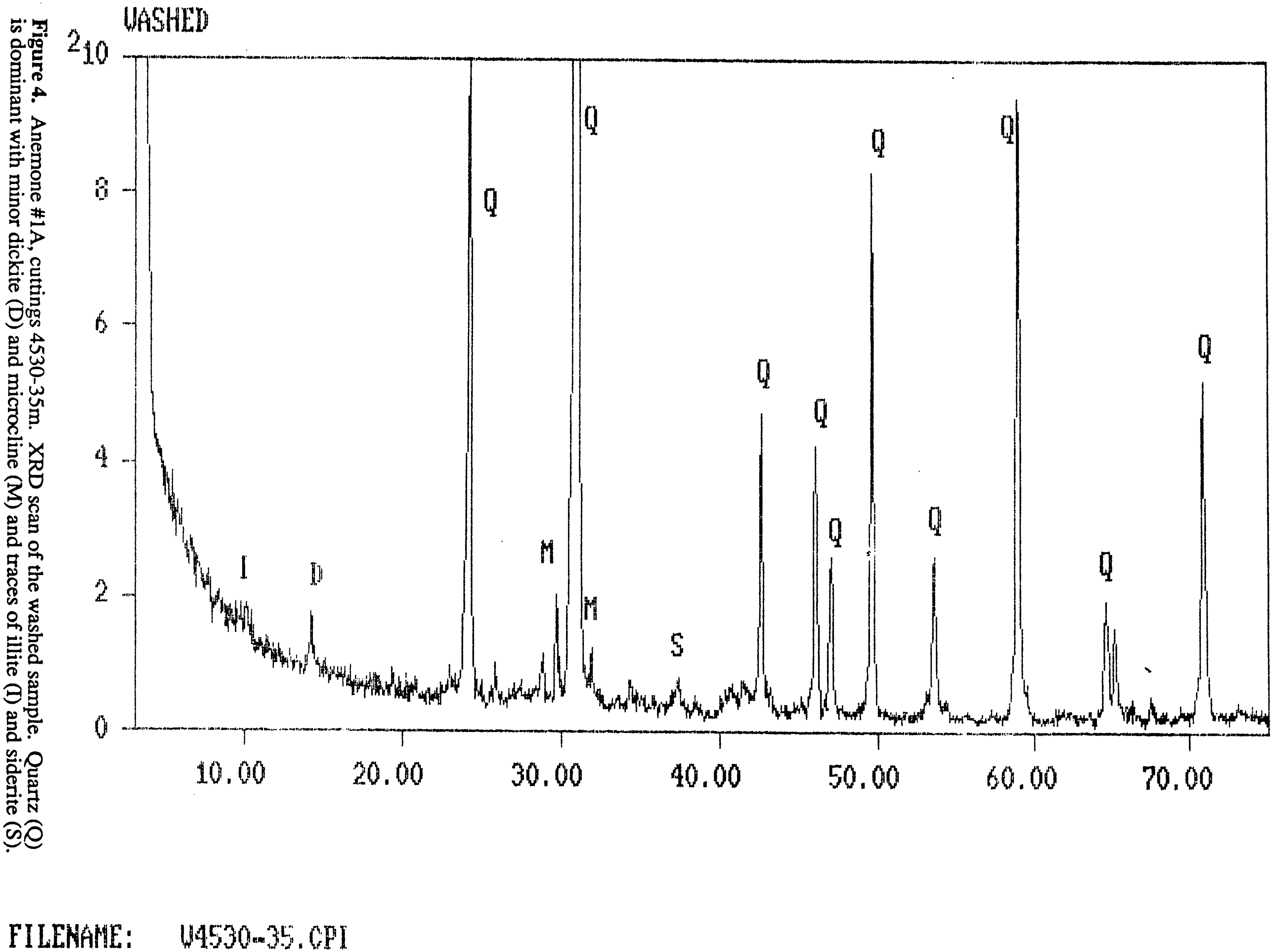

Figure 4. Anemone #1A, cuttings 4530-35m. XRD scan of the washed sample. Quartz (Q) is dominant with minor dickite (D) and microcline (M) and traces of illite (I) and siderite (S).

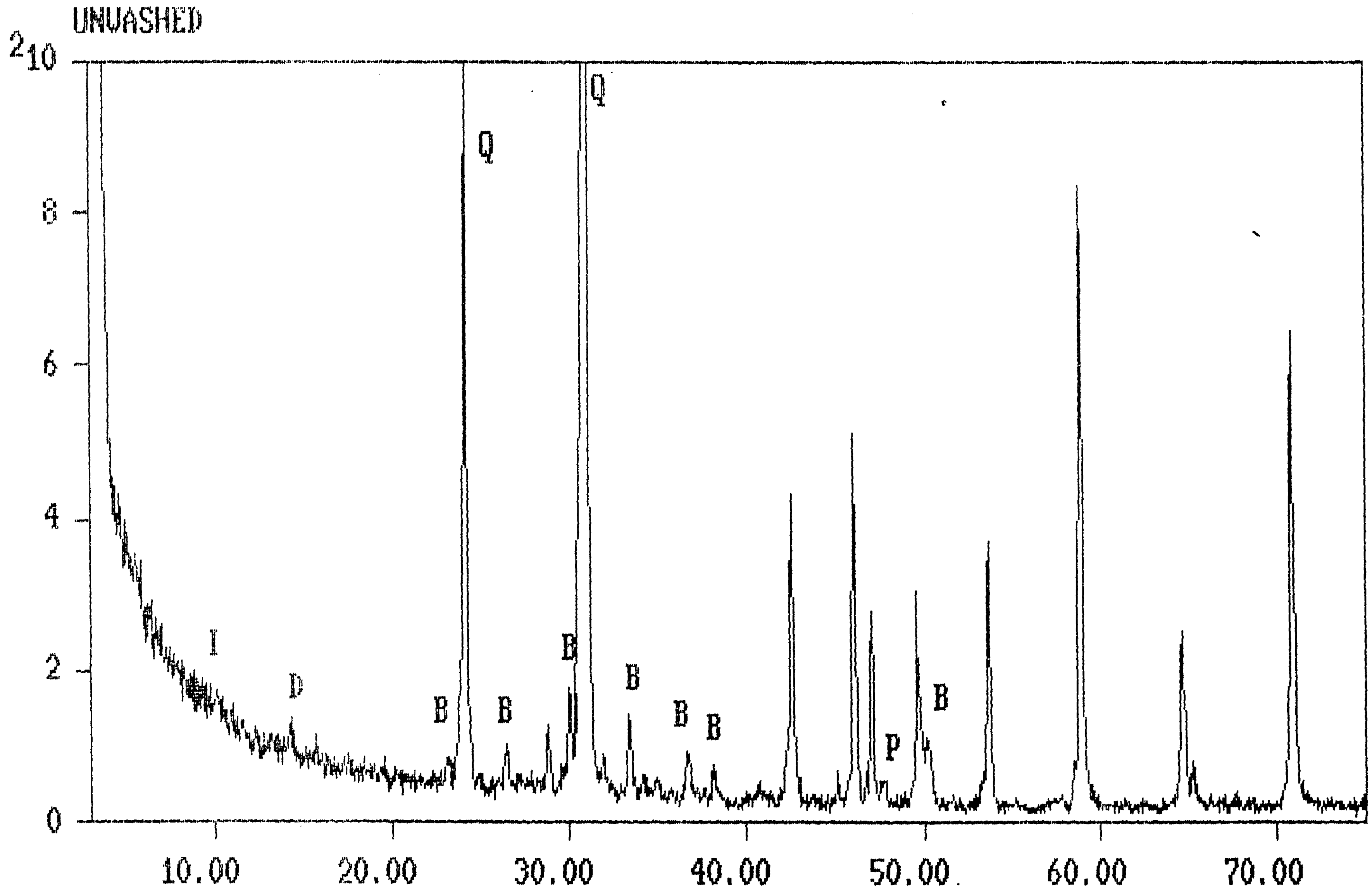

FILENAME: U4530-35.CPI

Figure 5. Anemone #1A, cuttings 4530-35m. XRD scan of the unwashed sample. Quartz (Q), dickite (D), microcline (M), and illite (I) are present as in the washed sample but barite (B) is the main contaminant from the drilling mud together with traces of halite (H) and pyrite (P).

PE906861

This is an enclosure indicator page.
The enclosure PE906861 is enclosed within the container PE906849 at this location in this document.

The enclosure PE906861 has the following characteristics:

ITEM_BARCODE =	PE906861
CONTAINER_BARCODE =	PE906849
NAME =	Core Photomicrograph
BASIN =	GIPPSLAND
PERMIT =	VIC/P20
TYPE =	WELL
SUBTYPE =	PHOTOMICROGRAPH
DESCRIPTION =	Core Photomicrograph, quartz, composite of sediment grains cemented by pore filled kaolin, (figure 6 from attachment to WCR--Petrographic Analysis Report) for Anemone-1 & 1A
REMARKS =	
DATE_CREATED =	31/12/89
DATE_RECEIVED =	17/01/90
W_NO =	W997
WELL_NAME =	ANEMONE-1 & 1A
CONTRACTOR =	CORE SERVICES OF AUSTRALIA
CLIENT_OP_CO =	PETROFINA EXPLORATION AUSTRALIA S.A.

PE906862

This is an enclosure indicator page.
The enclosure PE906862 is enclosed within the container PE906849 at this location in this document.

The enclosure PE906862 has the following characteristics:

ITEM_BARCODE =	PE906862
CONTAINER_BARCODE =	PE906849
NAME =	Core Photomicrograph
BASIN =	GIPPSLAND
PERMIT =	VIC/P20
TYPE =	WELL
SUBTYPE =	PHOTOMICROGRAPH
DESCRIPTION =	Core Photomicrograph, kaolinitic pore filling with illite matrix, (figure 7 from attachment to WCR--Petrographic Analysis Report) for Anemone-1 & 1A
REMARKS =	
DATE_CREATED =	31/12/89
DATE_RECEIVED =	17/01/90
W_NO =	W997
WELL_NAME =	ANEMONE-1 & 1A
CONTRACTOR =	CORE SERVICES OF AUSTRALIA
CLIENT_OP_CO =	PETROFINA EXPLORATION AUSTRALIA S.A.

(Inserted by DNRE - Vic Govt Mines Dept)

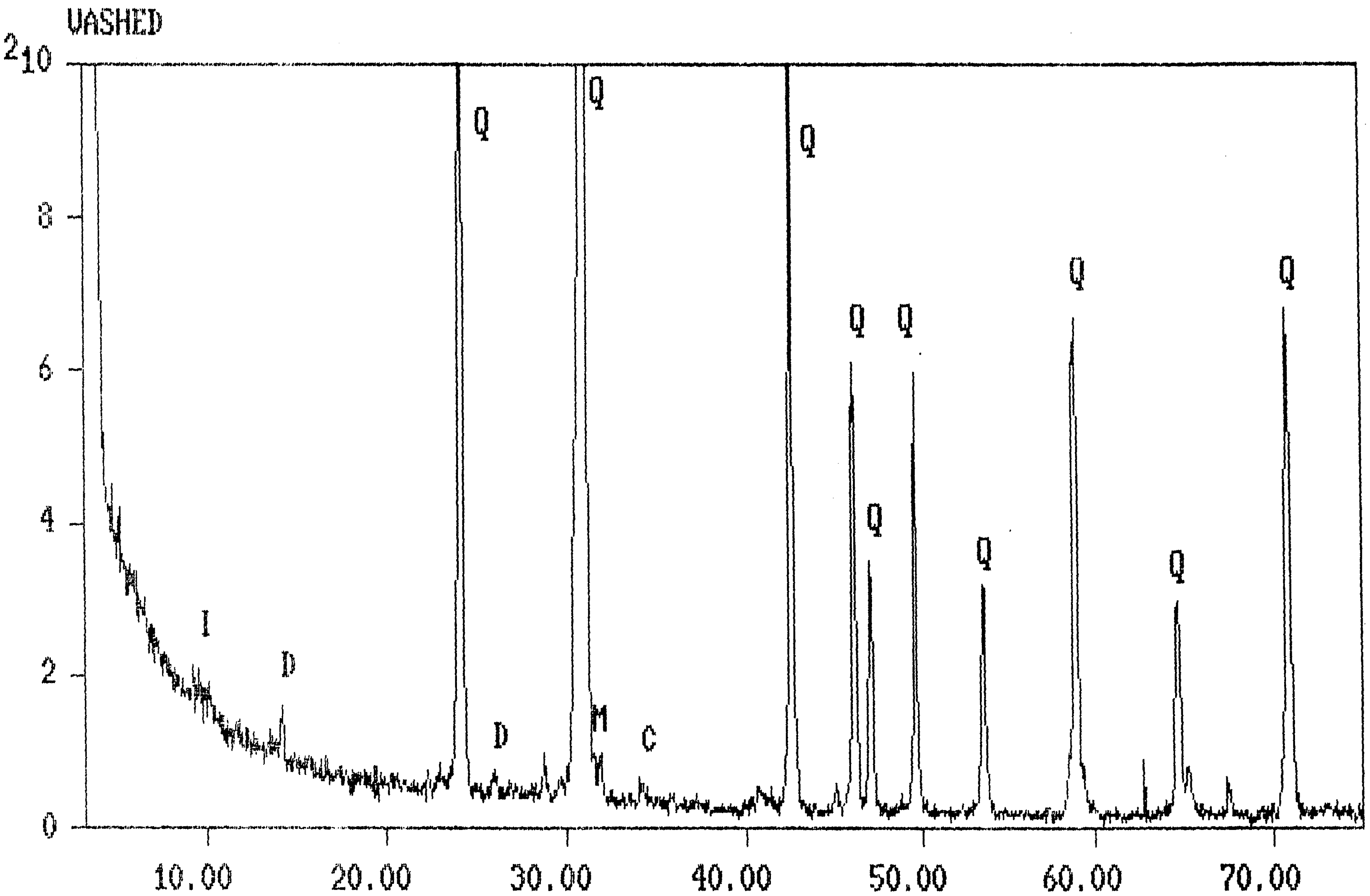

Figure 8. Anemone #1A, cuttings 4535-40m. XRD scan of the washed sample. Quartz (Q) is the dominant mineral with minor amounts of microcline (M). These are cemented by the clays, dickite (D) and illite (I) and traces of calcite (C).

FILENAME: V4535-40.CPI

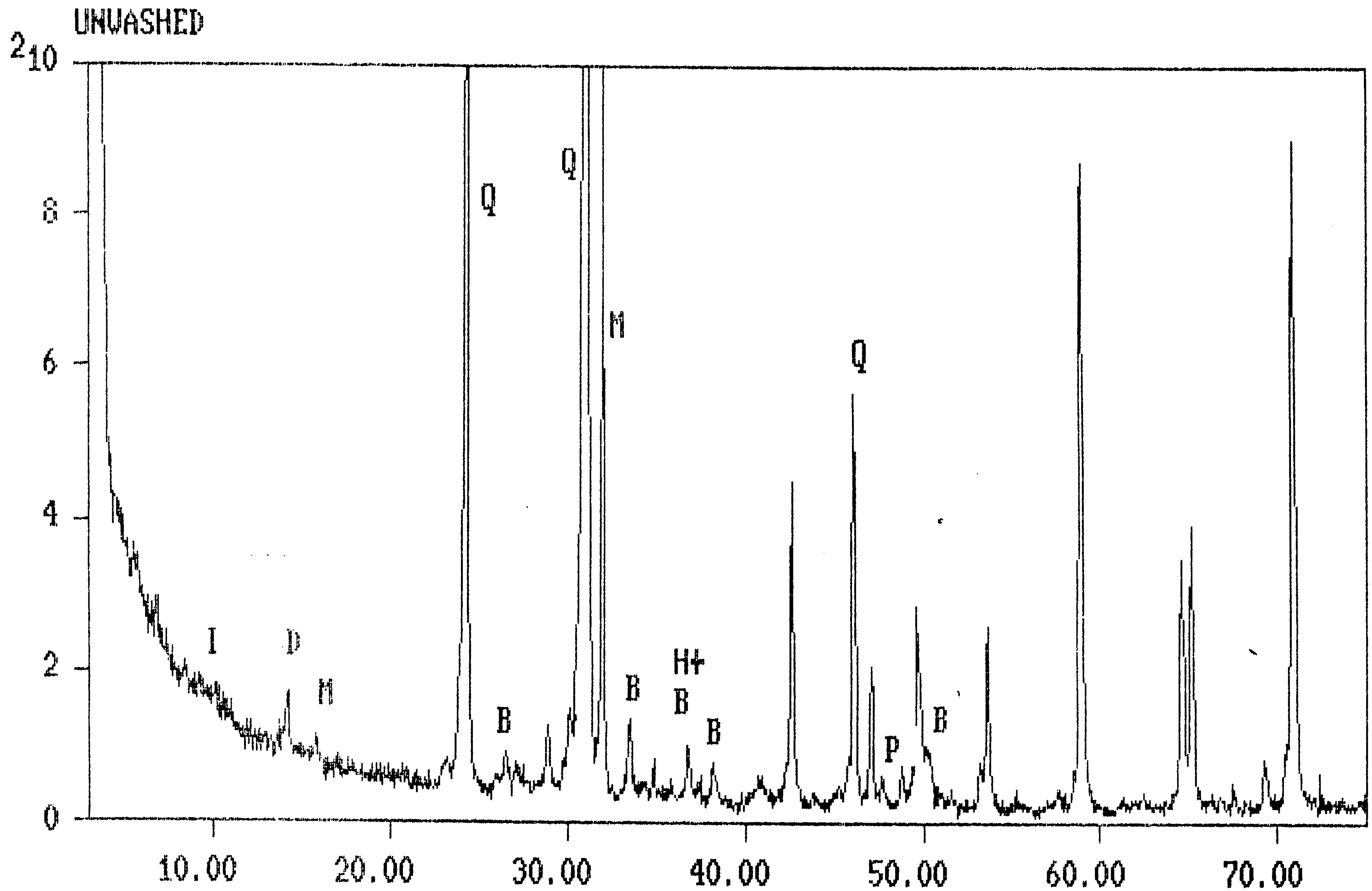

FILENAME: U4535-40.CPI

Figure 9. Anemone #1A, cuttings 4535-40m. XRD scan of the unwashed sample. Contamination by barite (B) with traces of halite (H) and pyrite (P) is superimposed on the minerals in the washed sample, quartz (Q), dickite (D) and illite (I). The dramatic increase in the microcline (M) peak is probably a function of sampling such a coarse sediment. One or two granules of microcline in the small XRD sample appear to have biased the results.

PE906863

This is an enclosure indicator page.
The enclosure PE906863 is enclosed within the container PE906849 at this location in this document.

The enclosure PE906863 has the following characteristics:

ITEM_BARCODE =	PE906863
CONTAINER_BARCODE =	PE906849
NAME =	Core Photomicrograph
BASIN =	GIPPSLAND
PERMIT =	VIC/P20
TYPE =	WELL
SUBTYPE =	PHOTOMICROGRAPH
DESCRIPTION =	Core Photomicrograph, microline dissolving to create secondary porosity, biotite altering to chlorite and plagioclase to sericite and kaolin, (figure 10 from attachment to WCR--Petrographic Analysis Report) for Anemone-1 & 1A
REMARKS =	
DATE_CREATED =	31/12/89
DATE_RECEIVED =	17/01/90
W_NO =	W997
WELL_NAME =	ANEMONE-1 & 1A
CONTRACTOR =	CORE SERVICES OF AUSTRALIA
CLIENT_OP_CO =	PETROFINA EXPLORATION AUSTRALIA S.A.

(Inserted by DNRE - Vic Govt Mines Dept)

PE906864

This is an enclosure indicator page.
The enclosure PE906864 is enclosed within the container PE906849 at this location in this document.

The enclosure PE906864 has the following characteristics:

ITEM_BARCODE =	PE906864
CONTAINER_BARCODE =	PE906849
NAME =	Core Photomicrograph
BASIN =	GIPPSLAND
PERMIT =	VIC/P20
TYPE =	WELL
SUBTYPE =	PHOTOMICROGRAPH
DESCRIPTION =	Core Photomicrograph, micritic carbonate around grain rim, (figure 11 from attachment to WCR--Petrographic Analysis Report) for Anemone-1 & 1A
REMARKS =	
DATE_CREATED =	31/12/89
DATE_RECEIVED =	17/01/90
W_NO =	W997
WELL_NAME =	ANEMONE-1 & 1A
CONTRACTOR =	CORE SERVICES OF AUSTRALIA
CLIENT_OP_CO =	PETROFINA EXPLORATION AUSTRALIA S.A.

(Inserted by DNRE - Vic Govt Mines Dept)

PE906865

This is an enclosure indicator page.
The enclosure PE906865 is enclosed within the container PE906849 at this location in this document.

The enclosure PE906865 has the following characteristics:

ITEM_BARCODE =	PE906865
CONTAINER_BARCODE =	PE906849
NAME =	Core Photomicrograph
BASIN =	GIPPSLAND
PERMIT =	VIC/P20
TYPE =	WELL
SUBTYPE =	PHOTOMICROGRAPH
DESCRIPTION =	Core Photomicrograph, composite microline-orthoclase grain which has been dissolved to create secondary porosity, (figure 12 from attachment to WCR--Petrographic Analysis Report) for Anemone-1 & 1A
REMARKS =	
DATE_CREATED =	31/12/89
DATE_RECEIVED =	17/01/90
W_NO =	W997
WELL_NAME =	ANEMONE-1 & 1A
CONTRACTOR =	CORE SERVICES OF AUSTRALIA
CLIENT_OP_CO =	PETROFINA EXPLORATION AUSTRALIA S.A.

PE906866

This is an enclosure indicator page.
The enclosure PE906866 is enclosed within the container PE906849 at this location in this document.

The enclosure PE906866 has the following characteristics:

ITEM_BARCODE =	PE906866
CONTAINER_BARCODE =	PE906849
NAME =	Core Photomicrograph
BASIN =	GIPPSLAND
PERMIT =	VIC/P20
TYPE =	WELL
SUBTYPE =	PHOTOMICROGRAPH
DESCRIPTION =	Core Photomicrograph, bright yellow pore lining illite and dark pore filling kaolin, (figure 13 from attachment to WCR--Petrographic Analysis Report) for Anemone-1 & 1A
REMARKS =	
DATE_CREATED =	31/12/89
DATE_RECEIVED =	17/01/90
W_NO =	W997
WELL_NAME =	ANEMONE-1 & 1A
CONTRACTOR =	CORE SERVICES OF AUSTRALIA
CLIENT_OP_CO =	PETROFINA EXPLORATION AUSTRALIA S.A.

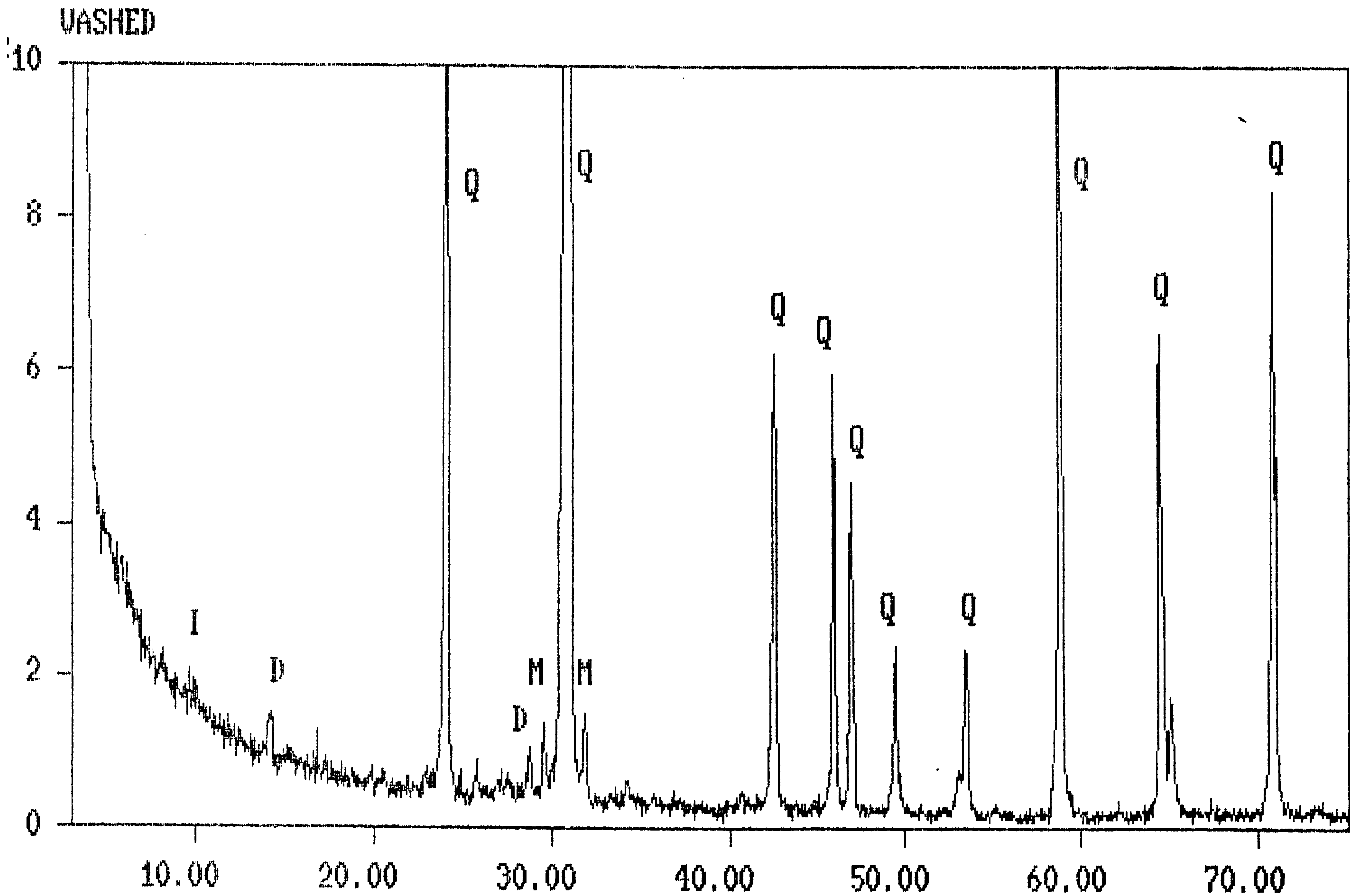

Figure 14. Anemone #1A, cuttings 4540-45m. XRD scan of the washed sample. Quartz (Q) is the dominant mineral with minor microcline (M). There are traces of the clays, illite (I) and dickite (D).

FILENAME: W4540-45.CPI

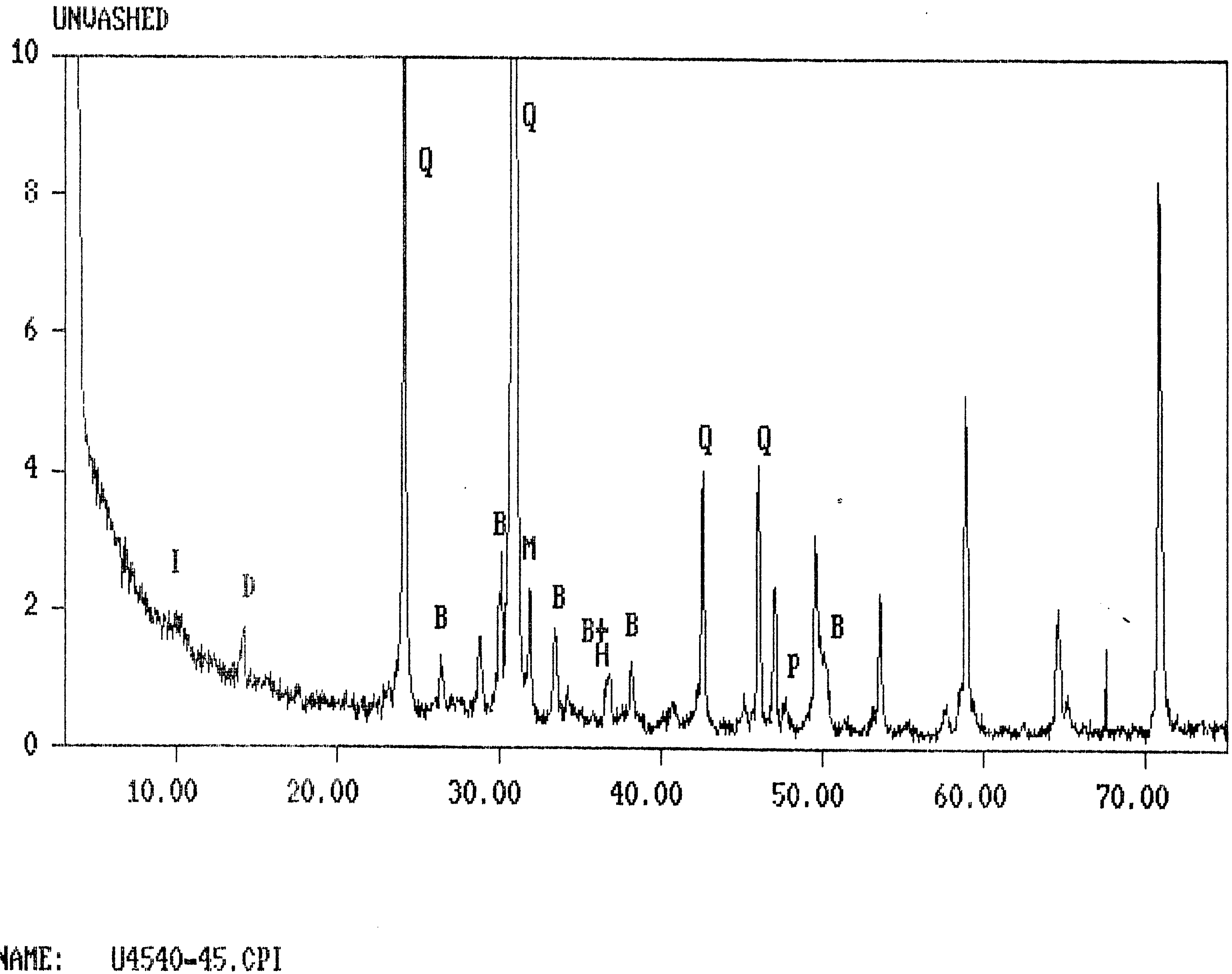

Figure 15. Anemone #1A, cuttings 4540-45m. XRD scan of the unwashed sample. Contaminants from the drilling mud, barite (B) with traces of halite (H) and pyrite (P), are superimposed on the minerals observed in the clean sample, quartz (Q), microcline (M), illite (I) and dickite (D).

PE906867

This is an enclosure indicator page.
The enclosure PE906867 is enclosed within the container PE906849 at this location in this document.

The enclosure PE906867 has the following characteristics:

ITEM_BARCODE =	PE906867
CONTAINER_BARCODE =	PE906849
NAME =	Core Photomicrograph
BASIN =	GIPPSLAND
PERMIT =	VIC/P20
TYPE =	WELL
SUBTYPE =	PHOTOMICROGRAPH
DESCRIPTION =	Core Photomicrograph, plagioclase in perthite creates secondary porosity, orthoclase with sericite alteration and micritic siderite recrystallizing to sparry scalenohedra, (figure 16 from attachment to WCR--Petrographic Analysis Report) for Anemone-1 & 1A
REMARKS =	
DATE_CREATED =	31/12/89
DATE_RECEIVED =	17/01/90
W_NO =	W997
WELL_NAME =	ANEMONE-1 & 1A
CONTRACTOR =	CORE SERVICES OF AUSTRALIA

PE906868

This is an enclosure indicator page.
The enclosure PE906868 is enclosed within the container PE906849 at this location in this document.

The enclosure PE906868 has the following characteristics:

ITEM_BARCODE =	PE906868
CONTAINER_BARCODE =	PE906849
NAME =	Core Photomicrograph
BASIN =	GIPPSLAND
PERMIT =	VIC/P20
TYPE =	WELL
SUBTYPE =	PHOTOMICROGRAPH
DESCRIPTION =	Core Photomicrograph, quartz filled with vacuole trails, (figure 17 from attachment to WCR--Petrographic Analysis Report) for Anemone-1 & 1A
REMARKS =	
DATE_CREATED =	31/12/89
DATE_RECEIVED =	17/01/90
W_NO =	W997
WELL_NAME =	ANEMONE-1 & 1A
CONTRACTOR =	CORE SERVICES OF AUSTRALIA
CLIENT_OP_CO =	PETROFINA EXPLORATION AUSTRALIA S.A.

(Inserted by DNRE - Vic Govt Mines Dept)

PE906869

This is an enclosure indicator page.
The enclosure PE906869 is enclosed within the container PE906849 at this location in this document.

The enclosure PE906869 has the following characteristics:

ITEM_BARCODE = PE906869
CONTAINER_BARCODE = PE906849
NAME = Core Photomicrograph
BASIN = GIPPSLAND
PERMIT = VIC/P20
TYPE = WELL
SUBTYPE = PHOTOMICROGRAPH
DESCRIPTION = Core Photomicrograph, primary porosity lined by a thin film of illite then filled with kaolin, (figure 18 from attachment to WCR--Petrographic Analysis Report) for Anemone-1 & 1A
REMARKS =
DATE_CREATED = 31/12/89
DATE_RECEIVED = 17/01/90
W_NO = W997
WELL_NAME = ANEMONE-1 & 1A
CONTRACTOR = CORE SERVICES OF AUSTRALIA
CLIENT_OP_CO = PETROFINA EXPLORATION AUSTRALIA S.A.

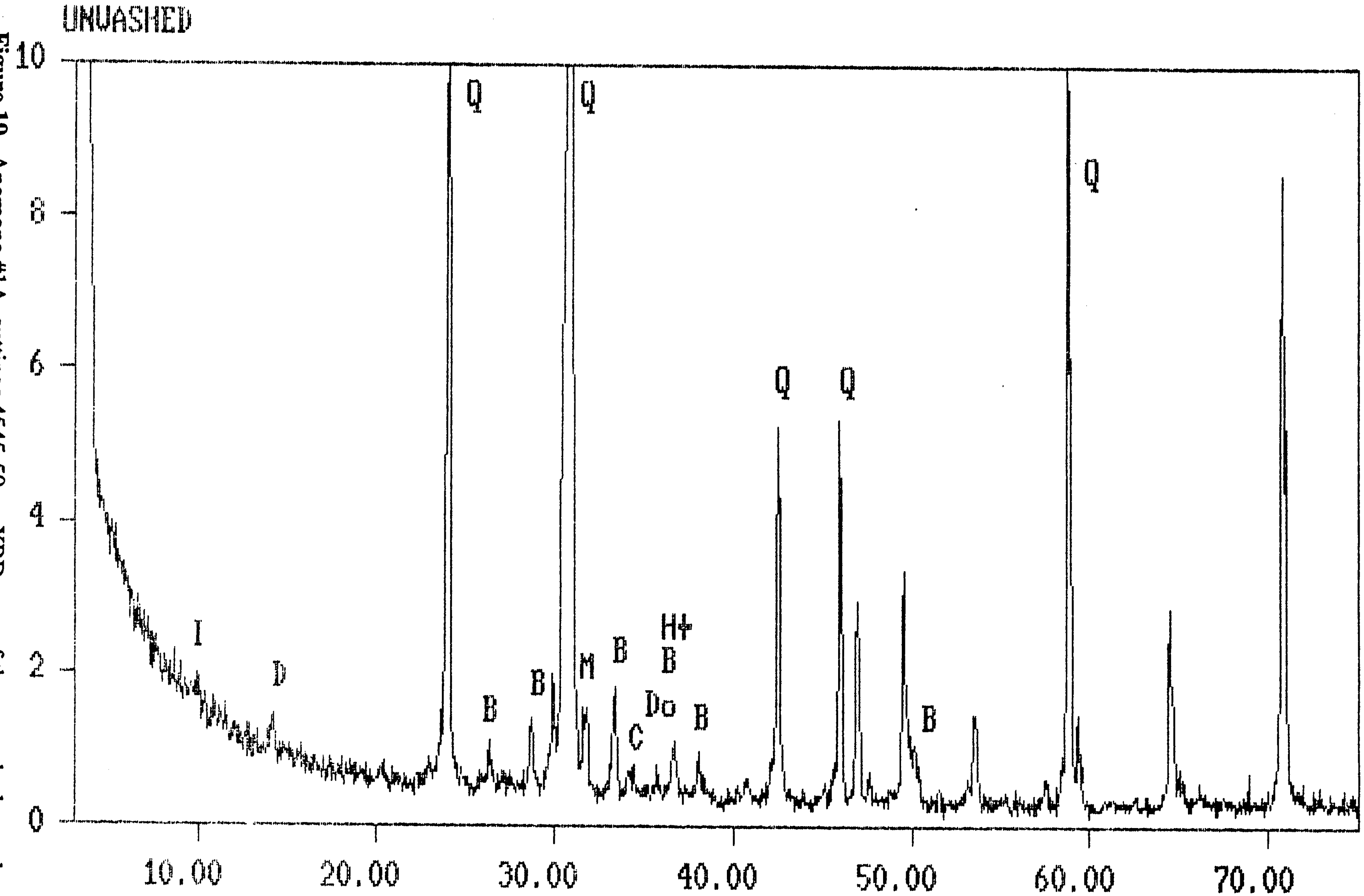

FILENAME: U4545-50.CPI

Figure 19. Anemone #1A, cuttings 4545-50m. XRD scan of the unwashed sample. Quartz (Q) dominates this sample with minor amounts of microcline (M). Traces amounts of dickite (D), illite (I), calcite (C) and dolomite (D) are seen. Barite is the main contaminant from the drilling mud, with traces of halite (H).

4. APPENDIX III

ANEMONE #1A, Junk sub samples

INDEX

4.1. INTRODUCTION

This report contains petrographic descriptions of 7 junk sub samples from Anemone #1A well in the Gippsland Basin. Samples were forwarded by Petrofina Exploration Australia S.A. Bulk X-ray diffraction was used to investigate mineralogy, particularly of clays. The three lighter coloured, more porous samples were studied using scanning electron microscopy.

The samples analysed were:

JS4575m
JS4676a m
JS4676b m
JS4676c m
JS4676d m
JS4676e m
JS4676f m

4.2. METHODS

All samples were briefly described in hand specimen. Part of each sample was then impregnated with blue-dyed araldite before thin section preparation in order to describe porosity and permeability. Thin sections were scanned to determine lithology, composition, porosity and textural relationships, then photographed. Composition was determined for each sample by counting 300 points.

To determine bulk mineralogy by X-ray diffraction, sub-samples were hand-ground in acetone then prepared as oriented smears. This technique is necessary to recognize and distinguish detrital and authigenic clays in such small samples. Smears were run from 3 to 75 degrees 2 theta, at 1 degree/minute, using Co $K\alpha$ radiation, 50kV and 35mA, on a Philips PW1050 diffractometer.

Sub-samples of the three more porous, lighter coloured rocks (JS4676c, JS4676d and JS4676f) were mounted in araldite on aluminium pin-type stubs for scanning electron microscopy. They were evaporatively coated with carbon (15nm) and gold/palladium (20nm) prior to viewing in a Philips 505 at 20kV. Double coatings were used to bind friable sediment on the fresh surfaces to be viewed. The elemental composition of each mineral photographed was identified using a Tracor Northern (TN 5500) energy dispersive spectrometer.

4.3. PETROGRAPHIC DESCRIPTIONS

4.3.1 Anemone #1A, junk sub sample, 4575 metres

Macro description
A moderately well sorted, coarse to very coarse grained sub-feldsarenite. This specimen appears to be more quartz rich than those from 4676 m. Many of the feldspars display alteration features, giving an opaque white colour to the grains. The specimen is not reactive to 10% HCl and shows only moderate porosity.

Micro description
This sample consists of well-cemented, moderately sorted, angular, low sphericity granules in an illitic matrix. Grain size ranges from silt-4 mm, averaging 2.5 mm.

Primary porosity has been reduced by compaction and quartz overgrowth. Grain contacts are straight to slightly sutured as a result. Euhedral quartz overgrowths are evident, terminating in clean pores. Porosity is mainly secondary, due to dissolution of feldspars (especially perthitic Kspar) and quartz (Figs. 1,2). Some fractures remain unhealed to give secondary porosity, or have encouraged dissolution along them (Fig. 3). Clay may have microporosity associated but this is not obvious.

Cementation is afforded by quartz overgrowth, illite and traces of carbonate spar and pyrite. Sericite replaces some grains, following feldspar cleavage. Figure 4 shows sericitic grain replacement. The matrix illite is largely detrital.

The framework consists of quartzose and quartzo-feldspathic rock fragments and single grains of quartz, microcline, perthite and muscovite (Fig. 5). Traces of organic matter occur in the matrix. All feldspars are highly altered. Quartz displays polycrystalline forms, fracturing, dissolution, abundant vacuole trails, slightly undulose extinction, inclusions and rare striations. Euhedral quartz growth is illustrated in Figures 6 and 7.

Quartz characteristics and granule mineralogy indicate a granitic provenance.

X-ray diffraction
As shown in Figure 8, this sample is dominated by quartz. A broad clay peak indicates traces of illite, possibly interstratified with other clays. Detrital illite (2M2) was detected.

4.3.2 Anemone #1A, junk sub sample, 4676a metres

Macro description
A grey, very poorly sorted, matrix-supported, very coarse sub-feldsarenite and granule conglomerate which is very well cemented. Most grains are angular to subangular.

The 2-5 mm granules are largely composed of K feldspars, some showing simple twinning and all displaying cleavage steps on broken faces. Most of these grains are milky white to clear with some grains showing yellow alteration. The dark grey matrix of silt and very fine sand is micaceous.

There is no reaction to dilute HCl and the sample displays negligible porosity.

The sample is of a quite immature sediment, texturally and mineralogically, and could well be described as a diamictite, probably derived from a nearby granitic source. There is no fabric in the rock and it is difficult to see that it is a sediment.

Micro description
A poorly sorted sub-feldsarenite and conglomerate with angular, low sphericity granules floating in a poorly laminated, clay-rich matrix. Grain size distribution is bimodal, with clast size ranging from silt to 4 mm and averaging 2 mm. Grain contacts range from floating to moderately sutured with stylolitic accumulations of organics and pyrite Fig. 9).

Secondary porosity has developed through dissolution of K feldspar. Dissolution tends to be along cleavage traces or of the plagioclase component of perthite. Fracture porosity is rare. Microporosity may be associated with clay but blue dye uptake is rarely observed.

Illite, grading to muscovite, is abundant through the matrix. Sericite partially or totally replaces feldspars (Fig. 10). The kaolin form, dickite, has reduced porosity by infilling fractures with booklets and partial replacement of K feldspar. One fracture shows clay zoning, with dickite at the edges and a core of illite. Interstitial lime-green chlorite is rare.

Clays, microspar, micrite and pyrite act as cements (Figs. 11,12).

Quartz and quartzo-feldspathic rock fragments are common. Quartz displays undulose extinction (rarely moderately strained), inclusions and abundant vacuoles. Microcline and perthites are common and moderately to severely altered (Fig. 13). Totally replaced laths in fragments are probably plagioclase. Organics, including wood fragments, concentrate in laminae, aggregates or stylolites at grain boundaries. Under reflected light, some organics are white and others are brown to black. Some bitumen staining is evident. Pyrite coexists with organics and can only be clearly distinguished under reflected light. It occurs as finely disseminated crystals, aggregates or framboids and rarely occurs in fractures or mineral cleavage. Muscovite is common in the matrix and intergrown with chlorite, sometimes hosting spar along cleavage (Fig. 14). Carbonate occurs as subhedral to euhedral scalenohedra or micritic masses and is often associated with organics. Detrital heavy minerals are rare.

Quartz and rock fragment characteristics such as inclusions and straight internal crystal boundaries, suggest a granitic source terrain.

X-ray diffraction
Figure 15 shows that quartz is dominant, though less so than in most other samples. Microcline and pyrite are minor constituents. Minor illite/muscovite has a broad peak, suggesting a detrital origin or random interstratification with material such as chlorite. Some illite is of 2M form, reflecting its detrital origin. A sharp peak indicates that highly crystalline dickite is a minor component. Traces of siderite, ankerite and calcite occur. A continuum of compositions between these end-members is evidenced by fluctuations in the carbonate spectrum. The calcite peak represents a Ca:Mg composition of 80:20. Carbon produces an elevated background effect.

4.3.3 Anemone #1A, junk sub sample, 4676b metres

Macro description
A light grey, poorly sorted, fine to very coarse sub-feldsarenite with some granules. Most grains are angular to subangular. Most of the feldspars are milky white to clear with about 30% of

them white and altered, some completely altered to clay. Porosity is very low. There is no reaction with 10% HCl. No bedding is visible.

Micro description
A poorly sorted sub-feldsarenite with subangular to angular clasts in an illite-rich matrix. Smaller grains tend to be more angular. Grain size ranges from silt to 5 mm. Grain contacts are tangential to slightly sutured.

Secondary porosity has developed by dissolution of feldspars, particularly microcline and perthite (Fig. 16). Dissolution follows cleavage or replaces presumably more sodic blebs. Fracture porosity is rare and microporosity is not obviously abundant.

Illite is abundant in the matrix (Fig. 17). Sericite follows feldspar cleavage and authigenic illite coats grains. The kaolin form, dickite, has developed in patches along cleavage and fractures in K feldspar.

Cementing agents are clays, carbonate microspar and pyrite.

The framework grains are dominantly quartz and quartzo-feldspathic rock fragments. Quartz displays vacuole trails, needle inclusions, undulose extinction and fractures. Polycrystalline grains are common and a few grains are moderately strained. Fragments occasionally contain inclusions and have relatively straight internal boundaries. Feldspars are highly altered and dominated by microcline and perthite. Bent muscovite is intergrown with chlorite and contains fine pyrite in the cleavage. Pyrite has grown as scattered crystals or aggregates within various fragments and in the matrix. Organics of various types frequently coexist with pyrite in the matrix and along sutured grain boundaries. Detrital heavy minerals are rare. Euhedral scalenohedra of microspar tend to be concentrated in the matrix, associated with organic matter, and in micaceous cleavage (Figs. 18,19).

Quartz and rock fragment characteristics suggest a granitic sediment source.

X-ray diffraction
Figure 20 reveals that quartz is dominant and microcline subdominant. Illite is a minor component and may be interstratified with other clays such as chlorite, resulting in a broad peak. The 2M1 illite is detrital. Dickite is a trace component, with the sharp peak reflecting high crystallinity. Pyrite, siderite and ankerite were detected in trace amounts. A continuum of carbonate compositions, from ankerite to siderite, exists. Carbon gives an elevated background effect.

4.3.4 Anemone #1A, junk sub sample, 4676c metres

Macro description
A pale greenish-grey, very poorly sorted, medium to very coarse sub-feldsarenite and granule conglomerate. Quartz dominates the sample. Weak bedding is outlined by flaky biotite accumulations. The larger feldspar grains are clear to milky white and many granules are composites of quartz and feldspar. Most of the smaller feldspar grains are opaque white, indicating some form of alteration. The sample shows moderate porosity. There is no reaction to 10% HCl.

Micro description
This conglomeratic sub-feldsarenite consists of poorly sorted, angular, low sphericity clasts in an illite-rich matrix. Grain size ranges from silt to 6 mm, averaging 1.5 mm. Grain contacts are tangential to slightly sutured and rarely straight.

Porosity is good at 10.3%. Secondary porosity is associated with varying degrees of K feldspar dissolution and fracturing (Fig. 21). Microporosity in clays and matrix is 2.3%. Any primary porosity which may have existed has been destroyed by compaction, evidenced by tangential to stylolitic grain boundaries.

Dickite has infilled some fractures and replaced grains. Sericite occurs as a grain replacement and illite is abundant in the matrix. Grain replacement is illustrated in Figure 22.

Cementation is afforded by microspar, micrite, clay and rare quartz overgrowths.

Framework grains consist mainly of quartz, K feldspar and quartzo-feldspathic rock fragments. Quartz displays fracturing, vacuoles, undulose extinction, inclusions and rare euhedral and anhedral overgrowths. The latter show corrosion by clays. Feldspars show considerable alteration, leaving remnants of microcline, perthites and orthoclase. Muscovite is common and seen altering to chlorite. Pyrite, organics and heavy minerals are scattered, and highlight sutured boundaries between grains (Figs. 23,24). Subhedral microspar scalenohedra and micrite cause mild to severe corrosion and totally replace some grains.

A granitic source terrain is evident from quartz and rock fragment character (Fig. 25).

X-ray diffraction
Quartz is dominant and microcline subdominant, as shown in Figure 26. Highly crystalline dickite (2M1) is minor. A broad illite peak, including detrital illite (2M2), indicates random interstratification of this minor component with other material. Traces of siderite and pyrite were detected, and there is a suggestion of the presence of ankerite and calcite. The fluctuating spectrum reflects a range of carbonate compositions. A background effect is produced by carbon.

Scanning electron microscopy
The sample is clay rich and displays very low porosity (Fig. 27), which is largely due to secondary dissolution of feldspars along preferred crystallographic axes (Figs. 28,29) and microporosity associated with some clays. An abundance of small barite spheres is evidence of drilling mud infiltration. Authigenic illite (Figs. 30,31) and patchy kaolin (Figs. 32,33) are common in the matrix and often mixed. Grain alteration is occasionally evident, such as alteration of K feldspar to patchy kaolin. Figures 34 and 35 record unaltered K feldspar. Euhedral quartz overgrowths (Fig. 36) have further reduced porosity, and are rarely intergrown

with kaolin (Fig. 37). Illite presence apparently retards overgrowth development. Siderite scalenohedra and rhombohedra are rare, and were seen intergrown with mica (Figs. 38,39).

4.3.5 Anemone #1A, junk sub sample, 4676d metres

Macro description
A pale brownish grey, moderately sorted fine to coarse grained sub-feldsarenite. Weak bedding is shown by the alignment of biotite and some muscovite. Quartz and feldspar are the main components of the rock. Most of the feldspars are opaque white, indicating some form of alteration. Porosity is poor and there is no reaction with 10% HCl.

Micro description
A moderately to poorly sorted sub-feldsarenite with angular to subangular grains and a few granules in a clay matrix. Grain size ranges from silt to 2 mm and averages 0.4 mm.

The good porosity (10.3%) is mainly due to K feldspar dissolution, with minor fracture porosity and microporosity (Fig. 40). A large area in the centre of the thin section shows excellent porosity, but this is due to slide preparation, as evidenced by fractured and floating grains.

Porosity has been reduced by grain-coating illite and pore-filling dickite, clearly shown in Figure 41. Dickite and illite replace grains to various degrees and illite is common in the matrix (Fig. 42). Compaction and quartz overgrowth have reduced porosity, resulting in straight to slightly sutured grain contacts.

Cementing agents are clay, carbonate, quartz and pyrite.

Most framework grains are quartz, commonly in rock fragments. Altered perthite, microcline and orthoclase are subdominant. Quartz is fractured, with undulose extinction and abundant vacuoles. Quartz cements of two types occur: unaltered overgrowths (Fig. 43) and corroded anhedral grains. The latter may not be first cycle sedimentary, having possibly been inherited from an earlier sediment. Muscovite is common, intermixed with minor chlorite. Pyrite, organics and heavy minerals are scattered throughout. Carbonate occurs as micritic aggregates, subhedral microspar scalenohedra and anhedral, subrounded spar. It is common in the matrix, causes mild to extreme corrosion and replaces some grains. Rock fragments are mainly quartzo-feldspathic but very rare chert and sandy micritic clasts occur.

The source terrain is mainly granitic with minor input of cherty preconsolidated sediment.

X-ray diffraction
The most common mineral is quartz, which is less dominant than in most other samples (Fig. 44). Microcline, siderite and highly crystalline dickite are minor components. Detrital illite (2M2) is minor and apparently mixed with randomly interstratified material such as chlorite. Traces of pyrite and ankerite occur. Background carbon and a range of carbonate compositions are likely.

Scanning electron microscopy
This sample has abundant clay and fair porosity of hybrid primary-secondary origin (Fig. 45). Oversized pores may have resulted from plucking during sample preparation or dissolution. Secondary dissolution and microporosity exist. Authigenic illite bridges pore throats, creating

permeability barriers to fluid flow (Figs. 46,47). Kaolin was observed replacing K feldspar. Illite and kaolin are often mixed (Figs. 48,49). Euhedral quartz overgrowths are common and may display intergrowth with kaolin (Fig. 50) or pyrite. Figure 51 shows intergrowth of quartz and pyrite, with the latter displaying two phases of growth represented by different crystal sizes. Euhedral authigenic anatase (Fig. 52) probably precipitated during alteration from Ti-rich biotite to muscovite. Subrounded detrital apatite was identified (Fig. 53).

4.3.6 Anemone #1A, junk sub sample, 4676e metres

Macro description
A pale grey, very poorly sorted, very fine to very coarse feldsarenite and granule conglomerate. Feldspar and quartz appear in equal proprtions and dominate the specimen. The granules are quartz and quartz-feldspar composites. Many of the sand-sized feldspar grains are opaque white indicating some alteration. The sample exhibits moderate porosity but is not reactive to 10% HCl.

Micro description
A poorly sorted feldsarenite and granule conglomerate with angular, low sphericity clasts in an illitic matrix. Grain size ranges from silt to 8 mm, and averages 0.5 mm.

Fair porosity (9.6%) results from dissolution, fracturing and micropores (Figs. 54,55,56) Primary porosity has been almost totally sealed by compaction and quartz overgrowth. These processes have produced straight to slightly sutured boundaries. One example of euhedral quartz overgrowth into a clean pore was seen.

Illite and pore-filling dickite have further reduced porosity. Illite is common in the matrix and sericite replaces K feldspar. Large patches of dickite suggest grain replacement. Grain replacement is demonstrated in Figure 57.

Apart from the clays, carbonate, quartz and pyrite act as cements.

The framework consists of quartz, granitic fragments, K feldspar, muscovite (altering to chlorite), organic matter and rare heavy minerals. Quartz displays fractures, vacuoles and rare dust rims and overgrowths. Some overgrowths are euhedral and others anhedral and corroded. One grain with two sets of overgrowths was seen. K feldspar includes highly altered perthite, microcline and orthoclase. Fine crystals of pyrite are widespread. Carbonate microspar and euhedral scalenohedra concentrations occur, possibly replacing sedimentary clasts.

Rock fragments and quartzose characteristics imply a dominantly granitic provenance with minor input from strained and sedimentary rocks.

X-ray diffraction
Figure 58 demonstrates that quartz is dominant and microcline subdominant. Minor components are siderite, highly crystalline dickite and illite with randomly interstratified, poorly crystalline, material. Trace minerals include pyrite and ankerite. A range of carbonate compositions and a background carbon effect are detectable.

4.3.7 Anemone #1A, junk sub sample, 4676f metres

Macro description
A pale grey, moderately sorted medium to very coarse sub-feldsarenite with some granules. Quartz and feldspar dominate the sample and are present in approximately equal proportions. There is some light grey silty matrix which is micaceous. The sample shows moderate porosity and does not react with 10% HCl.

Micro description
This sample is a poorly sorted, granule bearing sub-feldsarenite with angular to subangular, low sphericity grains in an illitic matrix. Grain size ranges from silt to 3.5 mm.

Dissolution (Figs. 59,60,61,62), fracturing and microporosity contribute to a total porosity of 9.6%. A reduction in porosity has occurred due to compaction and quartz overgrowth, resulting in straight to slightly sutured contacts and bent muscovite. Authigenic precipitation of clay has also occluded pores.

Illite is common in the matrix and along fractures. Patchy dickite is associated with Kspar alteration and has totally replaced some grains, possibly plagioclase. Grain-coating or scattered illite is occasionally mixed with dickite.

Cementing agents are clay, carbonate, quartz and pyrite.

The framework consists of quartz, K feldspar, granitic fragments, muscovite, chlorite, organics and rare heavy minerals. Organic matter includes traces of coal and wood. Small pyrite cubes are scattered or in aggregates. Carbonate occurs as subhedral to euhedral scalenohedra, which are mildly to moderately corrosive and invade muscovite cleavage (Figs. 63,64). Clusters of spar probably result from grain replacement.

The source terrain is granitic, as evidenced by quartzo-feldspathic fragments with straight internal crystal boundaries and inclusions. Some grains with slightly sutured internal boundaries may represent input from a strained lithotype.

X-ray diffraction
Quartz is the dominant mineral and siderite is minor, as shown in Figure 65. Minor illite of detrital origin (2M2) may be mixed with authigenic illite, muscovite and randomly interstratified material, accounting for the broad peak. Highly crystalline dickite (2M1), microcline, ankerite and pyrite are trace minerals. Fluctuations in the carbonate spectrum reveal a range of compositions. Carbon produces an elevated background.

Scanning electron microscopy
Like the previous samples, the sediment has a clay-rich matrix and is contaminated by drilling mud (Fig. 66). Porosity, which is fair, results from dissolution of feldspars (Fig. 68) and microporosity in clays. Authigenic illite and kaolin occur, occasionally together. Illite alteration of K feldspar was detected (Fig. 69). Muscovite has been bent by compaction. One example of druse quartz overgrowth was seen, as was a pyrite framboid and siderite.

TABLE 1. POINT COUNT SUMMARY
(giving mineral percentages)

Sample (m)	4575	4676a	4676b	4676c	4676d	4676e	4676f
Quartz	73.7	43.0	50.3	45.0	43.0	51.0	47.3
Feldspars							
orthoclase	-	0.3	0.6	0.6	2.7	2.0	2.7
microcline	0.3	4.7	6.3	3.3	3.7	4.0	4.3
perthite	2.0	4.7	3.3	6.0	6.7	5.3	4.7
indet.	-	1.3	1.0	0.6	0.3	0.3	0.7
total	2.3	11.0	11.2	10.5	13.2	21.6	12.4
Biotite	-	-	-	0.3	-	0.3	-
Muscovite	3.7	4.0	2.7	4.0	4.3	2.7	3.3
Sericite	4.0	2.7	2.3	3.0	5.0	7.7	8.0
Chlorite	0.6	5.7	4.0	2.7	0.3	1.0	0.6
Organics	1.3	10.7	5.0	5.3	3.0	3.0	3.7
Sed. minerals	-	0.6	-	-	-	-	-
Porosity							
primary	1.0	-	-	-	-	0.3	-
dissolution	5.0	4.3	6.0	5.3	8.7	5.3	7.3
fracture	3.0	-	1.0	2.7	1.0	2.0	1.0
micro.	1.7	1.0	0.6	2.3	0.6	2.0	1.3
total	10.7	5.3	7.6	10.3	10.3	9.6	9.6
Cement							
microsparite	-	1.7	3.0	7.3	5.3	3.0	9.0
micrite	-	-	-	0.6	4.0	-	-
quartz o/g	-	-	-	0.6	1.7	1.3	0.3
dickite	-	1.7	1.0	0.6	3.7	1.7	3.0
illite	3.3	5.7	7.0	5.0	3.3	4.3	2.7
pyrite	0.6	5.0	5.7	2.7	2.3	2.3	2.0
Matrix indet.	-	2.7	0.6	-	-	-	-
Polycrystalline grains	71.3	28.3	33.7	44.0	38.3	44.3	45.0
Total points	300	300	300	300	300	300	300

TABLE 2. X-RAY DIFFRACTION SUMMARY

Sample (m)	4575	4676a	4676b	4676c	4676d	4676e	4676f
Quartz	d	-d	d	d	-d	d	d
Microcline	-	m	sd	sd	m	sd	tr
Siderite	-	tr	tr	tr	m	m	m
Pyrite	-	m	tr	tr	tr	tr	tr
Ankerite	-	tr	tr	?	tr	tr	tr
Calcite	-	tr	-	?	-	-	-
Anatase	-	-	-	?	?	?	-
Dickite	-	m	m	m	m	m	tr
Illite/muscovite	tr	m	m	m	m	m	m

d=dominant (-d=less dominant than in other samples)
sd=subdominant
m=minor
tr=trace

4.5. CONCLUSIONS

All the samples in this suite had a similar granitic source area but there are compositional differences that divide the suite into groups. The sample from 4575 metres is a moderately sorted quartz arenite with less matrix and cement than other samples. The porosity is fair with primary porosity reduction due to compaction and suturing.

All the samples from 4676 metres are more closely related although they seem to form a series with respect to matrix content and porosity. These six samples were labelled a-f from the darkest and least porous to the lightest and apparently most porous, based on the hand specimen appearance. All are poorly sorted, silty, very fine to very coarse, sub-feldsarenites to feldsarenites and granule conglomerates composed of angular to subangular grains.

There are problems associated with junk sub samples. The exact position of each sample is unknown as are their relative depths. They are likely to be the most competant samples in the entire interval, possibly from hard ledges in the hole. Consequently, these samples will contain more matrix and be more strongly cemented than the sequence as a whole. An advantage is that perhaps all cements will be seen in these few samples and therefore the diagentic sequence derived from them will be almost complete.

The granitic source of all samples is indicated by a number of factors. The quartz grains all show low strain together with an abundance of vacuole trails. The feldspar content is usually high and dominated by the potassium (K) feldspars, orthoclase and microcline. Both these minerals often show a perthitic texture, exsolved blebs of plagioclase, another plutonic indicator. Many of the larger sand grains and granules are recognizable fragments of granite. The occurrence of muscovite and biotite, togther with traces of apatite and zircon, are consistent with a granitic source.

Although many of the larger grains are essentially rock fragments or lithics, individual components of these fragements have been counted separately to allow a direct comparison with finer grained samples. In these, the individual grains have merely been liberated from the composite fragments. This means all samples are classified as feldsarenites, sub-feldsarenites etc., rather than having the coarser grained samples of the same chemical composition being labelled as litharenites. The percentage of polycrystalline grains in Table 1 is largely an indicator of grain size.

Many of the framework grains show alteration to other minerals. While some of the alteration could be associated with hydrothermal activity in the source rock or have been a result of weathering in the source area, it is thought to be largely due to post-burial, authigenic processes. There are some large masses of sericite with minor kaolin which appear to have replaced plagioclase grains. In a few cases, faint plagioclase twinning can be seen through the alteration. Many of the K feldspars show incipient sericite alteration, which gives a dusty brown appearance to the grains. Although it is extremely difficult to pick between sericite , or finely divided muscovite, and illite, both in thin section and on XRD, a distinction was made by calling all altered feldspars sericite and clearly pore-filling authigenic or detrital matrix clay, illite. Muscovite was observed altering to kaolin and some K felspars have been replaced by kaolin. Many of the biotite grains have partially or completely altered to chlorite, with the subsequent release of finely divided magnetite.

Most of the samples have a fair proportion of matrix. The matrix consists of silt to fine sand sized quartz and feldspar grains together with illitic clay and is normally relatively high in pyrite and an organic component. The proportion of matrix in each sample can be roughly determined from Table 1 as the sum of the indeterminate matrix, about two thirds of the illite component and a proportion of quartz and feldspar, dependant on the grain size. This suggests that sample 4676a has about 8% matrix with samples b-f grading down progressively from 6% to about 2%.

Primary porosity in most of these samples is minimal, mainly due to the amount of matrix present or to infilling by authigenic cement. The exception is 4575m, where porosity reduction has been by compaction. Most of the grain-grain contacts in that sample are sutured.

There are substantial amounts of secondary porosity in all samples. This is largely due to dissolution of feldspars and is particularly evident in microcline grains, where dissolution has etched along the cleavages, and in perthite grains, where the plagioclase blebs have dissolved first, opening up a "Swiss cheese" pattern. Some secondary porosity was designated as fracture porosity but this includes fractures enhanced by dissolution.

A moderate amount of microporosity was observed in the samples and is mainly associated with areas of clay. Sericite alteration of plagioclase and kaolin replacement of K feldspar are often tinged blue with araldite dye uptake. The same is true of the pores filled with authigenic clays. This porosity will be measured by the porosity logs but will be largely ineffective with respect to hydrocarbons due to the large amounts of bound water held in such small pores.

Quartz, clays, carbonate, pyrite and anatase (authigenic TiO_2) all act as cements. The determination and sequence of these is a combined function of thin section microscopy, XRD analysis, SEM scanning and EDS analysis.

Quartz is a relatively early cement and is a minor component in most samples. It occurs as thin overgrowths on framework quartz grains which give straight edges to those grains with some euhedral terminations into porosity. Quartz cementation may well be associated with suturing between some grains during compaction; the lack of compaction being related to the minimal amount of cement.The presence of illite restricts quartz overgrowth, indicating some illite is pre-quartz cement. SEM work on several samples showed an intimate mixture of quartz and kaolin, indicating that the two minerals grew at the same time. Replacement of K feldspar by kaolin releases silica and explains both the intergrowth of the minerals and part of the source of the quartz. The extensive zones of quartz and kaolin intergrowth are unsual and may be associated with overpressure.

Kaolin also occurs as pore-filling booklets, which in some cases almost completely occlude primary porosity, leaving just a hint of microporosity. XRD analysis shows the kaolin to contain dickite, one of the forms of the kaolin group. It is most likely that the feldpsar replacement form is kaolinite and the pore-filling form is dickite. The sharpness of the kaolinite and dickite peaks (most of which are coincident) indicates that the minerals are authigenic.

Illite was seen in thin section and recognized on XRD traces and observed under SEM. The broad peak on the XRD traces suggests a range of compositions for that mineral. This could be due to a detrital origin for the matrix illite, to interference of the peaks with those of muscovite (and sericite) which are largely coincident or to random interstratification with another clay type such as chlorite. The two former reasons are likely to be the case with these samples. Thin section microscopy clearly showed a rim of illite lining many of the pores prior to the growth of pore-filling kaolin (dickite). This may be associated with alteration of the grains. Illite fibres growing on kaolin platelets were commonly seen under SEM. One sample, 4676d, showed illite fibres bridging between framework grains. While the porosity occlusion of this type of growth is small, it substantially reduces permeability.

Carbonate, both as micrite and as small euhedral crystals of spar, was observed within the matrix of the samples. Some coarser spar fills areas of primary porosity, cementing the framework grains and causing some corrosion of the quartz and feldspar. XRD scans show a range of compositions of the carbonate, from dolomite to ankerite with siderite. The micrite appears to be very early and is probably sideritic. The small euhedral crystals within the matrix are also siderite and form from recrystallization of the micrite. This also occurs early as the lines of crystals have been distorted by later compaction. There has been some corrosion of the grains prior to the clay cements and it may be associated with the siderite spar. A later period of spar cement, this time dolomitic to ankeritic, is post alteration of the feldspars and infills dissolution holes. There is more carbonate in the more porous samples, also inferring two phases of growth.

Pyrite is a very early cement as crystal aggregates have been surrounded by authigenic quartz. Euhedral crystals of anatase, seen under SEM in 4676d, are late stage as they are undistorted and not adorned by illite. Anatase is a polymorph of rutile and forms authigenically by alteration of other titanium minerals such as ilmenite. After it was recognized under SEM, traces of the mineral were noted in the XRD scans.

The diagenetic sequence derived from the junk sub samples is as follows:-

Micrite cement
Pyrite
Siderite spar
Compaction and quartz corrosion
Feldspar alteration
Pore-lining illite
Quartz overgrowth and pore-filling dickite
Dolomite and ankerite cement, dissolution
Illite fibre growth, bridging and on kaolin
Anatase

The position of hydrocarbon generation and migration is difficult to determine in this sequence as so little of it was seen in these tight samples. It does, however, postdate the feldspar alteration and possibly the pore-filling dickite.

The amount of matrix in these samples is important but not easily determined due to infiltration of drilling mud. The degree of contamination appeared higher in the SEM samples than in thin section. This anomaly was resolved by the strong barite signature from the mud in XRD scans of unwashed versus washed cuttings from 4530-50m. Barite was not picked up in the XRD of the junk sub samples, inferring low contamination by mud. The SEM samples are prepared by breaking chips from the sample. It appears that these fractures favour the more porous zones where mud is likely to infiltrate and is so prominent under SEM. Overall, there is confirmation of high matrix and low primary porosity in the junk sub samples. Re-assessment of the thin sections could only find 1-2% mud at most in the samples.

7. FIGURES AND CAPTIONS

Figure 1. Anemone #1A, junk sub sample, 4575 metres. Thin section micrograph in plane polarized light showing secondary porosity associated with fractures (f), and dissolution (d). Microporosity gives the brown clay areas a bluish tinge. The large microcline grains (M) display discolouration due to alteration.

Figure 2. Anemone #1A, junk sub sample, 4575 metres. The same view under crossed polars highlights the yellow illite rich matrix and areas of grain replacement (arrowed).

Figure 3. Anemone #1A, junk sub sample, 4575 metres. Thin section micrograph in plane polarized light demonstrating secondary porosity development by dissolution along fractures (arrowed) in highly vacuolated quartz (Q). Bluish areas in the matrix represent dissolution of highly altered grains and microporosity. A muscovite (Mu) and quartz intergrowth is an igneous fragment.

Figure 4. Anemone #1A, junk sub sample, 4575 metres. A crossed polars view of the previous figure shows the illite-rich matrix, sericite grain replacement (Se) and muscovite (Mu).

Figure 5. Anemone #1A, junk sub sample, 4575 metres. Detail of muscovite (Mu) corroding vacuolated quartz(Q) in an igneous fragment, under crossed polars. Carbonate spar (S) and fine opaque minerals arrowed (pyrite?) have precipitated along micaceous cleavage.

Figure 6. Anemone #1A, junk sub sample, 4575 metres. View in plane polarized light of authigenic euhedral-subhedral quartz growth in porous matrix. View is down the c crystallographic axis. Dark coloured matter includes organics and finely disseminated pyrite.

Figure 7. Anemone #1A, junk sub sample, 4575 metres. The same field of view as above under crossed polars, pore-lining illite (I) is evident.

Figure 8. Bulk XRD trace of Anemone #1A, junk sub sample, 4575 m. Q=quartz and I=illite. Only the strongest peaks have been labelled for each mineral.

Figure 9. Anemone #1A, junk sub sample, 4676a metres. Thin section micrograph in plane polarized light showing alteration of microcline (M) and a plutonic fragment on the right. Stylolitic organic matter and fine pyrite pervade the matrix. A small lime green area of chlorite (Ch) is visible. Vague bluish areas in the matrix may be microporosity.

Figure 10. Anemone #1A, junk sub sample, 4676a metres. A crossed polars view of the previous photo reveals patchy alteration of microcline and the granitic fragment to dickite (D) and minor yellowish sericite. The matrix is illite rich.

Figure 11. Anemone #1A, junk sub sample, 4676a metres. The central feldspar cleavage fragment shows alteration along cleavage in plane polarized light. Carbonate spar (S) is mildly corroding the feldspar. A structured organic fragment (?wood) occurs at the top right of the field of view and an aggregate of pyrite crystals (P) is visible.

Figure 12. Anemone #1A, junk sub sample, 4676a metres. Under crossed polars, the same view shows sericite in feldspar cleavage and illitic matrix. Brownish stringers in the previous photo are shown to consist of illite. Highly birefringent spar occurs in the matrix. A bright pink-yellow detrital mineral (apatite?) is evident in the lower right of the photo.

Figure 13. Anemone #1A, junk sub sample, 4676a metres. View under crossed polars of feldspars (F) displaying considerable alteration to dickite (D) and minor development of sericite along cleavage.

Figure 14. Anemone #1A, junk sub sample, 4676a metres. Carbonate spar (S) is corroding along cleavage of muscovite which is altering to grey chlorite. The quartz grain (Q) shows vacuole trails (arrowed) and inclusions. Dissolution is seen in the perthite grain (Pe).

Figure 15. Bulk XRD trace of Anemone #1A, junk sub sample, 4676a m. Q=quartz, I=illite/muscovite, D=dickite, M=microcline, P=pyrite, S=siderite and A=ankerite. Only the strongest peaks have been labelled for each mineral.

Figure 16. Anemone #1A, junk sub sample, 4676b metres. Thin section micrograph in plane polarized light demonstrating areas of secondary dissolution porosity (d) and fracture porosity (f). Microporosity may well be present. The stylolitic nature of organic matter (and opaques?) is evident. At the left of the photo is a concentration of spar crystals (S).

Figure 17. Anemone #1A, junk sub sample, 4676b metres. Seen under crossed polars, the illitic matrix and sericitic grain replacements (Se) of the previous figure are obvious. The concentration of spar (S) is seen to coincide with an abundance of clay and may represent grain replacement.

Figure 18. Anemone #1A, junk sub sample, 4676b metres. Anhedral to subhedral carbonate spar crystals (S) are seen here invading the less competent grains. Two feldspar fragments display alteration. The bent muscovite (Mu) shows cleavage development of pyrite, which is also disseminated around grain boundaries with organics. The spherical black object is probably an organic structure.

Figure 19. Anemone #1A, junk sub sample, 4676b metres. Under crossed polars, yellow illite is highlighted and one of the feldspars shows a patch of dickite (D).

Figure 20. Bulk XRD trace of Anemone #1A, junk sub sample, 4676b m. Q=quartz, I=illite/muscovite, D=dickite, M=microcline, P=pyrite, S=siderite and A=ankerite. Only the strongest peaks have been labelled for each mineral.

Figure 21. Anemone #1A, junk sub sample, 4676c metres. Thin section micrograph demonstrating secondary dissolution porosity (d),especially in the highly altered feldspar, and fracture porosity (f). Microporosity is arrowed in the grain on the right. Organics and aggregates of small anhedral-euhedral spar scalenohedra (S) occur in the matrix.

Figure 22. Anemone #1A, junk sub sample, 4676c metres. Under crossed polars, the central feldspar displays patchy dickite (D) and the microporosity in the previous figure is seen to coincide with a sericitized grain.

Figure 23. Anemone #1A, junk sub sample, 4676c metres. In plane polarized light, fine opaques and organics highlight the sutured boundaries between compacted quartz grains. Fine carbonate spar aggregates (S) are scattered through the matrix. Porosity in the quartzose grains has been produced by dissolution along fractures.

Figure 24. Anemone #1A, junk sub sample, 4676c metres. Detail from Figure 23 of finely divided pyrite and organics along a sutured contact and grain boundaries. Fracture porosity is indicated (f).

Figure 25. Anemone #1A, junk sub sample, 4676c metres. The plutonic nature of these quartzose grains is suggested by the vacuole trails (arrowed) and straight boundaries in the polycrystalline rock fragment, under crossed polars. Porosity is associated with fractures in the central quartz grain.

Figure 26. Bulk XRD trace of Anemone #1A, junk sub sample, 4676c m. Q=quartz, I=illite/muscovite, D=dickite, M=microcline, P=pyrite, S=siderite and A=ankerite. Only the strongest peaks have been labelled for each mineral.

Figure 27. Anemone #1A, junk sub sample, 4676c metres. Scanning electron micrograph showing general view of sediment with abundant clay matrix and probable drilling mud. No porosity is evident. Rare euhedral quartz overgrowths are evident from straight faces on quartz grains.

Figure 28. Anemone #1A, junk sub sample, 4676c metres. Scanning electron micrograph demonstrating dissolution of K feldspar along preferred crystallographic axes. Eventually this dissolution will lead to the development of secondary porosity.

Figure 29. Anemone #1A, junk sub sample, 4676c metres. EDS pattern of K feldspar from previous figure.

Figure 30. Anemone #1A, junk sub sample, 4676c metres. Long, unbroken fibres of illite suggest its authigenic origin.

Figure 31. Anemone #1A, junk sub sample, 4676c metres. EDS pattern of illite from the previous figure.

Figure 32. Anemone #1A, junk sub sample, 4676c metres. Detail of euhedral, pseudohexagonal kaolin booklets that suggest an authigenic origin. Associated microporosity and permeability are partially restricted by fibrous illite.

Figure 33. Anemone #1A, junk sub sample, 4676c metres. EDS pattern of kaolin from the previous figure.

Figure 34. Anemone #1A, junk sub sample, 4676c metres. Scanning electron micrograph showing kaolin booklets overlying an unaltered K feldspar grain. Wisps of authigenic illite are scattered over the surface of the feldspar and kaolin.

Figure 35. Anemone #1A, junk sub sample, 4676c metres. EDS pattern of K feldspar from previous figure.

Figure 36. Anemone #1A, junk sub sample, 4676c metres. Euhedral quartz overgrowths have reduced primary porosity. Step fracturing of quartz due to sample preparation is evident. Note that the presence of illite has limited the development of overgrowths in some zones.

Figure 37. Anemone #1A, junk sub sample, 4676c metres. Scanning electron micrograph demonstrating a very broad zone of intergrowth between kaolin booklets and authigenic quartz (Q).

Figure 38. Anemone #1A, junk sub sample, 4676c metres. SEM micrograph shows a subhedral siderite rhomb (S) is intergrown along cleavage of a biotite fragment. The small white crystals are drilling mud contaminants.

Figure 39. Anemone #1A, junk sub sample, 4676c metres. EDS pattern of siderite from the previous figure.

Figure 40. Anemone 1A, junk sub sample, 4676d metres. Thin section micrograph in plane polarized light showing high porosity which is partly dissolution porosity (d) but largely an artefact of slide preparation. Pyrite crystals occur in aggregates (P).

Figure 41. Anemone 1A, junk sub sample, 4676d metres. Crossed polars view revealing low birefringence dickite (D), grain-lining illite (I) and corroded quartz (arrowed). Aggregates of fine spar on the left coincide with illite-rich or opaque-rich zones.

Figure 42. Anemone 1A, junk sub sample, 4676d metres. Under crossed polars, illite is seen scattered throughout the matrix. Muscovite (Mu) is bent by compaction and polycrystalline rock fragments are evident. An unaltered quartz overgrowth is arrowed.

Figure 43. Anemone 1A, junk sub sample, 4676d metres. Detail of an altered quartz grain under crossed polars. A wide, unaltered, authigenic overgrowth (Og) forms a straight contact with the adjacent grain. The opposite side of the grain has a sutured contact, with the absence of an overgrowth suggesting that suturing was an earlier event.

Figure 44. Bulk XRD trace of Anemone #1A, junk sub sample, 4676d m. Q=quartz, I=illite/muscovite, D=dickite, M=microcline, P=pyrite, S=siderite and A=ankerite. Only the strongest peaks have been labelled for each mineral.

Figure 45. Anemone #1A, junk sub sample, 4676d metres. Scanning electron micrograph showing general view of sediment with abundant clay, including drilling mud. There is only minor porosity evident. Pores are of hybrid primary-secondary origin, since pore sizes are comparable to, or slightly larger than the average grain size. They may have resulted from whole grain dissolution.

Figure 46. Anemone #1A, junk sub sample, 4676d metres. Scanning electron micrograph demonstrating partial occlusion of pore throats by fibrous authigenic illite between dissolving feldspars. While it does not reduce porosity significantly, this type of bridging will create significant permeability barriers to fluid flow.

Figure 47. Anemone #1A, junk sub sample, 4676d metres. EDS pattern of K feldspar from previous figure.

Figure 48. Anemone #1A, junk sub sample, 4676d metres. Scanning electron micrograph showing detail of intergrowth of kaolin platelets and fibrous illite.

Figure 49. Anemone #1A, junk sub sample, 4676d metres. EDS pattern of illite from the previous figure.

Figure 50. Anemone #1A, junk sub sample, 4676d metres. Kaolin booklets lie adjacent to fractured quartz (Q) and show intergrowth at the contact. Platy and fibrous illite is apparent in the lower right of the micrograph.

Figure 51. Anemone #1A, junk sub sample, 4676d metres. Pyritic aggregates which have been engulfed by authigenic quartz. An early, fine crystal phase and a later coarse crystal phase of pyrite growth are evident. Moulds in the quartz indicate that some pyrite has probably been plucked during sample preparation.

Figure 52. Anemone #1A, junk sub sample, 4676d metres. Scanning electron micrograph showing euhedral anatase crystals (An) of authigenic origin.

Figure 53. Anemone #1A, junk sub sample, 4676d metres. A subhedral apatite crystal surrounded by clay matrix to the right and euhedral quartz to the left. Slight rounding of the crystal reflects its detrital origin.

Figure 54. Anemone #1A, junk sub sample, 4676e metres. Thin section micrograph in plane polarized light showing secondary porosity associated with dissolution (d) and microporosity (arrowed).

Figure 55. Anemone #1A, junk sub sample, 4676e metres. Microporosity is seen to be associated with a sericitized grain. Patches of spar scalenohedra are highlighted under crossed polars.

Figure 56. Anemone #1A, junk sub sample, 4676e metres. Extensive dissolution of feldspar grains has produced secondary porosity on the left of the field of view. Clay areas on the right have flecks of microporosity associated. Plane polarized light.

Figure 57. Anemone #1A, junk sub sample, 4676e metres. Sericitic (Se) and kaolinitic (K) grain replacement are revealed in the same scene as Fig.56 under crossed polars. The pore on the right has a thin lining of illite prior to the kaolin infill.

Figure 58. Bulk XRD trace of Anemone #1A, junk sub sample, 4676e m. Q=quartz, I=illite/muscovite, D=dickite, M=microcline, P=pyrite, S=siderite and A=ankerite. Only the strongest peaks have been labelled for each mineral.

Figure 59. Anemone #1A, junk sub sample, 4676f metres. General view in plane polarized light showing secondary dissolution porosity associated with highly altered microcline (M). Aggregates of spar scalenohedra (S) and pyrite (P) are evident.

Figure 60. Anemone #1A, junk sub sample, 4676f metres. In the same field of view as above, the highly altered microcline (M), spar (S) and quartzofeldspathic rock fragments (R) are clearly shown under crossed polars.

Figure 61. Anemone #1A, junk sub sample, 4676f metres. Feldspar grain displaying extreme alteration along cleavage and some secondary dissolution (d) and fracture (f) porosity development. Zones of bluish haze probably represent microporosity.

Figure 62. Anemone #1A, junk sub sample, 4676f metres. Cross polarized light of the scene above reveals the perthitic nature of the feldspar and remnant cross-hatching. The microporosity from the previous figure corresponds with zones of sericite and dickite (D).

Figure 63. Anemone #1A, junk sub sample, 4676f metres. Plane polar view of subhedral spar scalenohedra (S) growing between and displacing muscovite (Mu) plates. Structured organic matter (O) and an aggregation of pyrite crystals (P) are obvious.

Figure 64. Anemone #1A, junk sub sample, 4676f metres. View of previous figure under crossed polars.

Figure 65. Bulk XRD trace of Anemone #1A, junk sub sample, 4676f m. Q=quartz, I=illite/muscovite, D=dickite, M=microcline, P=pyrite, S=siderite and A=ankerite. Only the strongest peaks have been labelled for each mineral.

Figure 66. Anemone #1A, junk sub sample, 4676f metres. Scanning electron micrograph showing general view with abundant clay, (including drilling mud), fractured quartz (Q) and minor porosity.

Figure 67. Anemone #1A, junk sub sample, 4676f metres. An SEM micrograph shows dissolution of K feldspar has produced minor secondary porosity.

Figure 68. Anemone #1A, junk sub sample, 4676f metres. EDS pattern of K feldspar from previous figure.

Figure 69. Anemone #1A, junk sub sample, 4676f metres. A large dissolution pore is evident in the K feldspar on the left, adjacent to kaolin and minor illite. A thin border of illite between the pore and the kaolin probably represents alteration at the original boundary of the K feldspar.

PE906870

This is an enclosure indicator page.
The enclosure PE906870 is enclosed within the container PE906849 at this location in this document.

The enclosure PE906870 has the following characteristics:

ITEM_BARCODE =	PE906870
CONTAINER_BARCODE =	PE906849
NAME =	Core Photomicrograph
BASIN =	GIPPSLAND
PERMIT =	VIC/P20
TYPE =	WELL
SUBTYPE =	PHOTOMICROGRAPH
DESCRIPTION =	Core Photomicrograph, secondary porosity associated with fracture and dissolution, (figure 1 from attachment to WCR--Petrographic Analysis Report) for Anemone-1 & 1A
REMARKS =	
DATE_CREATED =	31/12/89
DATE_RECEIVED =	17/01/90
W_NO =	W997
WELL_NAME =	ANEMONE-1 & 1A
CONTRACTOR =	CORE SERVICES OF AUSTRALIA
CLIENT_OP_CO =	PETROFINA EXPLORATION AUSTRALIA S.A.

PE906871

This is an enclosure indicator page.
The enclosure PE906871 is enclosed within the container PE906849 at this location in this document.

The enclosure PE906871 has the following characteristics:

ITEM_BARCODE = PE906871
CONTAINER_BARCODE = PE906849
NAME = Core Photomicrograph
BASIN = GIPPSLAND
PERMIT = VIC/P20
TYPE = WELL
SUBTYPE = PHOTOMICROGRAPH
DESCRIPTION = Core Photomicrograph, yellow illite rich matrix and areas of grain replacement, (figure 2 from attachment to WCR--Petrographic Analysis Report) for Anemone-1 & 1A
REMARKS =
DATE_CREATED = 31/12/89
DATE_RECEIVED = 17/01/90
W_NO = W997
WELL_NAME = ANEMONE-1 & 1A
CONTRACTOR = CORE SERVICES OF AUSTRALIA
CLIENT_OP_CO = PETROFINA EXPLORATION AUSTRALIA S.A.

PE906872

This is an enclosure indicator page.
The enclosure PE906872 is enclosed within the container PE906849 at this location in this document.

The enclosure PE906872 has the following characteristics:

ITEM_BARCODE = PE906872
CONTAINER_BARCODE = PE906849
NAME = Core Photomicrograph
BASIN = GIPPSLAND
PERMIT = VIC/P20
TYPE = WELL
SUBTYPE = PHOTOMICROGRAPH
DESCRIPTION = Core Photomicrograph, secondary porosity developed by dissolution along fractures in highly vacuolated quartz, (figure 3 from attachment to WCR--Petrographic Analysis Report) for Anemone-1 & 1A
REMARKS =
DATE_CREATED = 31/12/89
DATE_RECEIVED = 17/01/90
W_NO = W997
WELL_NAME = ANEMONE-1 & 1A
CONTRACTOR = CORE SERVICES OF AUSTRALIA
CLIENT_OP_CO = PETROFINA EXPLORATION AUSTRALIA S.A.

PE906873

This is an enclosure indicator page.
The enclosure PE906873 is enclosed within the container PE906849 at this location in this document.

The enclosure PE906873 has the following characteristics:

ITEM_BARCODE = PE906873
CONTAINER_BARCODE = PE906849
NAME = Core Photomicrograph
BASIN = GIPPSLAND
PERMIT = VIC/P20
TYPE = WELL
SUBTYPE = PHOTOMICROGRAPH
DESCRIPTION = Core Photomicrograph, illite rich matrix,sericite grain replacement and muscovite, (figure 4 from attachment to WCR--Petrographic Analysis Report) for Anemone-1 & 1A
REMARKS =
DATE_CREATED = 31/12/89
DATE_RECEIVED = 17/01/90
W_NO = W997
WELL_NAME = ANEMONE-1 & 1A
CONTRACTOR = CORE SERVICES OF AUSTRALIA
CLIENT_OP_CO = PETROFINA EXPLORATION AUSTRALIA S.A.

PE906874

This is an enclosure indicator page.
The enclosure PE906874 is enclosed within the container PE906849 at this location in this document.

The enclosure PE906874 has the following characteristics:

ITEM_BARCODE =	PE906874
CONTAINER_BARCODE =	PE906849
NAME =	Core Photomicrograph
BASIN =	GIPPSLAND
PERMIT =	VIC/P20
TYPE =	WELL
SUBTYPE =	PHOTOMICROGRAPH
DESCRIPTION =	Core Photomicrograph, muscovite corroding vacuolated quartz in an igneous fragment under crossed polars, (figure 5 from attachment to WCR--Petrographic Analysis Report) for Anemone-1 & 1A
REMARKS =	
DATE_CREATED =	31/12/89
DATE_RECEIVED =	17/01/90
W_NO =	W997
WELL_NAME =	ANEMONE-1 & 1A
CONTRACTOR =	CORE SERVICES OF AUSTRALIA
CLIENT_OP_CO =	PETROFINA EXPLORATION AUSTRALIA S.A.

PE906875

This is an enclosure indicator page.
The enclosure PE906875 is enclosed within the container PE906849 at this location in this document.

The enclosure PE906875 has the following characteristics:

ITEM_BARCODE = PE906875
CONTAINER_BARCODE = PE906849
NAME = Core Photomicrograph
BASIN = GIPPSLAND
PERMIT = VIC/P20
TYPE = WELL
SUBTYPE = PHOTOMICROGRAPH
DESCRIPTION = Core Photomicrograph, authigenic euhedral-subhedral quartz growth in porous matrix , (figure 6 from attachment to WCR--Petrographic Analysis Report) for Anemone-1 & 1A
REMARKS =
DATE_CREATED = 31/12/89
DATE_RECEIVED = 17/01/90
W_NO = W997
WELL_NAME = ANEMONE-1 & 1A
CONTRACTOR = CORE SERVICES OF AUSTRALIA
CLIENT_OP_CO = PETROFINA EXPLORATION AUSTRALIA S.A.

PE906876

This is an enclosure indicator page.
The enclosure PE906876 is enclosed within the container PE906849 at this location in this document.

The enclosure PE906876 has the following characteristics:

ITEM_BARCODE =	PE906876
CONTAINER_BARCODE =	PE906849
NAME =	Core Photomicrograph
BASIN =	GIPPSLAND
PERMIT =	VIC/P20
TYPE =	WELL
SUBTYPE =	PHOTOMICROGRAPH
DESCRIPTION =	Core Photomicrograph, pore lining illite is evident under crossed polars, (figure 7 from attachment to WCR--Petrographic Analysis Report) for Anemone-1 & 1A
REMARKS =	
DATE_CREATED =	31/12/89
DATE_RECEIVED =	17/01/90
W_NO =	W997
WELL_NAME =	ANEMONE-1 & 1A
CONTRACTOR =	CORE SERVICES OF AUSTRALIA
CLIENT_OP_CO =	PETROFINA EXPLORATION AUSTRALIA S.A.

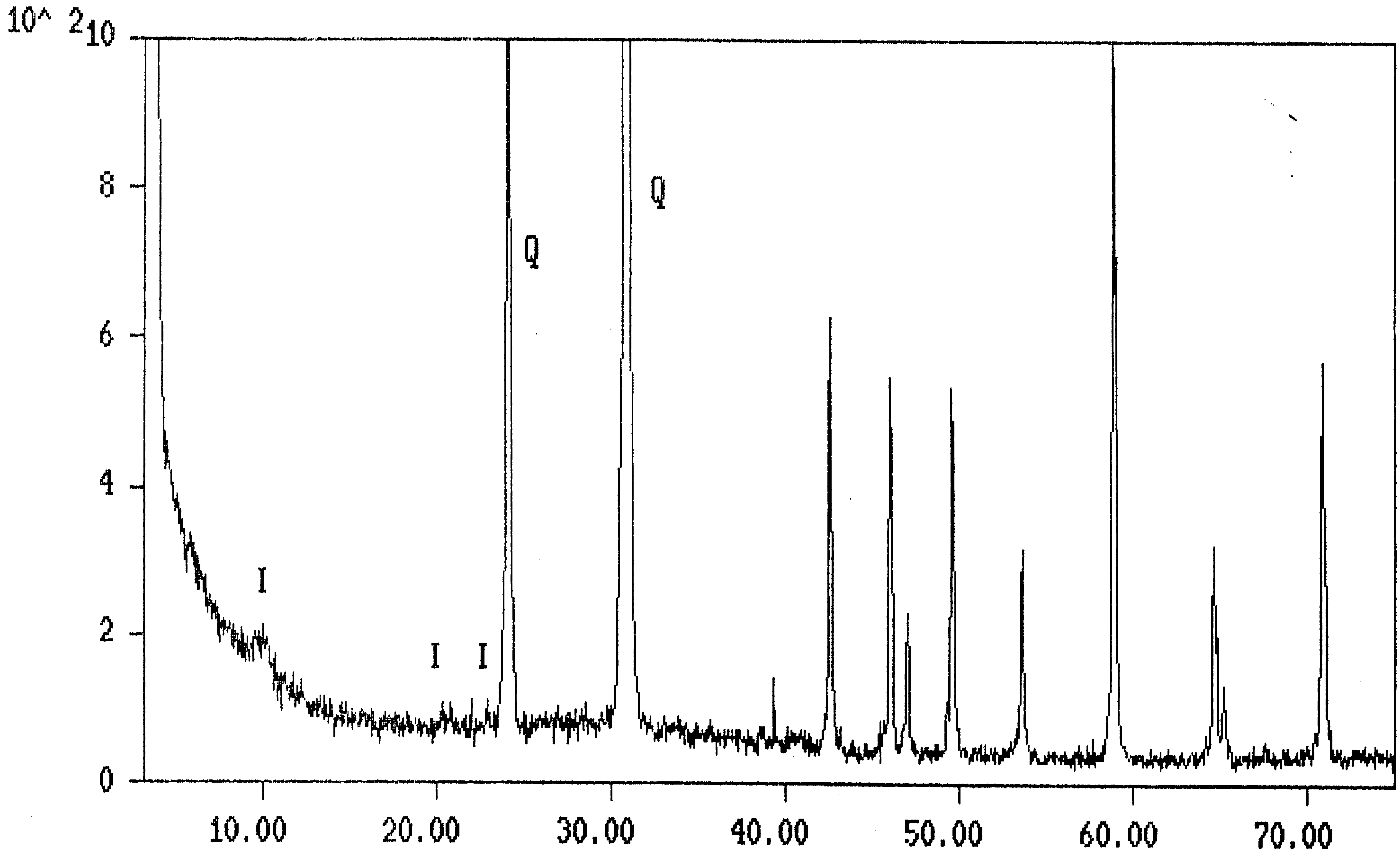

Figure 8. Bulk XRD trace of Anemone #1A, junk sub sample, 4575 m. Q=quartz and I=illite. Only the strongest peaks have been labelled for each mineral.

FILENAME: NL-4575.CPI

PE906877

This is an enclosure indicator page.
The enclosure PE906877 is enclosed within the container PE906849 at this location in this document.

The enclosure PE906877 has the following characteristics:

ITEM_BARCODE =	PE906877
CONTAINER_BARCODE =	PE906849
NAME =	Core Photomicrograph
BASIN =	GIPPSLAND
PERMIT =	VIC/P20
TYPE =	WELL
SUBTYPE =	PHOTOMICROGRAPH
DESCRIPTION =	Core Photomicrograph, alteration of microline,organic matter and pyrite matrix with chlorite visible, (figure 9 from attachment to WCR--Petrographic Analysis Report) for Anemone-1 & 1A
REMARKS =	
DATE_CREATED =	31/12/89
DATE_RECEIVED =	17/01/90
W_NO =	W997
WELL_NAME =	ANEMONE-1 & 1A
CONTRACTOR =	CORE SERVICES OF AUSTRALIA
CLIENT_OP_CO =	PETROFINA EXPLORATION AUSTRALIA S.A.

PE906878

This is an enclosure indicator page.
The enclosure PE906878 is enclosed within the container PE906849 at this location in this document.

The enclosure PE906878 has the following characteristics:

ITEM_BARCODE = PE906878
CONTAINER_BARCODE = PE906849
NAME = Core Photomicrograph
BASIN = GIPPSLAND
PERMIT = VIC/P20
TYPE = WELL
SUBTYPE = PHOTOMICROGRAPH
DESCRIPTION = Core Photomicrograph, alteration of micoline and granitic fragment to dicktite and minor yellowish sericite with an illite rich matrix, (figure 10 from attachment to WCR--Petrographic Analysis Report) for Anemone-1 & 1A
REMARKS =
DATE_CREATED = 31/12/89
DATE_RECEIVED = 17/01/90
W_NO = W997
WELL_NAME = ANEMONE-1 & 1A
CONTRACTOR = CORE SERVICES OF AUSTRALIA
CLIENT_OP_CO = PETROFINA EXPLORATION AUSTRALIA S.A.

PE906879

This is an enclosure indicator page.
The enclosure PE906879 is enclosed within the container PE906849 at this location in this document.

The enclosure PE906879 has the following characteristics:

ITEM_BARCODE = PE906879
CONTAINER_BARCODE = PE906849
NAME = Core Photomicrograph
BASIN = GIPPSLAND
PERMIT = VIC/P20
TYPE = WELL
SUBTYPE = PHOTOMICROGRAPH
DESCRIPTION = Core Photomicrograph, alteration in cleavage of feldspar as carbonate srap corrodes the feldspar, (figure 11 from attachment to WCR--Petrographic Analysis Report) for Anemone-1 & 1A
REMARKS =
DATE_CREATED = 31/12/89
DATE_RECEIVED = 17/01/90
W_NO = W997
WELL_NAME = ANEMONE-1 & 1A
CONTRACTOR = CORE SERVICES OF AUSTRALIA
CLIENT_OP_CO = PETROFINA EXPLORATION AUSTRALIA S.A.

PE906880

This is an enclosure indicator page.
The enclosure PE906880 is enclosed within the container PE906849 at this location in this document.

The enclosure PE906880 has the following characteristics:

ITEM_BARCODE =	PE906880
CONTAINER_BARCODE =	PE906849
NAME =	Core Photomicrograph
BASIN =	GIPPSLAND
PERMIT =	VIC/P20
TYPE =	WELL
SUBTYPE =	PHOTOMICROGRAPH
DESCRIPTION =	Core Photomicrograph, sericite in feldspar cleavage and illitic matrix, (figure 12 from attachment to WCR--Petrographic Analysis Report) for Anemone-1 & 1A
REMARKS =	
DATE_CREATED =	31/12/89
DATE_RECEIVED =	17/01/90
W_NO =	W997
WELL_NAME =	ANEMONE-1 & 1A
CONTRACTOR =	CORE SERVICES OF AUSTRALIA
CLIENT_OP_CO =	PETROFINA EXPLORATION AUSTRALIA S.A.

PE906881

This is an enclosure indicator page.
The enclosure PE906881 is enclosed within the container PE906849 at this location in this document.

The enclosure PE906881 has the following characteristics:

ITEM_BARCODE =	PE906881
CONTAINER_BARCODE =	PE906849
NAME =	Core Photomicrograph
BASIN =	GIPPSLAND
PERMIT =	VIC/P20
TYPE =	WELL
SUBTYPE =	PHOTOMICROGRAPH
DESCRIPTION =	Core Photomicrograph, feldspar alteration to dicktite and development of sericite along cleavage, (figure 13 from attachment to WCR--Petrographic Analysis Report) for Anemone-1 & 1A
REMARKS =	
DATE_CREATED =	31/12/89
DATE_RECEIVED =	17/01/90
W_NO =	W997
WELL_NAME =	ANEMONE-1 & 1A
CONTRACTOR =	CORE SERVICES OF AUSTRALIA
CLIENT_OP_CO =	PETROFINA EXPLORATION AUSTRALIA S.A.

PE906882

This is an enclosure indicator page.
The enclosure PE906882 is enclosed within the container PE906849 at this location in this document.

The enclosure PE906882 has the following characteristics:

ITEM_BARCODE =	PE906882
CONTAINER_BARCODE =	PE906849
NAME =	Core Photomicrograph
BASIN =	GIPPSLAND
PERMIT =	VIC/P20
TYPE =	WELL
SUBTYPE =	PHOTOMICROGRAPH
DESCRIPTION =	Core Photomicrograph, carbonate spar corroding along muscovite cleavage which is altering to grey chlorite, (figure 14 from attachment to WCR--Petrographic Analysis Report) for Anemone-1 & 1A
REMARKS =	
DATE_CREATED =	31/12/89
DATE_RECEIVED =	17/01/90
W_NO =	W997
WELL_NAME =	ANEMONE-1 & 1A
CONTRACTOR =	CORE SERVICES OF AUSTRALIA
CLIENT_OP_CO =	PETROFINA EXPLORATION AUSTRALIA S.A.

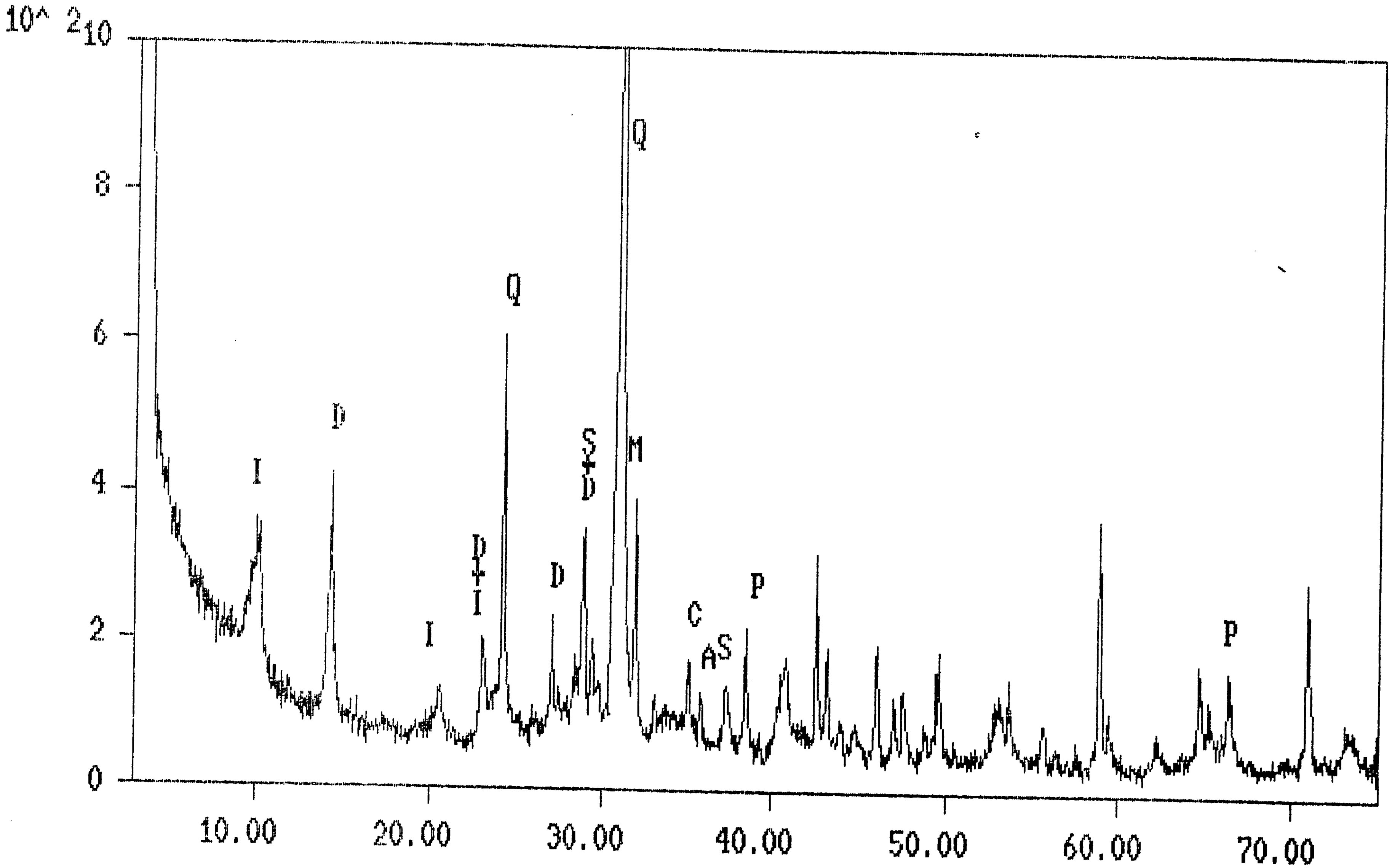

Figure 15. Bulk XRD trace of Anemone #1A, junk sub sample, 4676a m. Q=quartz, I=illite/muscovite, D=dickite, M=microcline, P=pyrite, S=siderite and A=ankerite. Only the strongest peaks have been labelled for each mineral.

FILENAME: NL-4676A.CPI

PE906883

This is an enclosure indicator page.
The enclosure PE906883 is enclosed within the container PE906849 at this location in this document.

The enclosure PE906883 has the following characteristics:

ITEM_BARCODE = PE906883
CONTAINER_BARCODE = PE906849
NAME = Core Photomicrograph
BASIN = GIPPSLAND
PERMIT = VIC/P20
TYPE = WELL
SUBTYPE = PHOTOMICROGRAPH
DESCRIPTION = Core Photomicrograph, dissolution, porosity and fracture porosity evident; the organic matter has a styolitic nature, (figure 16 from attachment to WCR--Petrographic Analysis Report) for Anemone-1 & 1A
REMARKS =
DATE_CREATED = 31/12/89
DATE_RECEIVED = 17/01/90
W_NO = W997
WELL_NAME = ANEMONE-1 & 1A
CONTRACTOR = CORE SERVICES OF AUSTRALIA
CLIENT_OP_CO = PETROFINA EXPLORATION AUSTRALIA S.A.

PE906884

This is an enclosure indicator page.
The enclosure PE906884 is enclosed within the container PE906849 at this location in this document.

The enclosure PE906884 has the following characteristics:

ITEM_BARCODE =	PE906884
CONTAINER_BARCODE =	PE906849
NAME =	Core Photomicrograph
BASIN =	GIPPSLAND
PERMIT =	VIC/P20
TYPE =	WELL
SUBTYPE =	PHOTOMICROGRAPH
DESCRIPTION =	Core Photomicrograph, illitic matrix and sericitic grain replacements, (figure 17 from attachment to WCR--Petrographic Analysis Report) for Anemone-1 & 1A
REMARKS =	
DATE_CREATED =	31/12/89
DATE_RECEIVED =	17/01/90
W_NO =	W997
WELL_NAME =	ANEMONE-1 & 1A
CONTRACTOR =	CORE SERVICES OF AUSTRALIA
CLIENT_OP_CO =	PETROFINA EXPLORATION AUSTRALIA S.A.

PE906885

This is an enclosure indicator page.
The enclosure PE906885 is enclosed within the container PE906849 at this location in this document.

The enclosure PE906885 has the following characteristics:

ITEM_BARCODE = PE906885
CONTAINER_BARCODE = PE906849
NAME = Core Photomicrograph
BASIN = GIPPSLAND
PERMIT = VIC/P20
TYPE = WELL
SUBTYPE = PHOTOMICROGRAPH
DESCRIPTION = Core Photomicrograph, anhedral-subhedral carbonate spar crystals invading less competant grains; feldspar shows alteration;muscovite shows cleavage development of pyrite, (figure 18 from attachment to WCR--Petrographic Analysis Report) for Anemone-1 & 1A
REMARKS =
DATE_CREATED = 31/12/89
DATE_RECEIVED = 17/01/90
W_NO = W997
WELL_NAME = ANEMONE-1 & 1A
CONTRACTOR = CORE SERVICES OF AUSTRALIA
CLIENT_OP_CO = PETROFINA EXPLORATION AUSTRALIA S.A.

(Inserted by DNRE - Vic Govt Mines Dept)

PE906886

This is an enclosure indicator page.
The enclosure PE906886 is enclosed within the container PE906849 at this location in this document.

The enclosure PE906886 has the following characteristics:

ITEM_BARCODE =	PE906886
CONTAINER_BARCODE =	PE906849
NAME =	Core Photomicrograph
BASIN =	GIPPSLAND
PERMIT =	VIC/P20
TYPE =	WELL
SUBTYPE =	PHOTOMICROGRAPH
DESCRIPTION =	Core Photomicrograph, yellow illite and one of the feldspars shows a patch of dickite, (figure 19 from attachment to WCR--Petrographic Analysis Report) for Anemone-1 & 1A
REMARKS =	
DATE_CREATED =	31/12/89
DATE_RECEIVED =	17/01/90
W_NO =	W997
WELL_NAME =	ANEMONE-1 & 1A
CONTRACTOR =	CORE SERVICES OF AUSTRALIA
CLIENT_OP_CO =	PETROFINA EXPLORATION AUSTRALIA S.A.

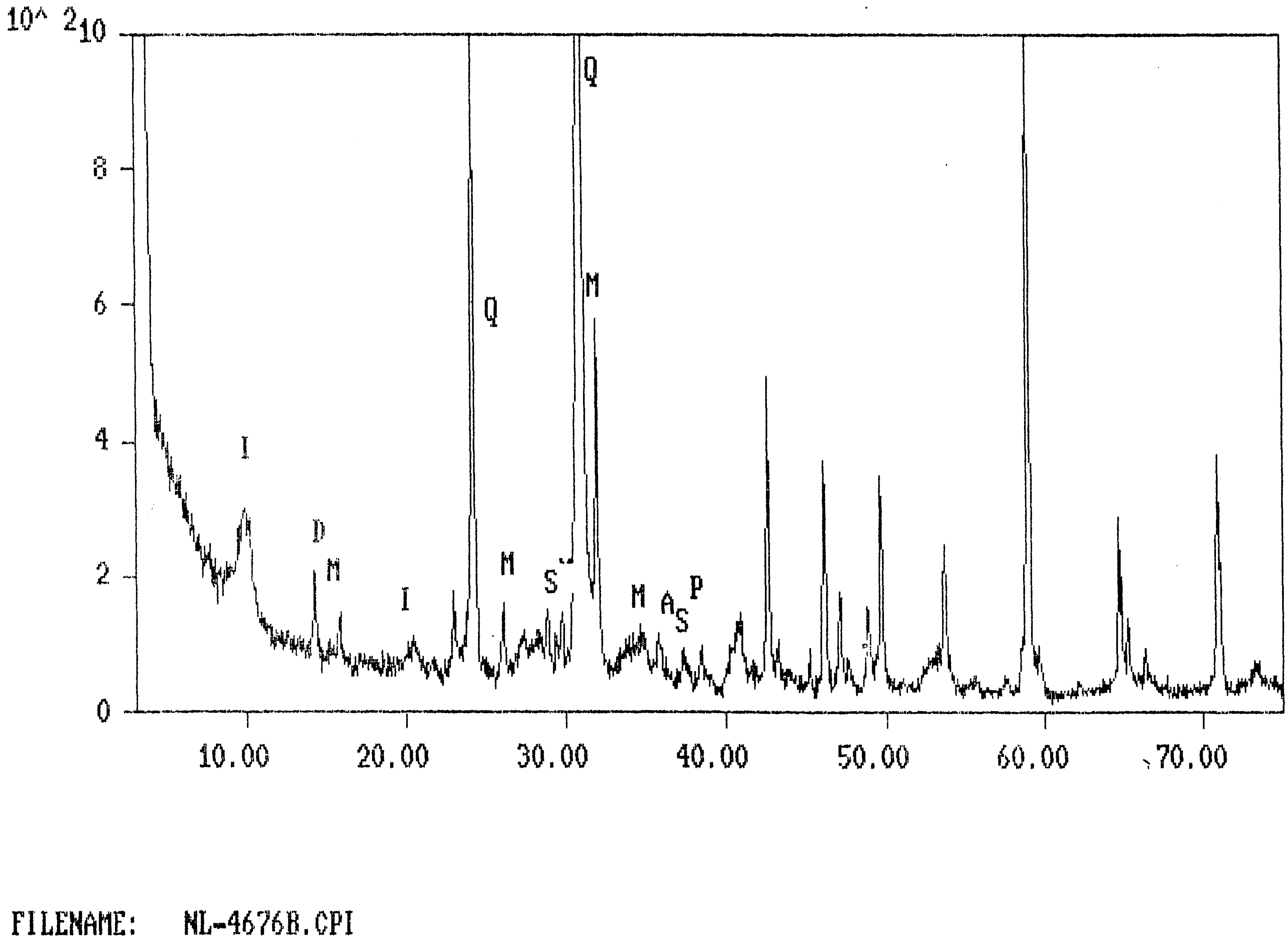

Figure 20. Bulk XRD trace of Anemone #1A, junk sub sample, 4676b m. Q=quartz, I=illite/muscovite, D=dickite, M=microcline, P=pyrite, S=siderite and A=ankerite. Only the strongest peaks have been labelled for each mineral.

PE906887

This is an enclosure indicator page.
The enclosure PE906887 is enclosed within the container PE906849 at this location in this document.

The enclosure PE906887 has the following characteristics:

ITEM_BARCODE =	PE906887
CONTAINER_BARCODE =	PE906849
NAME =	Core Photomicrograph
BASIN =	GIPPSLAND
PERMIT =	VIC/P20
TYPE =	WELL
SUBTYPE =	PHOTOMICROGRAPH
DESCRIPTION =	Core Photomicrograph, secondary dissolution porosity in the highly altered feldspar, and fracture porosity, (figure 21 from attachment to WCR--Petrographic Analysis Report) for Anemone-1 & 1A
REMARKS =	
DATE_CREATED =	31/12/89
DATE_RECEIVED =	17/01/90
W_NO =	W997
WELL_NAME =	ANEMONE-1 & 1A
CONTRACTOR =	CORE SERVICES OF AUSTRALIA
CLIENT_OP_CO =	PETROFINA EXPLORATION AUSTRALIA S.A.

PE906888

This is an enclosure indicator page.
The enclosure PE906888 is enclosed within the container PE906849 at this location in this document.

The enclosure PE906888 has the following characteristics:

ITEM_BARCODE =	PE906888
CONTAINER_BARCODE =	PE906849
NAME =	Core Photomicrograph
BASIN =	GIPPSLAND
PERMIT =	VIC/P20
TYPE =	WELL
SUBTYPE =	PHOTOMICROGRAPH
DESCRIPTION =	Core Photomicrograph, feldspar displays patchy dicktite and the microporosity coincides witha sericitized grain, (figure 22 from attachment to WCR--Petrographic Analysis Report) for Anemone-1 & 1A
REMARKS =	
DATE_CREATED =	31/12/89
DATE_RECEIVED =	17/01/90
W_NO =	W997
WELL_NAME =	ANEMONE-1 & 1A
CONTRACTOR =	CORE SERVICES OF AUSTRALIA
CLIENT_OP_CO =	PETROFINA EXPLORATION AUSTRALIA S.A.

PE906889

This is an enclosure indicator page.
The enclosure PE906889 is enclosed within the container PE906849 at this location in this document.

The enclosure PE906889 has the following characteristics:

ITEM_BARCODE = PE906889
CONTAINER_BARCODE = PE906849
NAME = Core Photomicrograph
BASIN = GIPPSLAND
PERMIT = VIC/P20
TYPE = WELL
SUBTYPE = PHOTOMICROGRAPH
DESCRIPTION = Core Photomicrograph, opaques and organics highlight the boundaries between quartz grains; carbonate spar is scattered in the matrix; porosity resulted from dissolution, (figure 23 from attachment to WCR--Petrographic Analysis Report) for Anemone-1 & 1A
REMARKS =
DATE_CREATED = 31/12/89
DATE_RECEIVED = 17/01/90
W_NO = W997
WELL_NAME = ANEMONE-1 & 1A
CONTRACTOR = CORE SERVICES OF AUSTRALIA
CLIENT_OP_CO = PETROFINA EXPLORATION AUSTRALIA S.A.

(Inserted by DNRE - Vic Govt Mines Dept)

PE906890

This is an enclosure indicator page.
The enclosure PE906890 is enclosed within the container PE906849 at this location in this document.

The enclosure PE906890 has the following characteristics:

ITEM_BARCODE = PE906890
CONTAINER_BARCODE = PE906849
NAME = Core Photomicrograph
BASIN = GIPPSLAND
PERMIT = VIC/P20
TYPE = WELL
SUBTYPE = PHOTOMICROGRAPH
DESCRIPTION = Core Photomicrograph, finely divided pyrite and organics along a sutured contact and grain boundaries with fracture porosity indicated, (figure 24 from attachment to WCR--Petrographic Analysis Report) for Anemone-1 & 1A
REMARKS =
DATE_CREATED = 31/12/89
DATE_RECEIVED = 17/01/90
W_NO = W997
WELL_NAME = ANEMONE-1 & 1A
CONTRACTOR = CORE SERVICES OF AUSTRALIA
CLIENT_OP_CO = PETROFINA EXPLORATION AUSTRALIA S.A.

PE906891

This is an enclosure indicator page.
The enclosure PE906891 is enclosed within the container PE906849 at this location in this document.

The enclosure PE906891 has the following characteristics:

ITEM_BARCODE =	PE906891
CONTAINER_BARCODE =	PE906849
NAME =	Core Photomicrograph
BASIN =	GIPPSLAND
PERMIT =	VIC/P20
TYPE =	WELL
SUBTYPE =	PHOTOMICROGRAPH
DESCRIPTION =	Core Photomicrograph, vacuole trails in quartzose grains and straight boundaries in the polycrystalline rock fragment, (figure 25 from attachment to WCR--Petrographic Analysis Report) for Anemone-1 & 1A
REMARKS =	
DATE_CREATED =	31/12/89
DATE_RECEIVED =	17/01/90
W_NO =	W997
WELL_NAME =	ANEMONE-1 & 1A
CONTRACTOR =	CORE SERVICES OF AUSTRALIA
CLIENT_OP_CO =	PETROFINA EXPLORATION AUSTRALIA S.A.

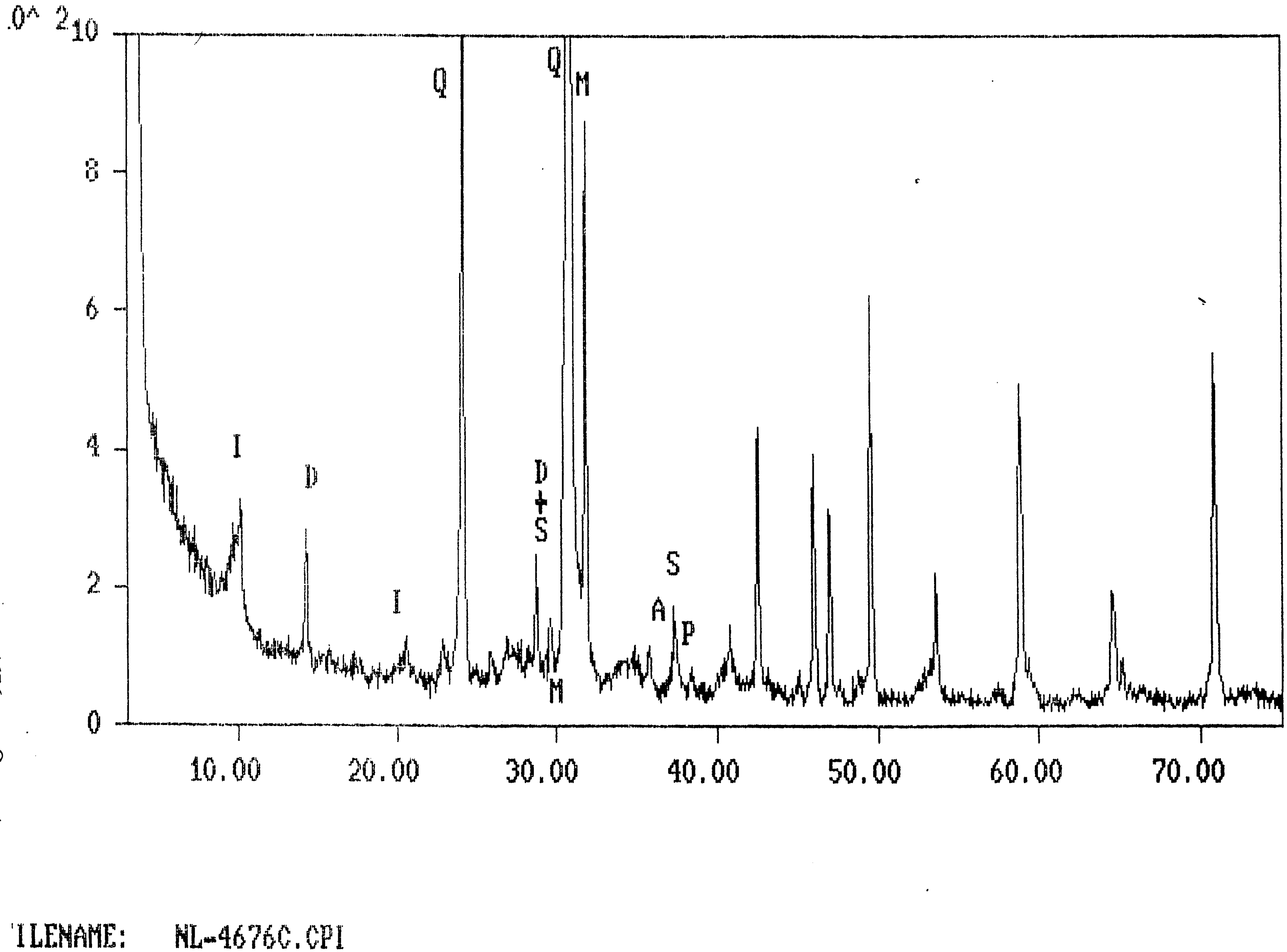

Figure 26. Bulk XRD trace of Anemone #1A, junk sub sample, 4676c m. Q=quartz, I=illite/muscovite, D=dickite, M=microcline, P=pyrite, S=siderite and A=ankerite. Only the strongest peaks have been labelled for each mineral.

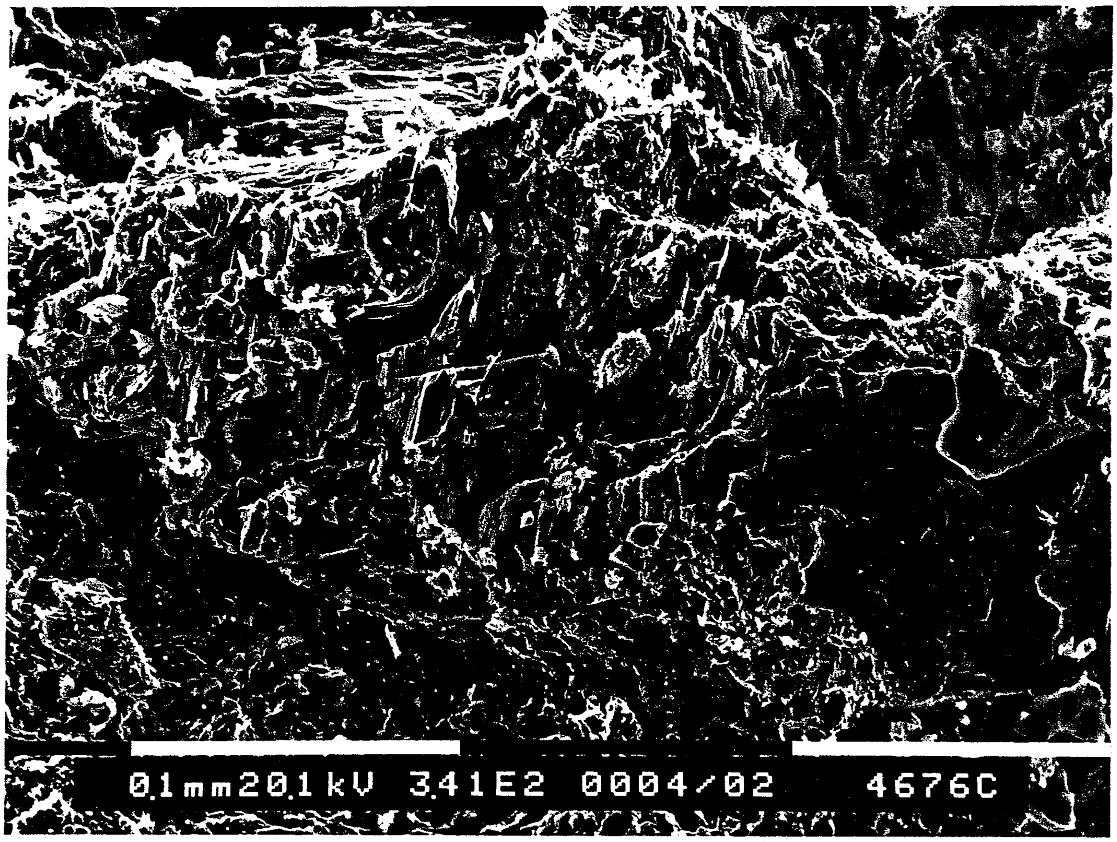

Figure 27 - Anemone #1A, junk sub sample, 4676c m. Scanning electron micrograph showing general view of sediment with abundant clay matrix and probable drilling mud. No porosity is evident. Rare euhedral quartz overgrowths are evident from straight faces on quartz grains.

2-98 Anemone 1A

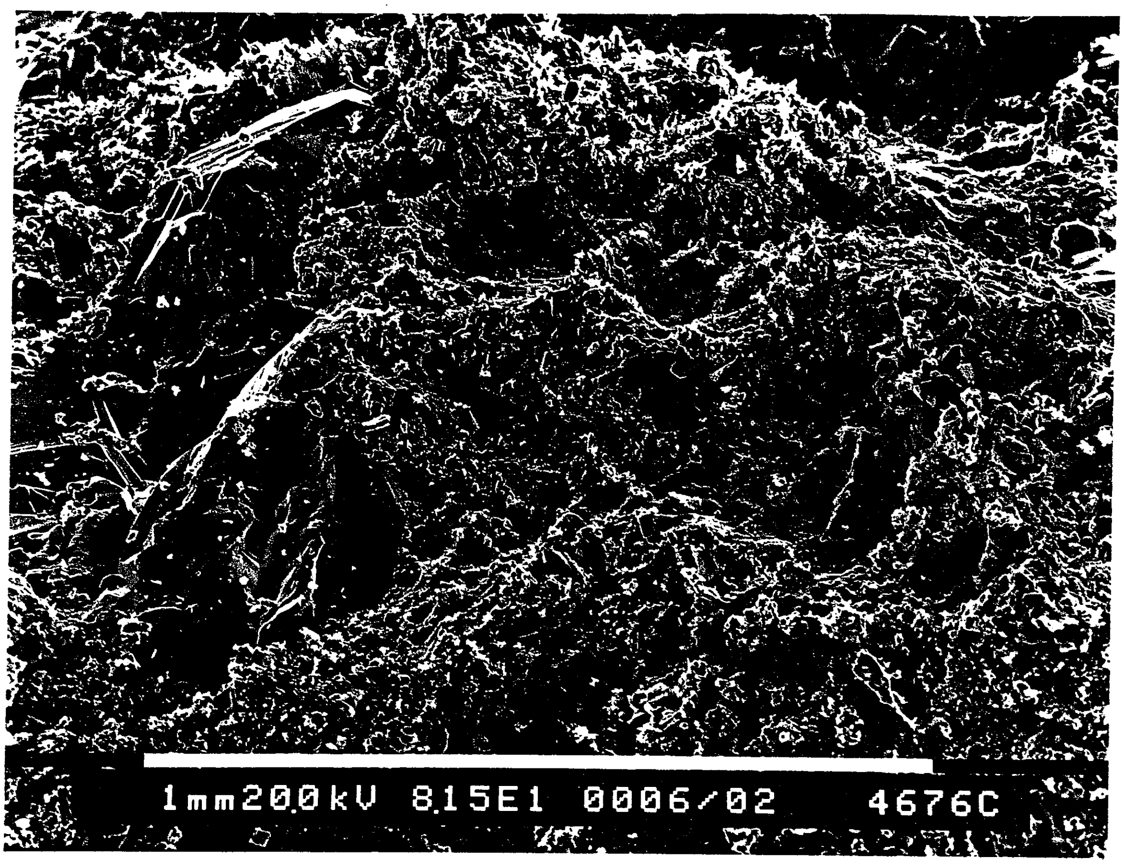

Figure 28 - Anemone #1A, junk sub sample, 4676c m. Scanning electron micrograph demonstrating dissolution of K feldspar along preferred crystallographic axes. Eventually this dissolution will lead to the development of secondary porosity.

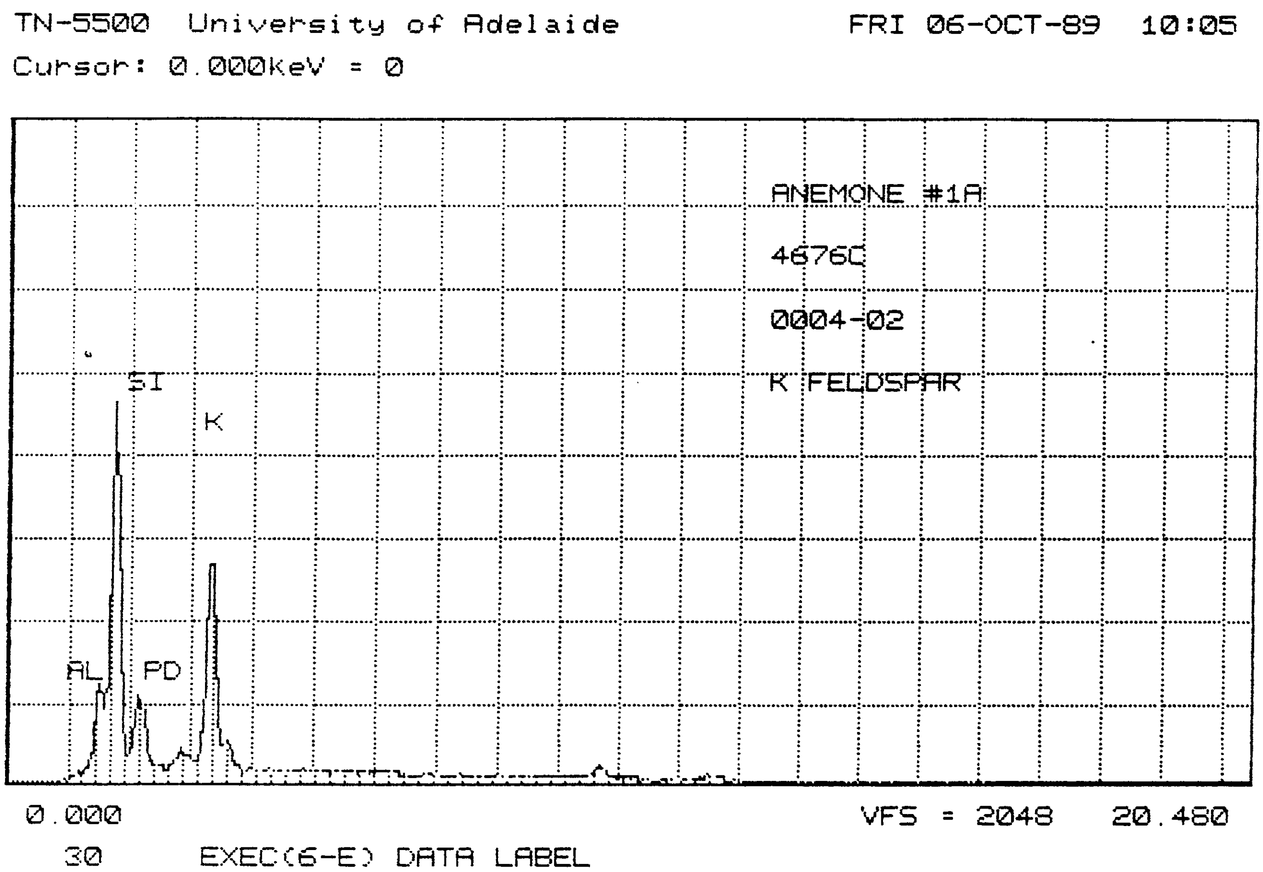

Figure 29. Anemone #1A, junk sub sample, 4676c metres. EDS pattern of K feldspar from previous figure.

Figure 30 - Anemone #1A, junk sub sample, 4676c m. Long, unbroken fibres of illite suggest its authigenic origin.

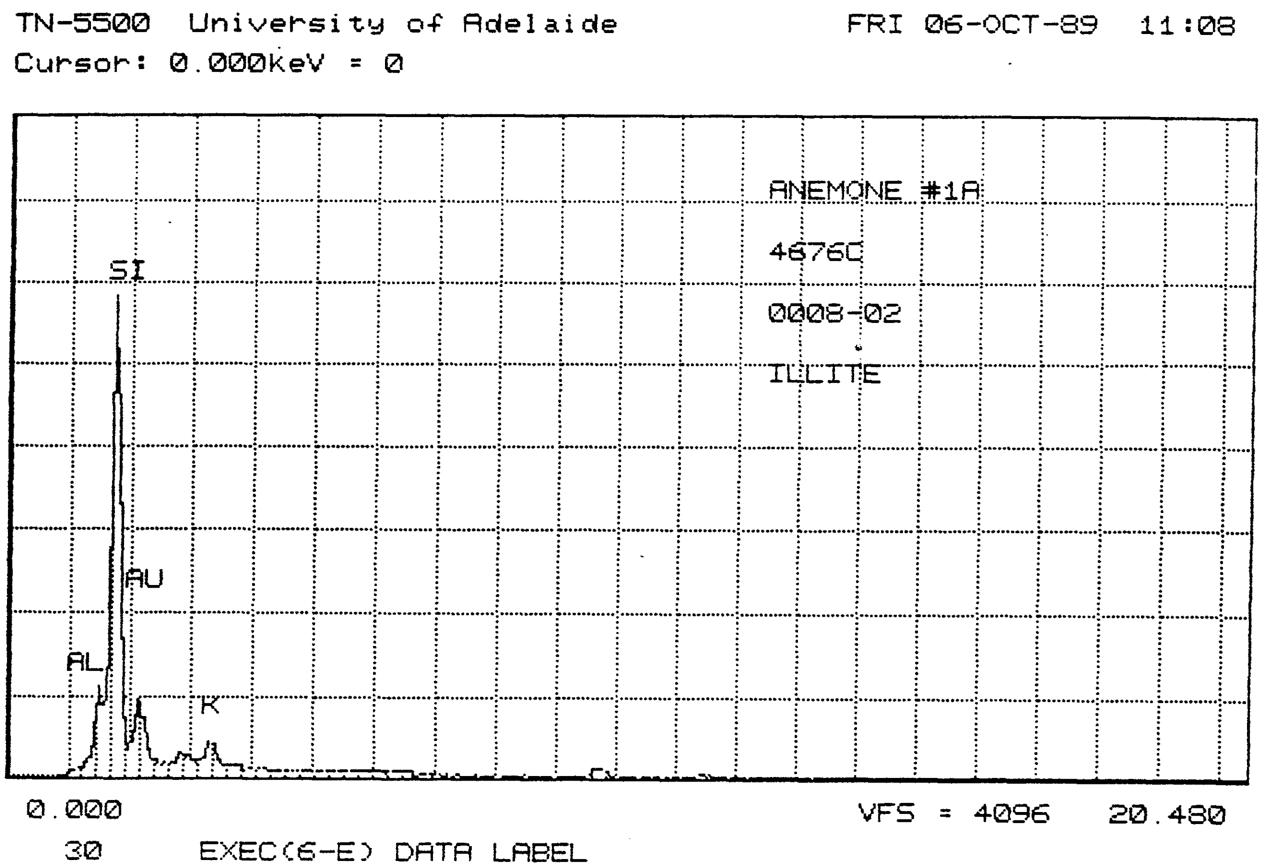

Figure 31. Anemone #1A, junk sub sample, 4676c metres. EDS pattern of illite from the previous figure.

2-98 Anemone 1A

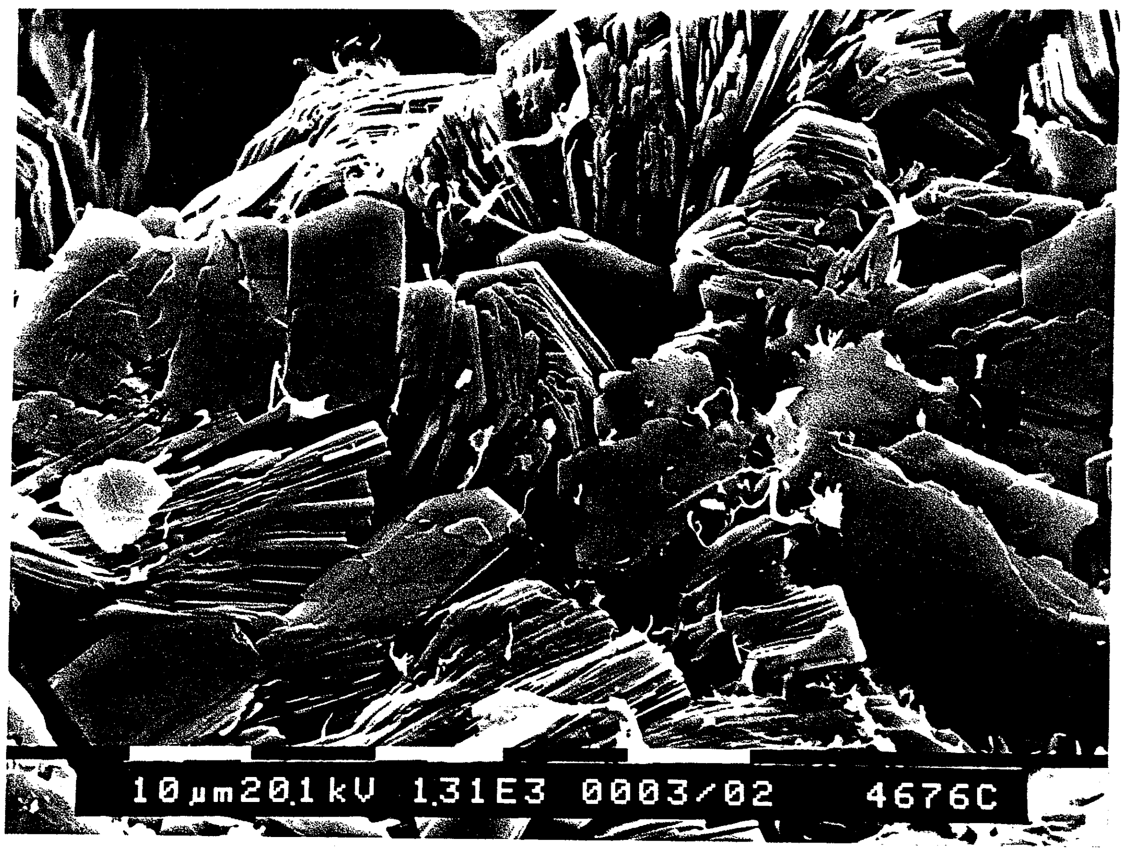

Figure 32 - Anemone #1A, junk sub sample, 4676c m. Detail of euhedral pseudohexagonal kaolin booklets that suggest an authigenic origin. Associated microporosity and permeability are partially restricted by fibrous illite.

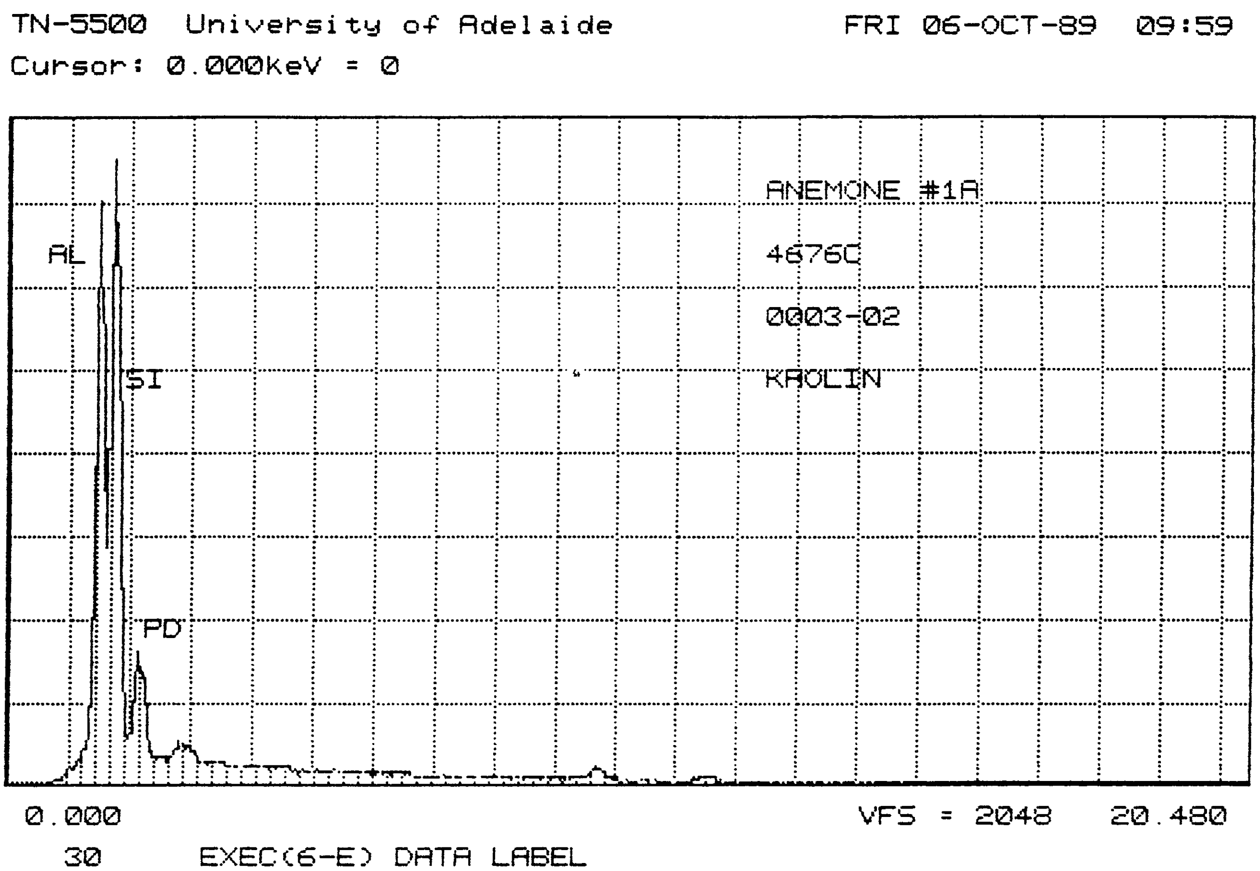

Figure 33. Anemone #1A, junk sub sample, 4676c metres. EDS pattern of kaolin from the previous figure.

Figure 34 - Anemone #1A, junk sub sample, 4676c m. Scanning electron micrograph showing kaolin booklets overlying an unaltered K feldspar grain. Wisps of authigenic illite are scattered over the surface of the feldspar and kaolin.

173712

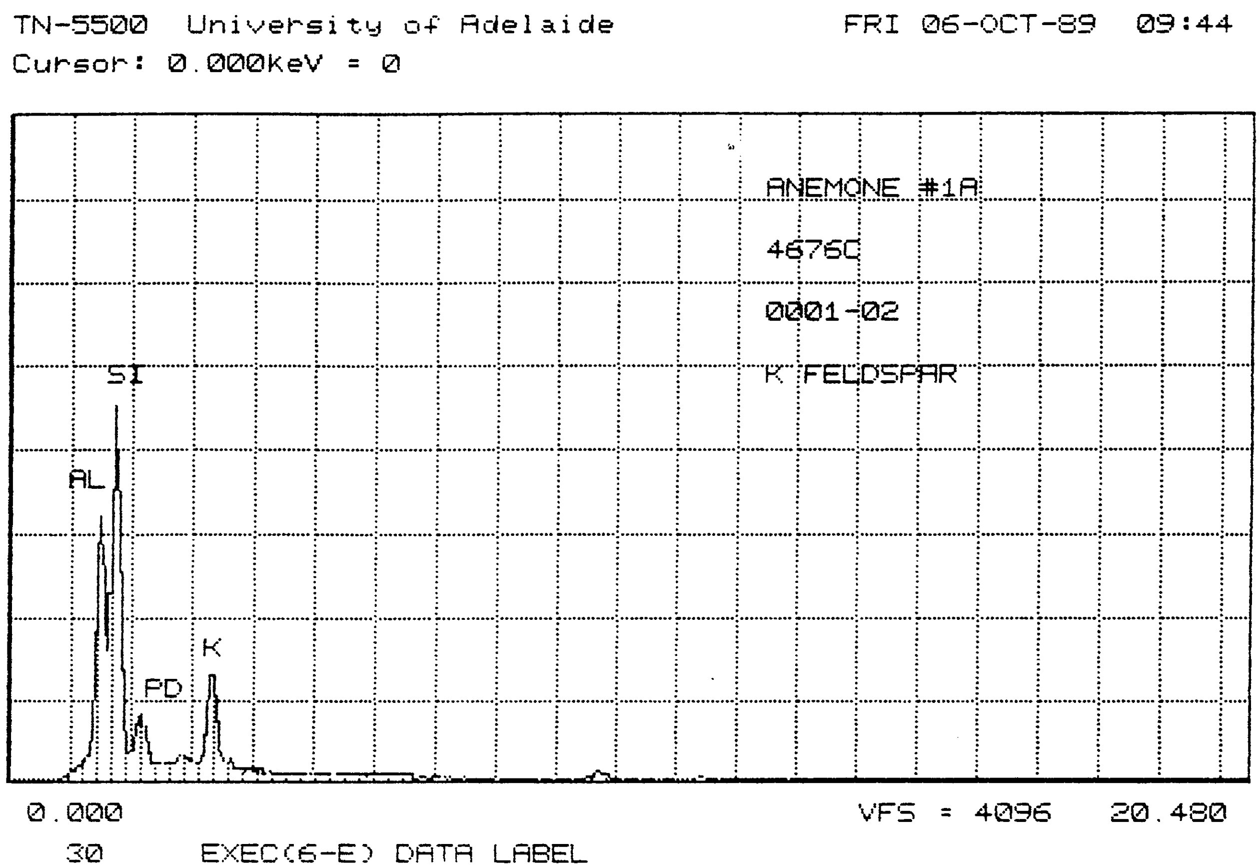

Figure 35. Anemone #1A, junk sub sample, 4676c metres. EDS pattern of K feldspar from previous figure.

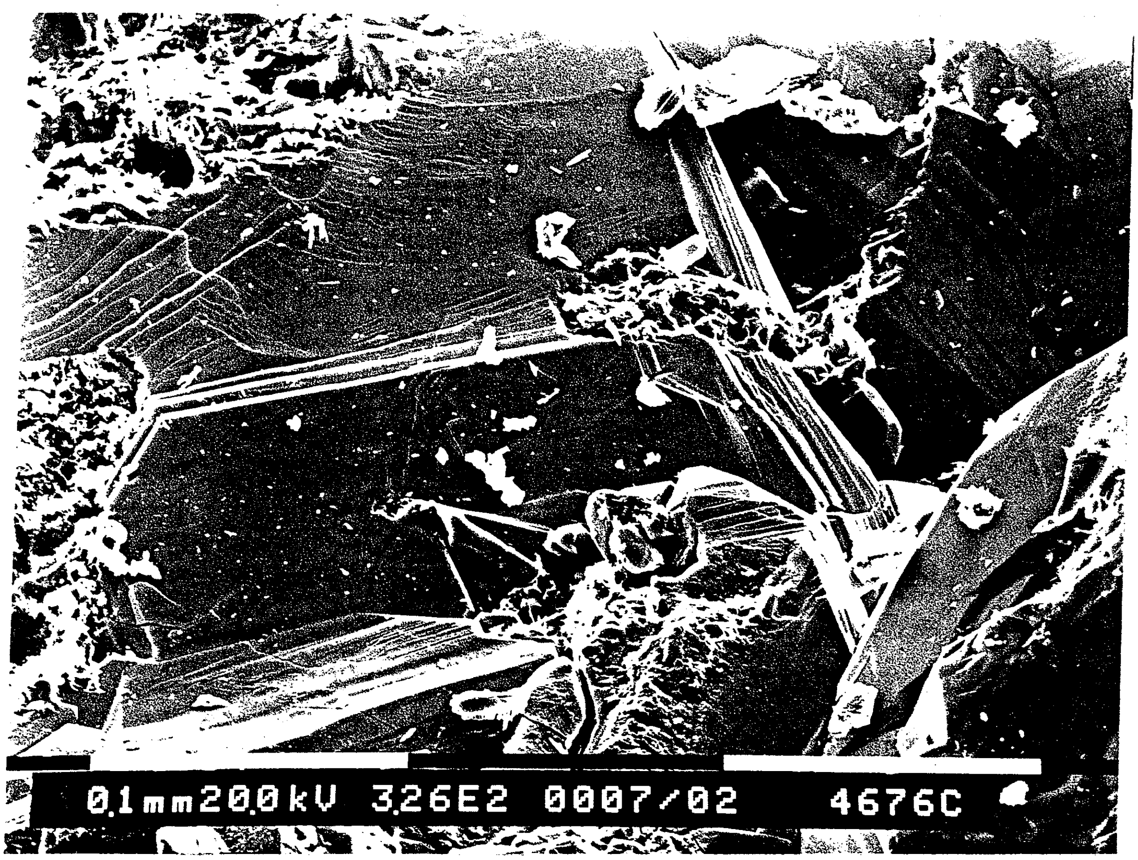

Figure 36, Anemone #1A, junk sub sample, 4676c m. Euhedral quartz overgrowths have reduced primary porosity. Step fracturing of quartz due to sample preparation is evident. Note that the presence of illite has limited the development of overgrowths in some zones.

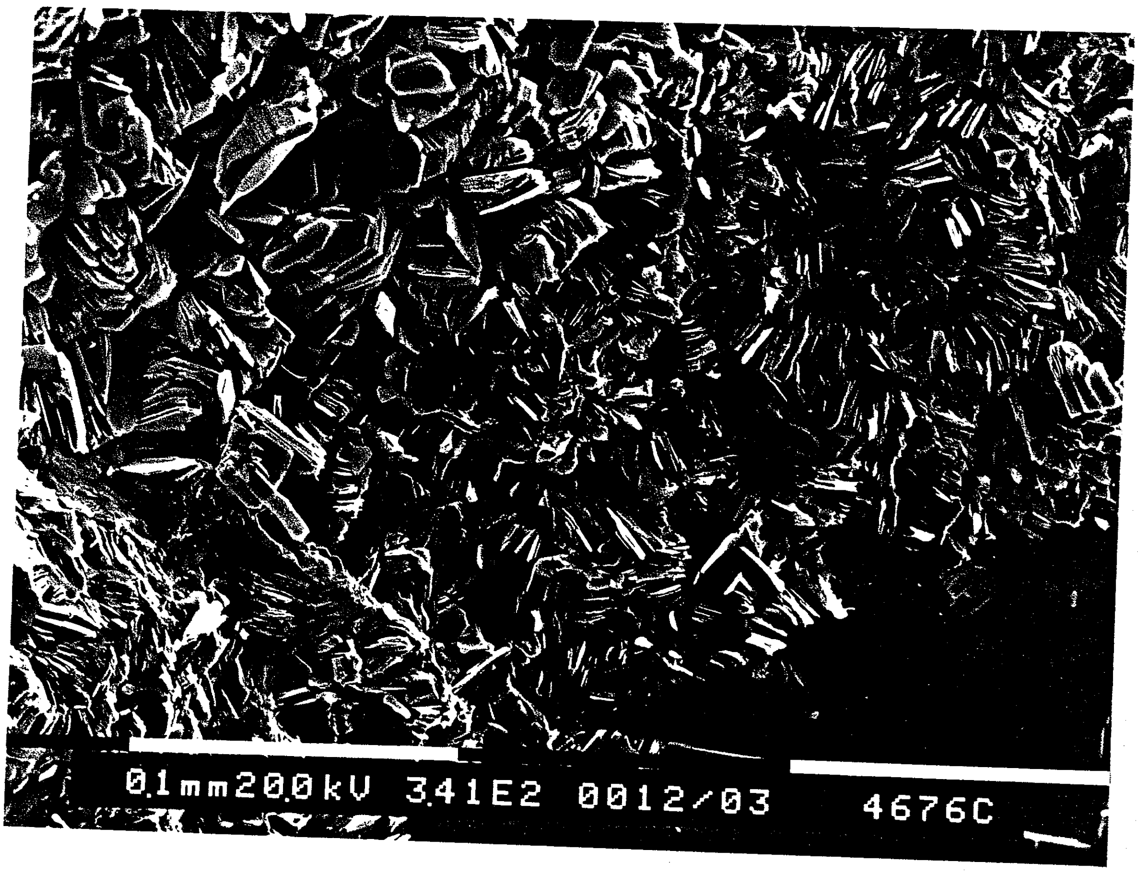

Figure 37 - Anemone #1A, junk sub sample, 4676c m.
Scanning electron micrograph demonstrating a very broad zone of intergrowth between kaolin booklets and authigenic quartz (Q).

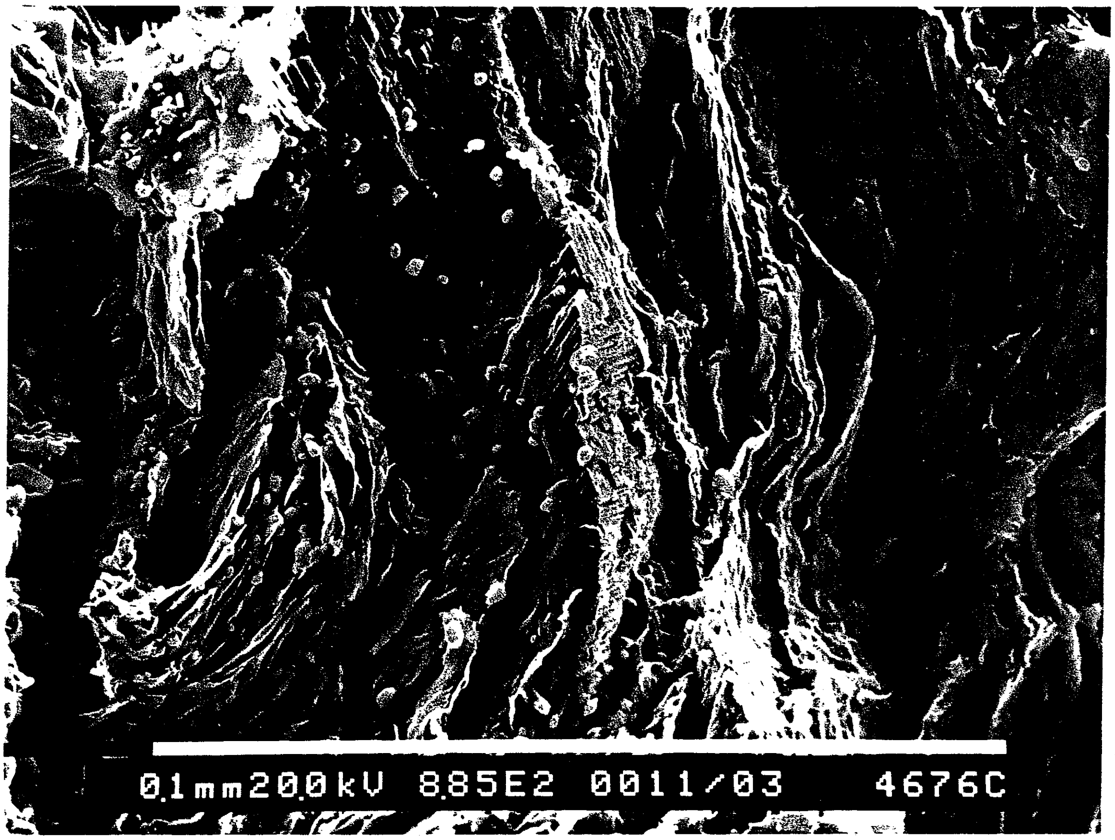

Figure 38 - Anemone #1A, junk sub sample, 4676c m. SEM micrograph shows a subhedral siderite rhomb (S) is intergrown along cleavage of a biotite fragment. The small white crystals are drilling mud contaminants.

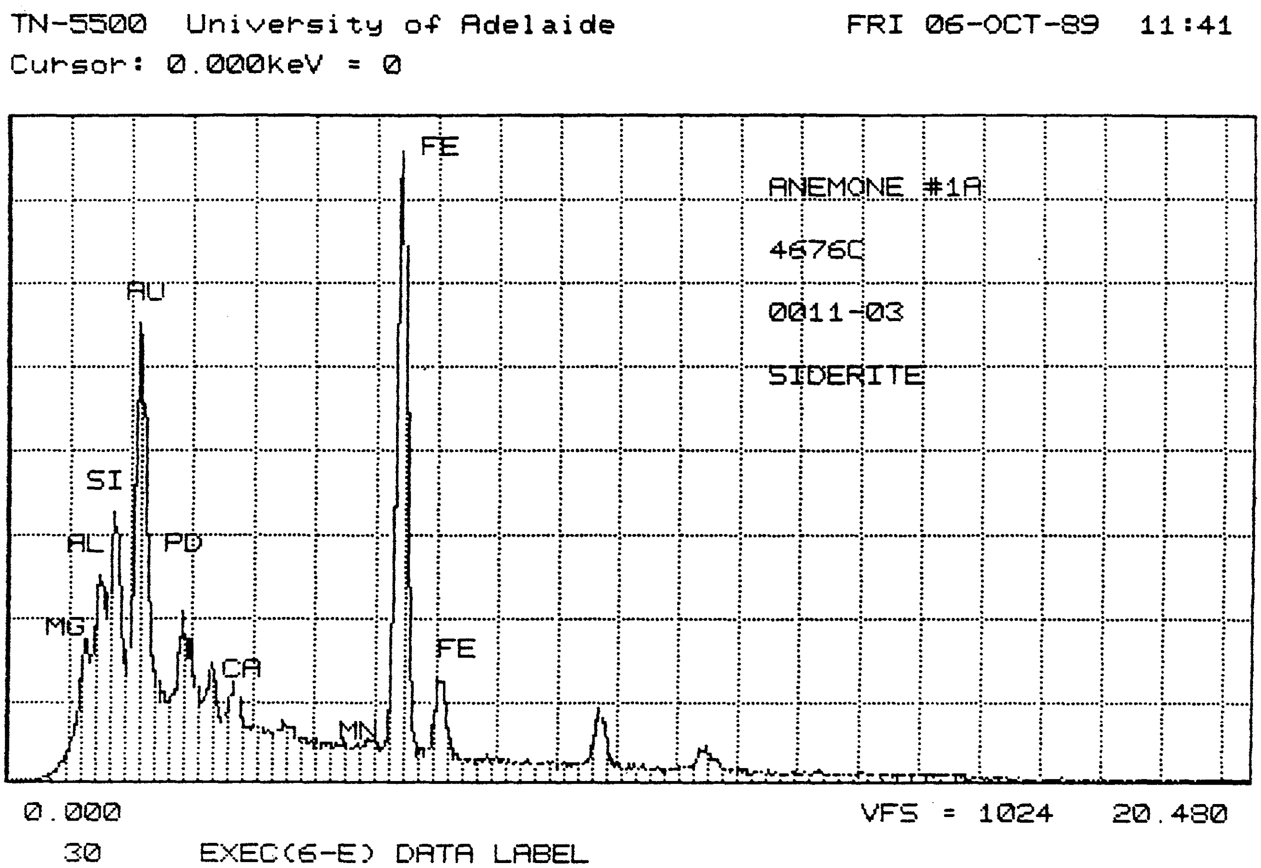

Figure 39. Anemone #1A, junk sub sample, 4676c metres. EDS pattern of siderite from the previous figure.

PE906892

This is an enclosure indicator page.
The enclosure PE906892 is enclosed within the container PE906849 at this location in this document.

The enclosure PE906892 has the following characteristics:

ITEM_BARCODE =	PE906892
CONTAINER_BARCODE =	PE906849
NAME =	Core Photomicrograph
BASIN =	GIPPSLAND
PERMIT =	VIC/P20
TYPE =	WELL
SUBTYPE =	PHOTOMICROGRAPH
DESCRIPTION =	Core Photomicrograph, porosity due to dissolution and slide preparation; pyrit crystals occur in aggregates, (figure 40 from attachment to WCR--Petrographic Analysis Report) for Anemone-1 & 1A
REMARKS =	
DATE_CREATED =	31/12/89
DATE_RECEIVED =	17/01/90
W_NO =	W997
WELL_NAME =	ANEMONE-1 & 1A
CONTRACTOR =	CORE SERVICES OF AUSTRALIA
CLIENT_OP_CO =	PETROFINA EXPLORATION AUSTRALIA S.A.

PE906893

This is an enclosure indicator page.
The enclosure PE906893 is enclosed within the container PE906849 at this location in this document.

The enclosure PE906893 has the following characteristics:

ITEM_BARCODE =	PE906893
CONTAINER_BARCODE =	PE906849
NAME =	Core Photomicrograph
BASIN =	GIPPSLAND
PERMIT =	VIC/P20
TYPE =	WELL
SUBTYPE =	PHOTOMICROGRAPH
DESCRIPTION =	Core Photomicrograph, low birefringence, grain-lining illite and corroded quartz, (figure 41 from attachment to WCR--Petrographic Analysis Report) for Anemone-1 & 1A
REMARKS =	
DATE_CREATED =	31/12/89
DATE_RECEIVED =	17/01/90
W_NO =	W997
WELL_NAME =	ANEMONE-1 & 1A
CONTRACTOR =	CORE SERVICES OF AUSTRALIA
CLIENT_OP_CO =	PETROFINA EXPLORATION AUSTRALIA S.A.

PE906894

This is an enclosure indicator page.
The enclosure PE906894 is enclosed within the container PE906849 at this location in this document.

The enclosure PE906894 has the following characteristics:

ITEM_BARCODE = PE906894
CONTAINER_BARCODE = PE906849
NAME = Core Photomicrograph
BASIN = GIPPSLAND
PERMIT = VIC/P20
TYPE = WELL
SUBTYPE = PHOTOMICROGRAPH
DESCRIPTION = Core Photomicrograph, scattered illite in the matrix; muscovite bent by compaction and polycrystalline rock fragments are evident, (figure 42 from attachment to WCR--Petrographic Analysis Report) for Anemone-1 & 1A
REMARKS =
DATE_CREATED = 31/12/89
DATE_RECEIVED = 17/01/90
W_NO = W997
WELL_NAME = ANEMONE-1 & 1A
CONTRACTOR = CORE SERVICES OF AUSTRALIA
CLIENT_OP_CO = PETROFINA EXPLORATION AUSTRALIA S.A.

PE906895

This is an enclosure indicator page.
The enclosure PE906895 is enclosed within the container PE906849 at this location in this document.

The enclosure PE906895 has the following characteristics:

ITEM_BARCODE	=	PE906895
CONTAINER_BARCODE	=	PE906849
NAME	=	Core Photomicrograph
BASIN	=	GIPPSLAND
PERMIT	=	VIC/P20
TYPE	=	WELL
SUBTYPE	=	PHOTOMICROGRAPH
DESCRIPTION	=	Core Photomicrograph, wide authigenic overgrowth forms a straight contact with the adjacent grain, the opposite side has a sutured contact which was an earlier event, (figure 43 from attachment to WCR--Petrographic Analysis Report) for Anemone-1 & 1A
REMARKS	=	
DATE_CREATED	=	31/12/89
DATE_RECEIVED	=	17/01/90
W_NO	=	W997
WELL_NAME	=	ANEMONE-1 & 1A
CONTRACTOR	=	CORE SERVICES OF AUSTRALIA
CLIENT_OP_CO	=	PETROFINA EXPLORATION AUSTRALIA S.A.

(Inserted by DNRE - Vic Govt Mines Dept)

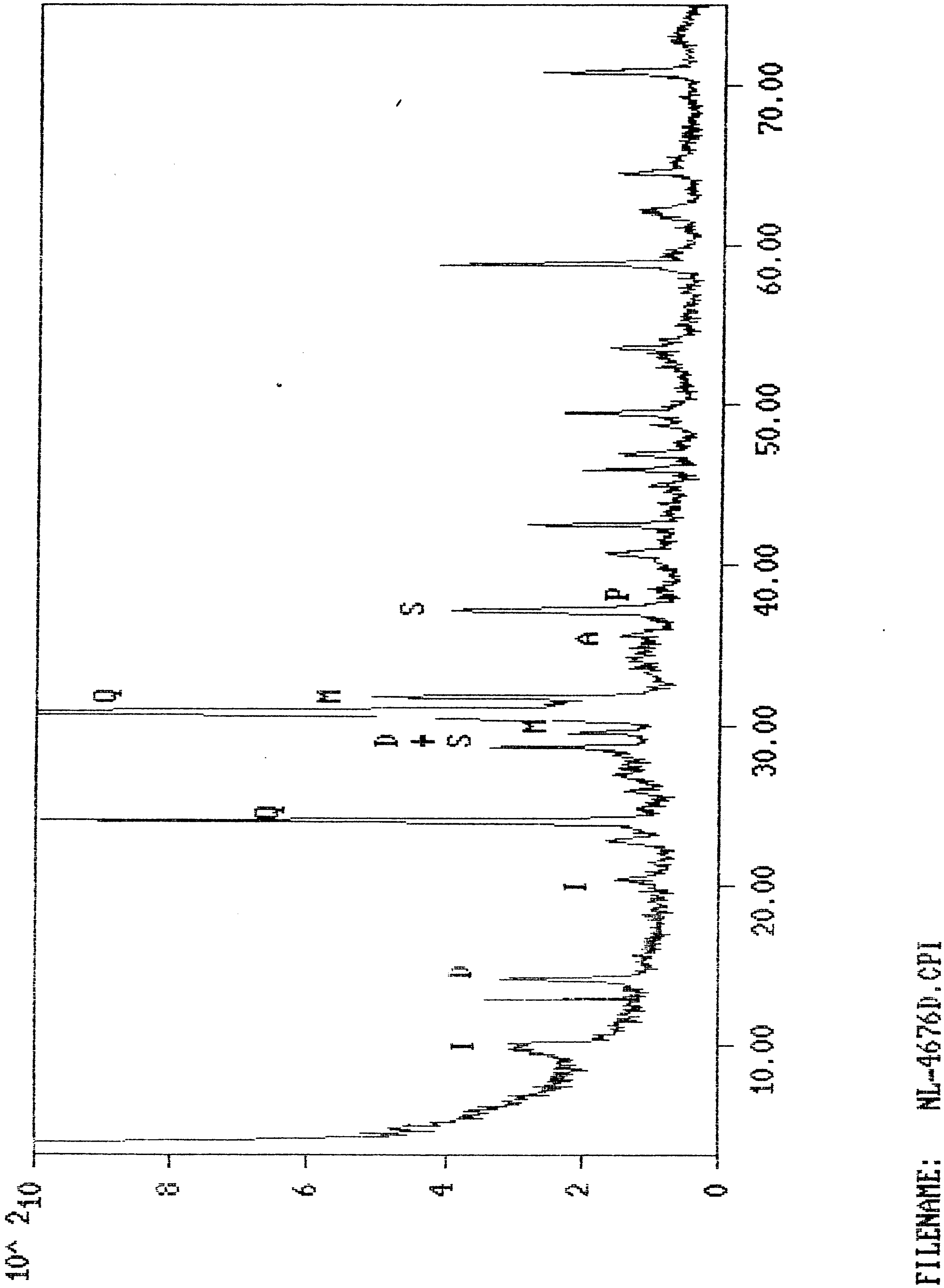

Figure 44. Bulk XRD trace of Anemone #1A, junk sub sample, 4676d m. Q=quartz, I=illite/muscovite, D=dickite, M=microcline, P=pyrite, S=siderite and A=ankerite. Only the strongest peaks have been labelled for each mineral.

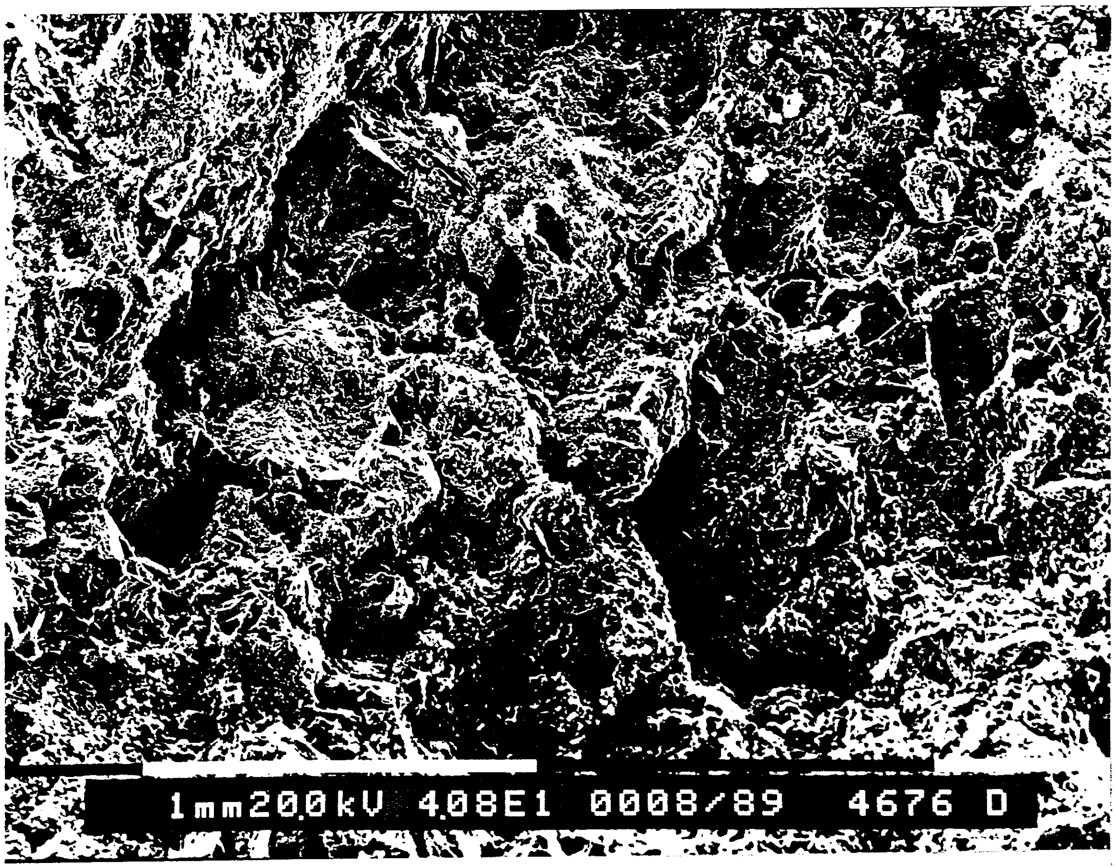

Figure 45 - Anemone #1A, junk sub sample, 4676d m. Scanning electron micrograph showing general view of sediment with abundant clay, including drilling mud. There is only minor porosity evident. Pores are of hybrid primary-secondary origin, since pore sizes are comparable to, or slightly larger than the average grain size. They may have resulted from whole grain dissolution.

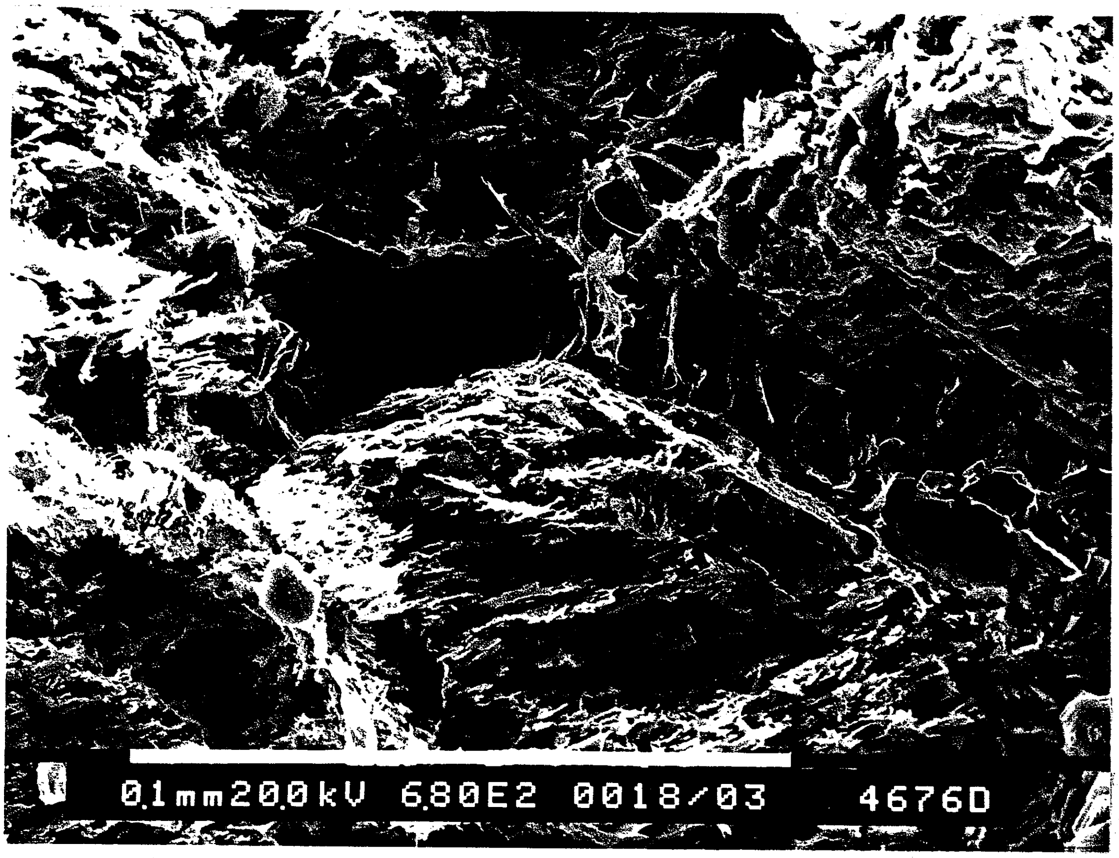

Figure 46, Anemone #1A, junk sub sample, 4676d m. Scanning electron micrograph demonstrating partial occlusion of pore throats by fibrous authigenic illite between dissolving feldspars. While it does not reduce porosity significantly, this type of bridging will create significant permeability barriers to flow.

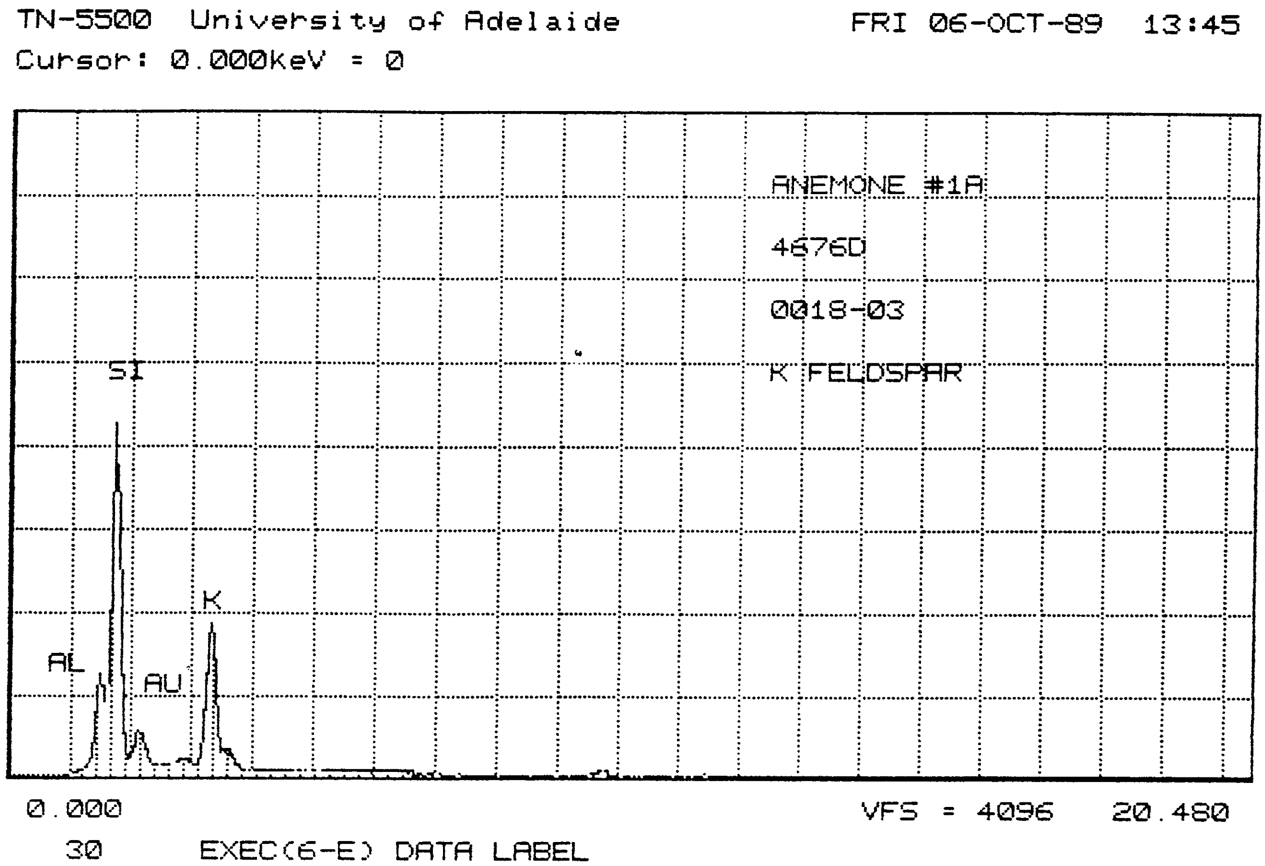

Figure 47. Anemone #1A, junk sub sample, 4676d metres. EDS pattern of K feldspar from previous figure.

2-98 Anemone 1A

Figure 48 - Anemone #1A, junk sub sample, 4676d m. Scanning electron micrograph showing detail of intergrowth of kaolin platelets and fibrous illite.

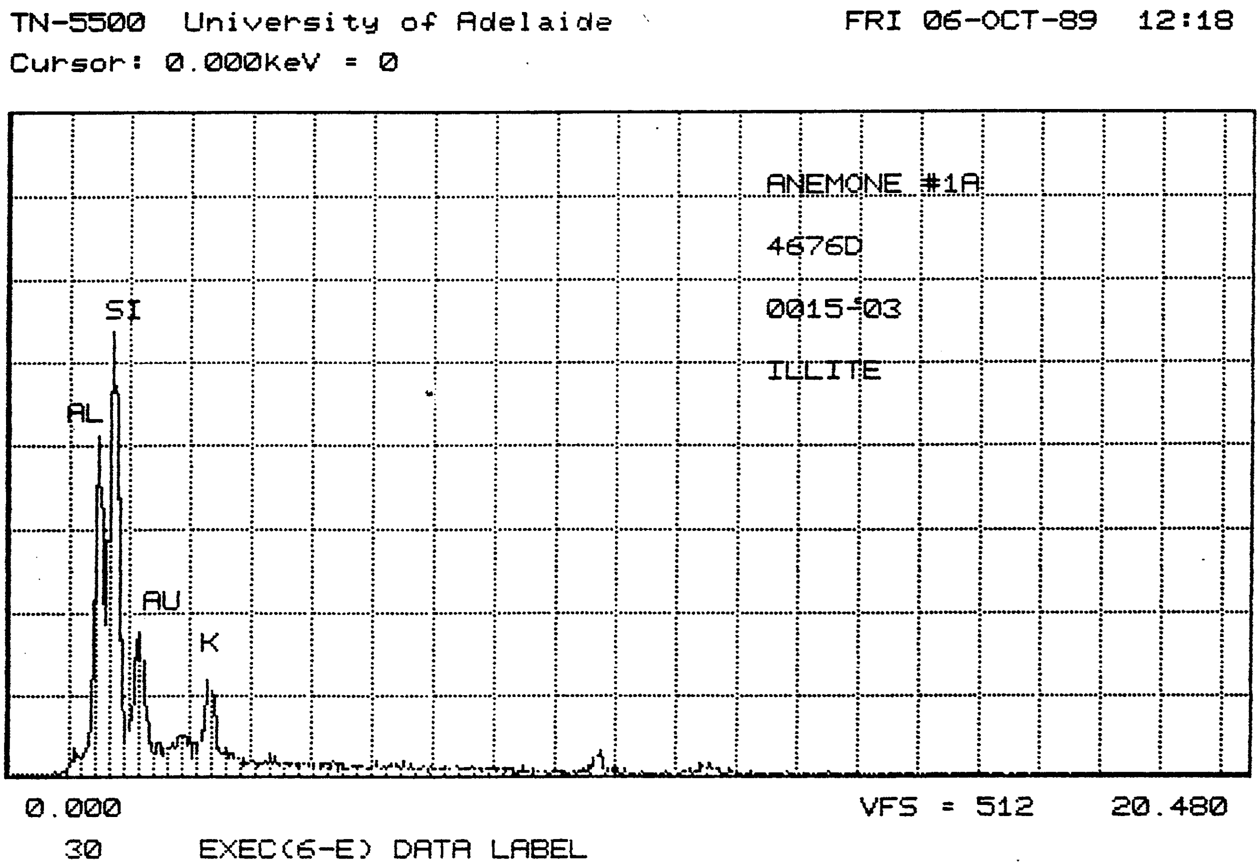

Figure 49. Anemone #1A, junk sub sample, 4676d metres. EDS pattern of illite from the previous figure.

Figure 50 - Anemone #1A, junk sub sample, 4676d m. Kaolin booklets lie adjacent to fractured quartz (q) and show intergrowth at the contact. Platy and fibrous illite is apparent in the lower right of the micrograph.

Figure 51 - Anemone #1A, junk sub sample, 4676d m. Pyritic aggregates which have been engulfed by authigenic quartz. An early, fine crystal phase and a later coarse crystal phase of pyrite growth are evident. Moulds in the quartz indicate that some pyrite has probably been plucked during sample preparation.

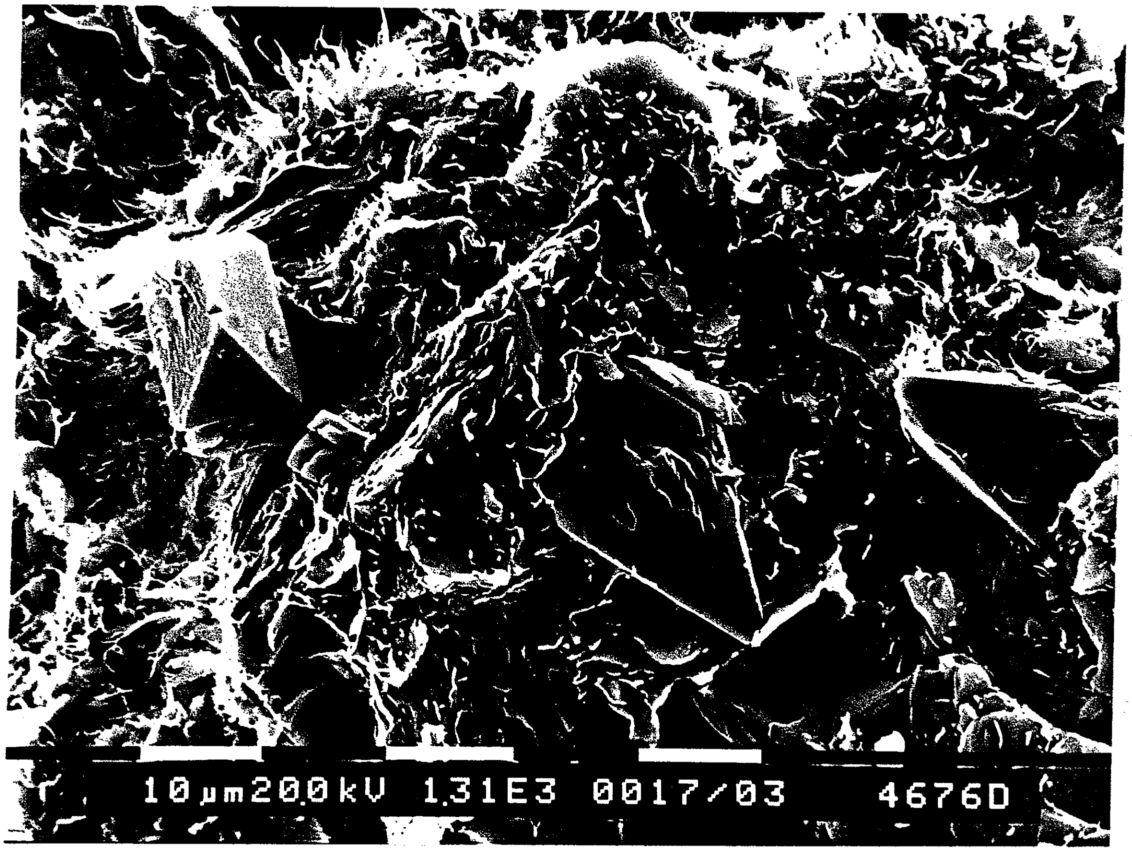

Figure 52 - Anemone #1A, junk sub sample, 4676d. Scanning electron micrograph showing euhedral anatase crystals (An) of authigenic origin.

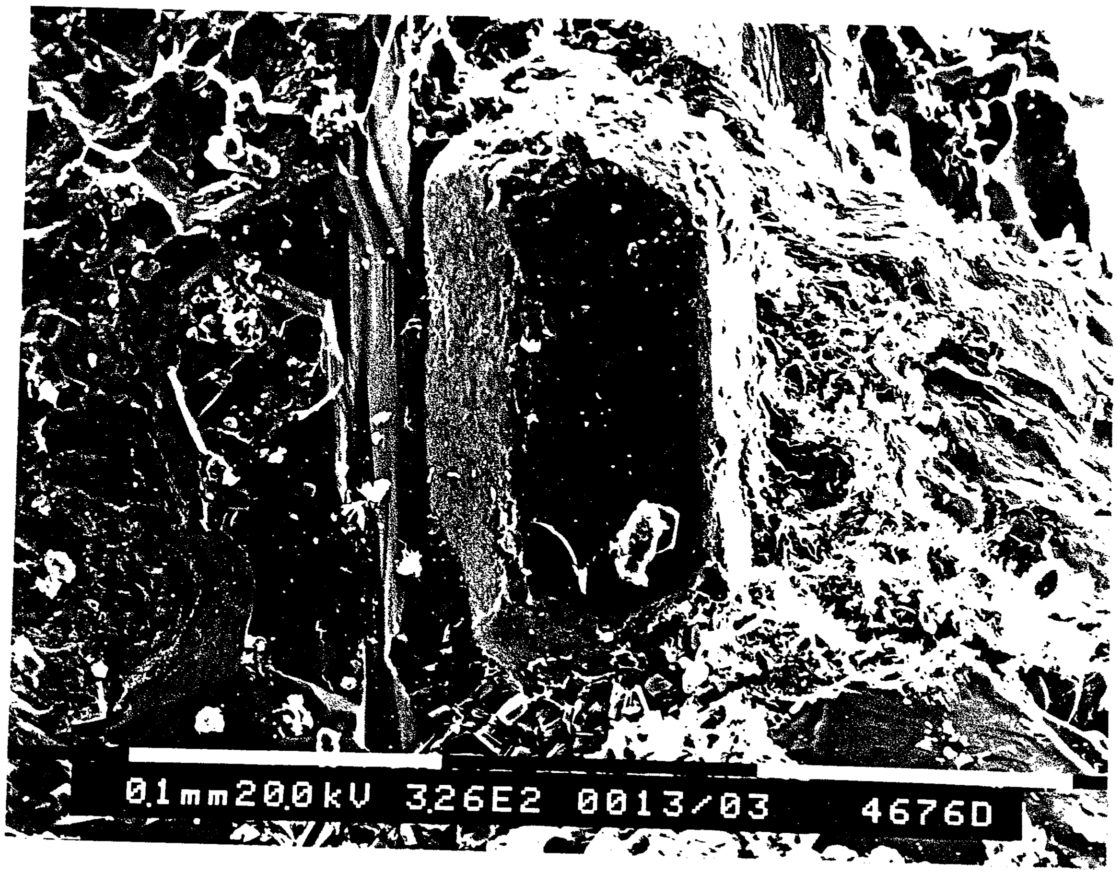

Figure 53, Anemone #1A, junk sub sample, 4676d m. A subhedral apatite crystal surrounded by clay matrix to the right and euhedral quartz to the left. Slight rounding of the crystal reflects it's detrital origin.

PE906896

This is an enclosure indicator page.
The enclosure PE906896 is enclosed within the container PE906849 at this location in this document.

The enclosure PE906896 has the following characteristics:

ITEM_BARCODE =	PE906896
CONTAINER_BARCODE =	PE906849
NAME =	Core Photomicrograph
BASIN =	GIPPSLAND
PERMIT =	VIC/P20
TYPE =	WELL
SUBTYPE =	PHOTOMICROGRAPH
DESCRIPTION =	Core Photomicrograph, secondary porosity associated with dissolution and microporosity, (figure 54 from attachment to WCR--Petrographic Analysis Report) for Anemone-1 & 1A
REMARKS =	
DATE_CREATED =	31/12/89
DATE_RECEIVED =	17/01/90
W_NO =	W997
WELL_NAME =	ANEMONE-1 & 1A
CONTRACTOR =	CORE SERVICES OF AUSTRALIA
CLIENT_OP_CO =	PETROFINA EXPLORATION AUSTRALIA S.A.

PE906897

This is an enclosure indicator page.
The enclosure PE906897 is enclosed within the container PE906849 at this location in this document.

The enclosure PE906897 has the following characteristics:

ITEM_BARCODE =	PE906897
CONTAINER_BARCODE =	PE906849
NAME =	Core Photomicrograph
BASIN =	GIPPSLAND
PERMIT =	VIC/P20
TYPE =	WELL
SUBTYPE =	PHOTOMICROGRAPH
DESCRIPTION =	Core Photomicrograph, microporosity associated with a seriticized grain with patches of spar scalenohedra, (figure 55 from attachment to WCR--Petrographic Analysis Report) for Anemone-1 & 1A
REMARKS =	
DATE_CREATED =	31/12/89
DATE_RECEIVED =	17/01/90
W_NO =	W997
WELL_NAME =	ANEMONE-1 & 1A
CONTRACTOR =	CORE SERVICES OF AUSTRALIA
CLIENT_OP_CO =	PETROFINA EXPLORATION AUSTRALIA S.A.

PE906898

This is an enclosure indicator page.
The enclosure PE906898 is enclosed within the container PE906849 at this location in this document.

The enclosure PE906898 has the following characteristics:

ITEM_BARCODE =	PE906898
CONTAINER_BARCODE =	PE906849
NAME =	Core Photomicrograph
BASIN =	GIPPSLAND
PERMIT =	VIC/P20
TYPE =	WELL
SUBTYPE =	PHOTOMICROGRAPH
DESCRIPTION =	Core Photomicrograph, extensive dissolution of feldspar producing seondary prosity; clay areas have flecks of microporosity., (figure 56 from attachment to WCR--Petrographic Analysis Report) for Anemone-1 & 1A
REMARKS =	
DATE_CREATED =	31/12/89
DATE_RECEIVED =	17/01/90
W_NO =	W997
WELL_NAME =	ANEMONE-1 & 1A
CONTRACTOR =	CORE SERVICES OF AUSTRALIA
CLIENT_OP_CO =	PETROFINA EXPLORATION AUSTRALIA S.A.

PE906899

This is an enclosure indicator page.
The enclosure PE906899 is enclosed within the container PE906849 at this location in this document.

The enclosure PE906899 has the following characteristics:

ITEM_BARCODE =	PE906899
CONTAINER_BARCODE =	PE906849
NAME =	Core Photomicrograph
BASIN =	GIPPSLAND
PERMIT =	VIC/P20
TYPE =	WELL
SUBTYPE =	PHOTOMICROGRAPH
DESCRIPTION =	Core Photomicrograph, Sericitic and kaolinitic grain replacement, (figure 57 from attachment to WCR--Petrographic Analysis Report) for Anemone-1 & 1A
REMARKS =	
DATE_CREATED =	31/12/89
DATE_RECEIVED =	17/01/90
W_NO =	W997
WELL_NAME =	ANEMONE-1 & 1A
CONTRACTOR =	CORE SERVICES OF AUSTRALIA
CLIENT_OP_CO =	PETROFINA EXPLORATION AUSTRALIA S.A.

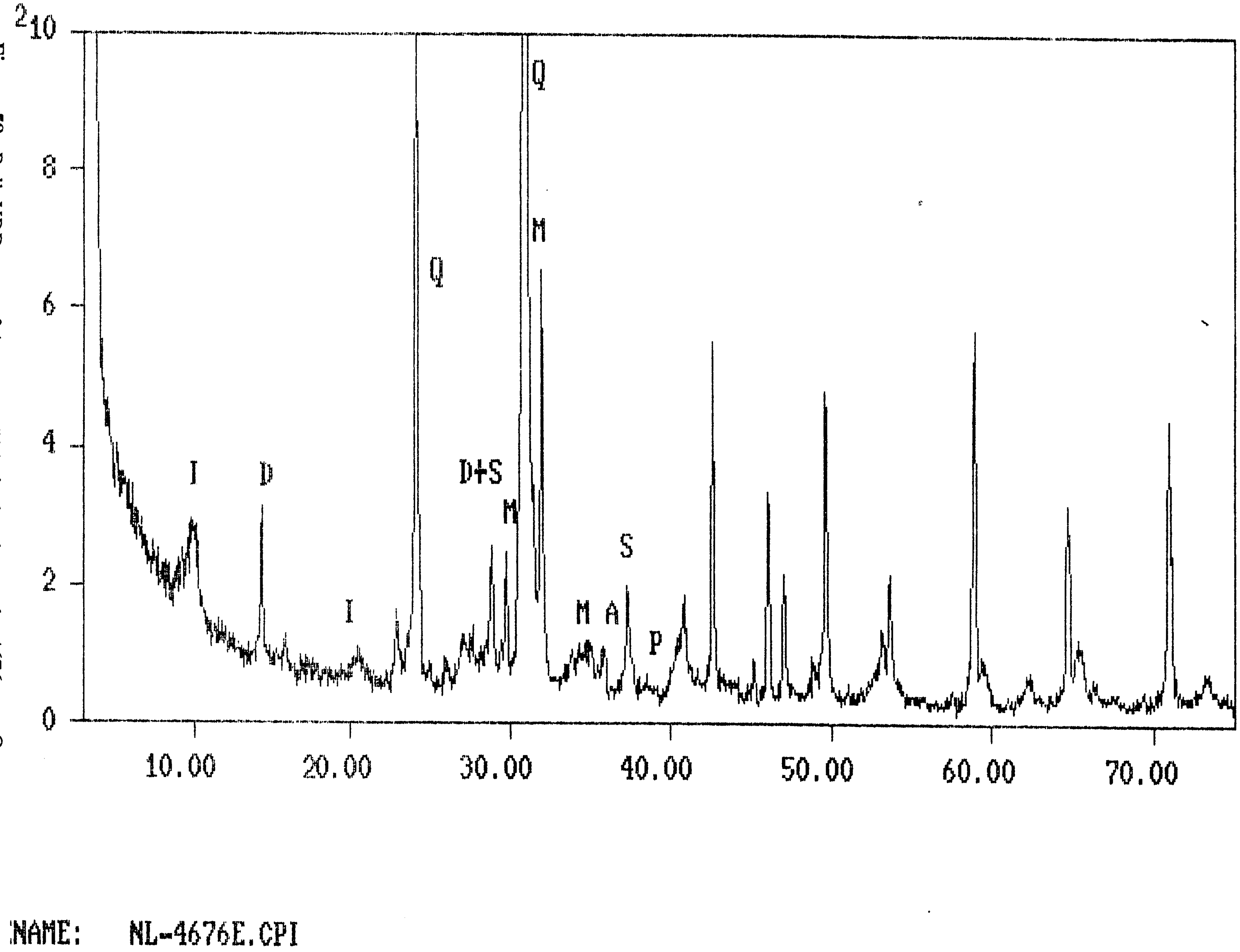

Figure 58. Bulk XRD trace of Anemone #1A, junk sub sample, 4676e m. Q=quartz, I=illite/muscovite, D=dickite, M=microcline, P=pyrite, S=siderite and A=ankerite. Only the strongest peaks have been labelled for each mineral.

PE906900

This is an enclosure indicator page.
The enclosure PE906900 is enclosed within the container PE906849 at this location in this document.

The enclosure PE906900 has the following characteristics:

ITEM_BARCODE =	PE906900
CONTAINER_BARCODE =	PE906849
NAME =	Core Photomicrograph
BASIN =	GIPPSLAND
PERMIT =	VIC/P20
TYPE =	WELL
SUBTYPE =	PHOTOMICROGRAPH
DESCRIPTION =	Core Photomicrograph, secondary dissolution porosity associated with highly altered microcline, (figure 59 from attachment to WCR--Petrographic Analysis Report) for Anemone-1 & 1A
REMARKS =	
DATE_CREATED =	31/12/89
DATE_RECEIVED =	17/01/90
W_NO =	W997
WELL_NAME =	ANEMONE-1 & 1A
CONTRACTOR =	CORE SERVICES OF AUSTRALIA
CLIENT_OP_CO =	PETROFINA EXPLORATION AUSTRALIA S.A.

PE906901

This is an enclosure indicator page.
The enclosure PE906901 is enclosed within the container PE906849 at this location in this document.

The enclosure PE906901 has the following characteristics:

ITEM_BARCODE =	PE906901
CONTAINER_BARCODE =	PE906849
NAME =	Core Photomicrograph
BASIN =	GIPPSLAND
PERMIT =	VIC/P20
TYPE =	WELL
SUBTYPE =	PHOTOMICROGRAPH
DESCRIPTION =	Core Photomicrograph, highly altered micrcline, spar and quartzofeldspathic rock fragments, (figure 60 from attachment to WCR--Petrographic Analysis Report) for Anemone-1 & 1A
REMARKS =	
DATE_CREATED =	31/12/89
DATE_RECEIVED =	17/01/90
W_NO =	W997
WELL_NAME =	ANEMONE-1 & 1A
CONTRACTOR =	CORE SERVICES OF AUSTRALIA
CLIENT_OP_CO =	PETROFINA EXPLORATION AUSTRALIA S.A.

PE906902

This is an enclosure indicator page.
The enclosure PE906902 is enclosed within the container PE906849 at this location in this document.

The enclosure PE906902 has the following characteristics:

ITEM_BARCODE =	PE906902
CONTAINER_BARCODE =	PE906849
NAME =	Core Photomicrograph
BASIN =	GIPPSLAND
PERMIT =	VIC/P20
TYPE =	WELL
SUBTYPE =	PHOTOMICROGRAPH
DESCRIPTION =	Core Photomicrograph, feldspar alteration along cleavage, secondary dissolution, fracture and porosity development, (figure6 1 from attachment to WCR--Petrographic Analysis Report) for Anemone-1 & 1A
REMARKS =	
DATE_CREATED =	31/12/89
DATE_RECEIVED =	17/01/90
W_NO =	W997
WELL_NAME =	ANEMONE-1 & 1A
CONTRACTOR =	CORE SERVICES OF AUSTRALIA
CLIENT_OP_CO =	PETROFINA EXPLORATION AUSTRALIA S.A.

PE906903

This is an enclosure indicator page.
The enclosure PE906903 is enclosed within the container PE906849 at this location in this document.

The enclosure PE906903 has the following characteristics:

ITEM_BARCODE = PE906903
CONTAINER_BARCODE = PE906849
NAME = Core Photomicrograph
BASIN = GIPPSLAND
PERMIT = VIC/P20
TYPE = WELL
SUBTYPE = PHOTOMICROGRAPH
DESCRIPTION = Core Photomicrograph, perthitic feldspar and cross-hatching, (figure 62 from attachment to WCR--Petrographic Analysis Report) for Anemone-1 & 1A
REMARKS =
DATE_CREATED = 31/12/89
DATE_RECEIVED = 17/01/90
W_NO = W997
WELL_NAME = ANEMONE-1 & 1A
CONTRACTOR = CORE SERVICES OF AUSTRALIA
CLIENT_OP_CO = PETROFINA EXPLORATION AUSTRALIA S.A.

(Inserted by DNRE - Vic Govt Mines Dept)

PE906904

This is an enclosure indicator page.
The enclosure PE906904 is enclosed within the container PE906849 at this location in this document.

The enclosure PE906904 has the following characteristics:

ITEM_BARCODE = PE906904
CONTAINER_BARCODE = PE906849
NAME = Core Photomicrograph
BASIN = GIPPSLAND
PERMIT = VIC/P20
TYPE = WELL
SUBTYPE = PHOTOMICROGRAPH
DESCRIPTION = Core Photomicrograph, subhedral spar scalenohedra growing between muscovite, (figure 63 from attachment to WCR--Petrographic Analysis Report) for Anemone-1 & 1A
REMARKS =
DATE_CREATED = 31/12/89
DATE_RECEIVED = 17/01/90
W_NO = W997
WELL_NAME = ANEMONE-1 & 1A
CONTRACTOR = CORE SERVICES OF AUSTRALIA
CLIENT_OP_CO = PETROFINA EXPLORATION AUSTRALIA S.A.

PE906905

This is an enclosure indicator page.
The enclosure PE906905 is enclosed within the container PE906849 at this location in this document.

The enclosure PE906905 has the following characteristics:

ITEM_BARCODE =	PE906905
CONTAINER_BARCODE =	PE906849
NAME =	Core Photomicrograph
BASIN =	GIPPSLAND
PERMIT =	VIC/P20
TYPE =	WELL
SUBTYPE =	PHOTOMICROGRAPH
DESCRIPTION =	Core Photomicrograph, subhedral spar scalenohedrite growing between the muscovite under crossed polars, (figure 64 from attachment to WCR--Petrographic Analysis Report) for Anemone-1 & 1A
REMARKS =	
DATE_CREATED =	31/12/89
DATE_RECEIVED =	17/01/90
W_NO =	W997
WELL_NAME =	ANEMONE-1 & 1A
CONTRACTOR =	CORE SERVICES OF AUSTRALIA
CLIENT_OP_CO =	PETROFINA EXPLORATION AUSTRALIA S.A.

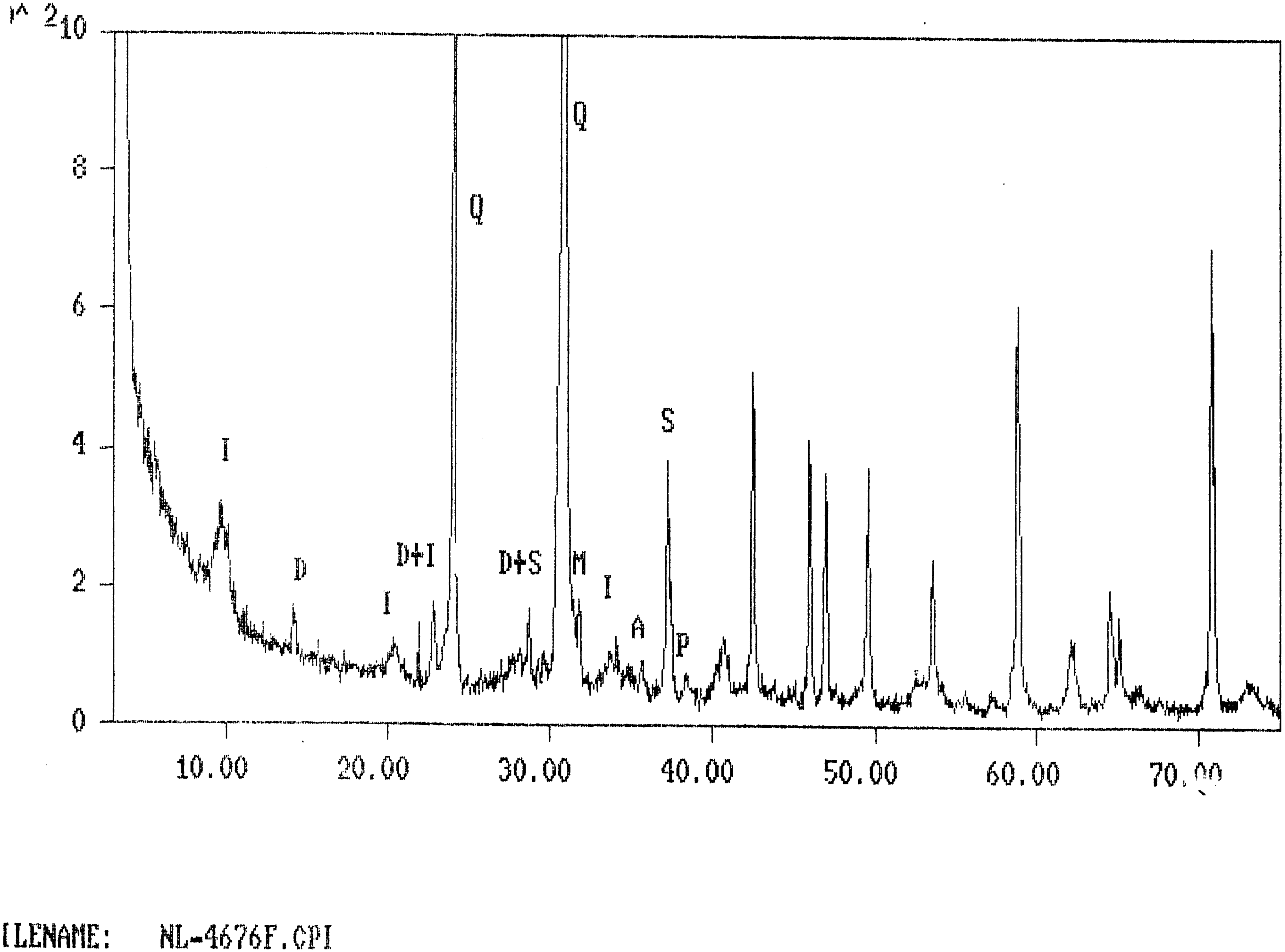

Figure 65. Bulk XRD trace of Anemone #1A, junk sub sample, 4676f m. Q=quartz, I=illite/muscovite, D=dickite, M=microcline, P=pyrite, S=siderite and A=ankerite. Only the strongest peaks have been labelled for each mineral.

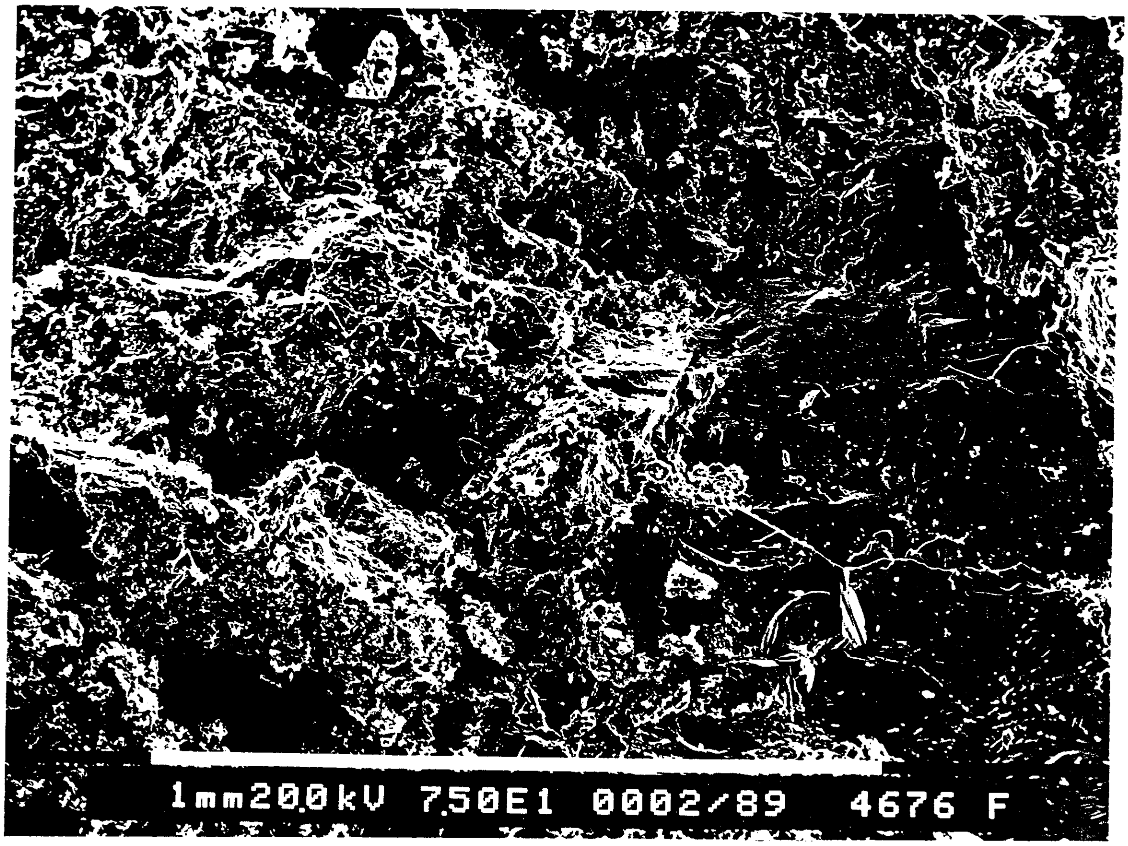

Figure 66 - Anemone #1A, junk sub sample, 4676f m. Scanning electron micrograph showing general view with abundant clay, (including drilling mud), fractured quartz (Q) and minor porosity.

2-98 Anemone 1A

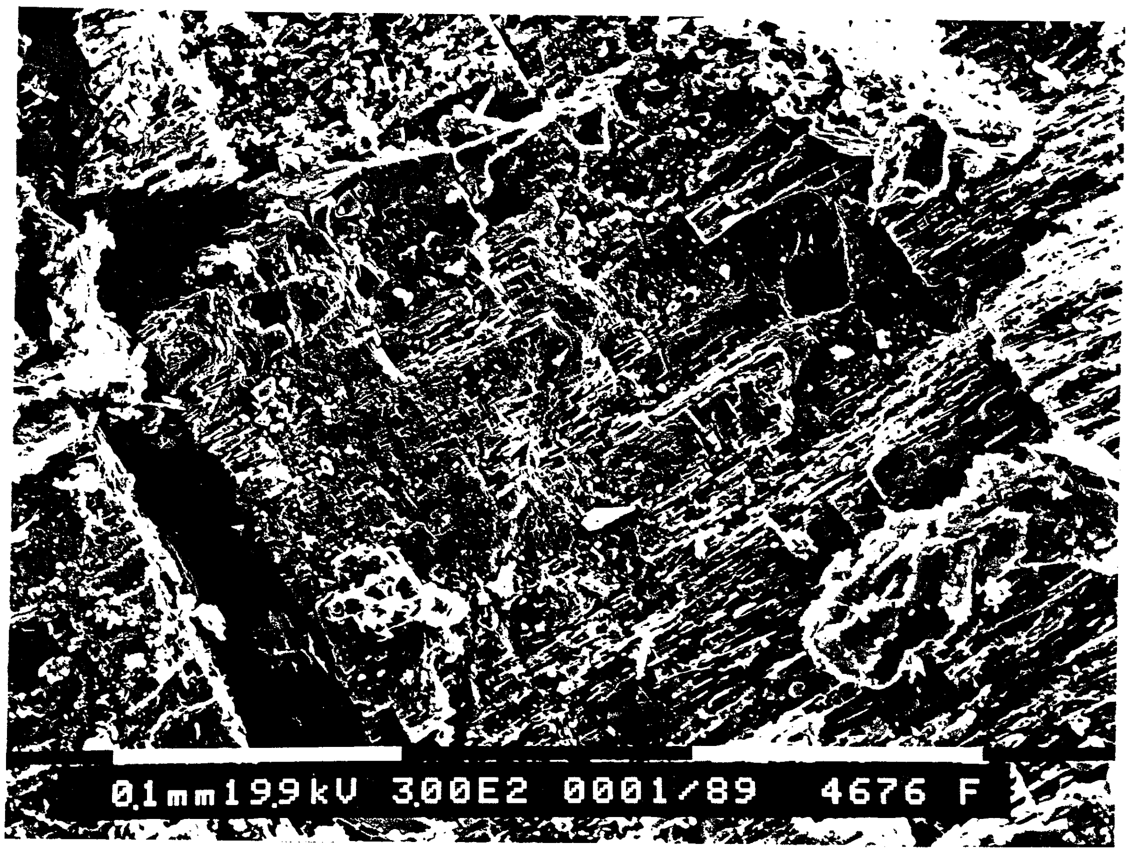

Figure 67 - Anemone #1A, junk sub sample, 4676f m. A SEM micrograph showing dissolution of K feldspar has produced minor secondary porosity.

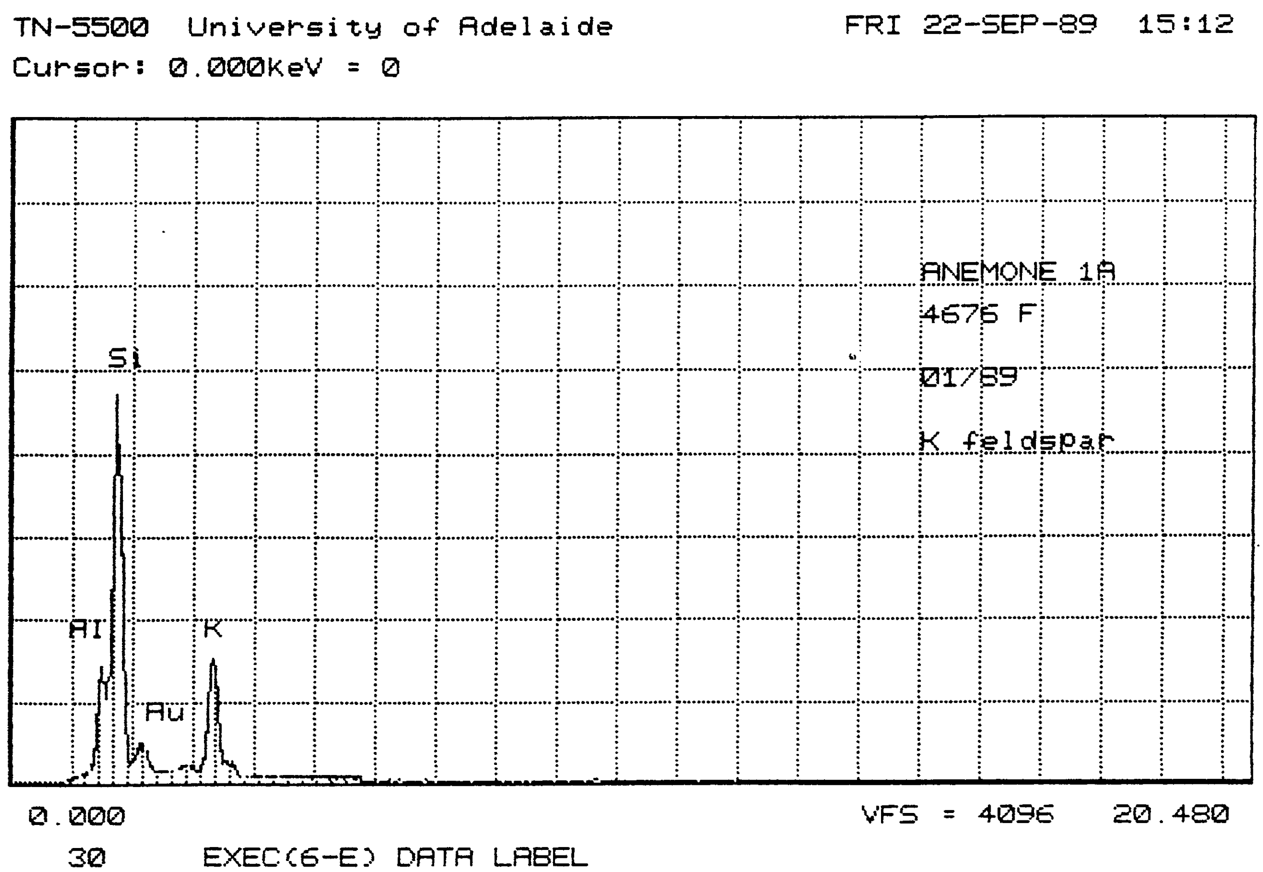

Figure 68. Anemone #1A, junk sub sample, 4676f metres. EDS pattern of K feldspar from previous figure.

2-98 Anemone 1A

Figure 69 - Anemone #1A, junk sub sample, 4676f m. A large dissolution pore is evident in the K feldspar on the left, adjacent to kaolin and minor illite. A thin border of illite between the pore and the kaolin probably represents alteration at the original boundary of the K. feldspar.